2011

ADAM10 exacerbation of allergic disease is potentially explained by its role in CD23 exosomal sorting.

Joel Mathews
Virginia Commonwealth University

ADAM10 exacerbation of allergic disease is potentially explained by its role in CD23 exosomal sorting.

A dissertation submitted in partial fulfillment of the requirements for the degree of Doctor of Philosophy at Virginia Commonwealth University

By

Joel Andrew Mathews
B.S., Brigham Young University, 2006

Director: Daniel H. Conrad, Professor, Department of Microbiology and Immunology

Virginia Commonwealth University
Richmond, Virginia
April, 2011

DEDICATION

This dissertation is dedicated to my family for all their encouragement to go to graduate school and then for the continual support during it. I would like to first thank my wife, Becky, for all of her support and encouragement, I never could have completed this without her. I would also like to thank my parents for all the help and support they gave me growing up to gain my education and to learn to work hard. Finally I would like to thank all my brothers and sisters, mother and father in-law for all the encouragement they have given me during this process, without them I never could have succeeded.

ACKNOWLEDGEMENTS

First off, I would like to thank my graduate advisor and mentor, Dr. Daniel H. Conrad. He has been a great friend. I will always remember all the things he has taught me as well as the patience and support he has given me.

Secondly, I would like to thank my graduate committee members, Dr. Barbour, Dr. Lloyd, Dr. Tew and Dr. Kepley for all their support and guidance they have given me throughout the PhD process.

I would also like to thank some of the past members of the Laboratory including Dr. Jill Ford for the work she did in determining the role of CD23 in experimental asthma with the CD23Tg as this was the bases for my project on ADAM10s role in experimental asthma. I would also like to thank her for all the advice she has given me while working on the project and writing up the paper.

I would also especially like to thank Dr. David Gibb for creating the ADAM10 B cell specific knockout mice as these mice have made possible much of my work. He has also been a great friend and support to me and I would like to thank him for that.

I would also like to thank Dr. Jamie Sturgill as she helped me start on doing much of my work. Including, the inhibitor studies on human B cells and ADAM10 involvement in proliferation. In addition, Jamie has always been a great friend and has given me a lot of guidance to help me in my work.

I would also like to thank one other past member of the laboratory Dr. Bing-Hung Chen who created all the recombinant CD23 mutants. With these I was able to show the region of CD23 important in binding ADAM10.

I would also like to thank the members of Dr. Stephan Galli laboratory who created the IgE/mast cell dependent experimental asthma model.

In addition I would also like to thank Dr. Peggy Scherle at the Incyte Corporation for providing the ADAM10 inhibitors. Without these none of my studies would have been possible.

I would also like to thank all of the current members of the laboratory for all of their support. Sarah Norton especially has been a big help in developing my mouse experiments and in interpreting the results. I would also like to thank Dae-Joong Kang who has been a great help in looking at gene expression by qRT-PCR in the lungs of the mice. I would finally like to thank Naty Chaimowitz, Becca Martin and Sheinei Saleem as well as Hannah Zellner and Yvette Orihuela for all their suggestions and help during my dissertation.

Finally, I would also like to thank my undergraduate mentor Dr. Eric Wilson. He was the first one to help me get started in immunology research. In addition, he has been a great friend and support.

Table of contents

LIST OF TABLES

TABLE

LIST OF FIGURES

FIGURES

LIST OF ABBREVIATIONS

-/-	Homozygous deletion of a gene
11E10	mAb recognizing the stalk region of human CD23
19G5	mAb recognizing the stalk region of murine CD23
293	Human embryonic kidney cell line
2H10	mAb recognizing the lectin domain of murine CD23
Ab	Antibody
ADAM	A disintegrin and metalloprotease
AHR	Airway hyperreactivity
Alum	Aluminum hydroxide
AP	Alkaline phosphatase
APC	Allophycocyanin
B3B4	mAb recognizing the lectin domain of murine CD23
BALB/C	Inbred mouse strain; high IgE responder
BALF	Bronchoalveolar lavage fluid
BSA	Bovine serum albumin
C57BL/6	Inbred mouse strain; intermediate IgE responder
CD	Clusters of differentiation
CD23Tg	CD23 transgenic
CFSE	Carboxyfluroscein diacetate succinimidyl ester
CHO	Chinese hamster ovary cell line

CM5	Biacore sensor chip suitable for coupling via -NH2, -SH, -CHO, -OH, or -COOH groups
COH2	Rat IgG_{2a}; isotype control for 19G5
CPM	Counts per minute
Cre	Causes Recombination – removes DNA between loxP sites
CSR	Class switch recombination
DMSO	Dimethyl sulfoxide
DN-ADAM10	Mutated A disintegrin and Metalloproteases where the prodomain has been spliced to the disintegrin, thus removing the protease domain
DNP	2,4-Dinitrophenol
EEA1	Early endosome antigen 1
ELISA	Enzyme-linked immunosorbent assay
ELISPOT	Enzyme-linked immunosorbent spot
endoH	Endoglycosidase H is a recombinant glycosidase which cleaves within the chitobiose core of high mannose and some hybrid oligosaccharides from N-linked glycoproteins
FACS	Fluorescence activated cell sorter
FBS	Fetal bovine serum
FITC	Fluorescein isothiocyanate
flox/flox	Homozygous for loxP sites on both sides of exon 9 of ADAM10
GI254023X	Glaxo ADAM10 inhibitor
H&E	Haematoxylin and eosin stain
HEPES	Buffering agent

HRP	Horseradish peroxidase
i.n.	Intranasal
i.p.	Intraperitoneal
IDEC-152	mAb recognizing the lectin domain of human CD23
Ig	Immunoglobulin
IgE	Immunoglobulin E
IL	Interleukine
INC000129	Incyte ADAM17 inhibitor
INC008765	Incyte ADAM10 inhibitor
INC009588	Incyte ADAM10 inhibitor
INF-γ	Interferon-gamma
IκB	A negative regulator of nuclear factor kappa B
Jijoye	Human B cell line – intermediate CD23 expression
Ka	Affinity constant
KC	Keratinocyte-derived chemokine
kD	Kilodalton
LAMP1	Lysosomal-associated membrane protein 1
LM	Littermate
LPS	Lipopolysaccharide
Luc	Luciferases units
lz-CD23	Chimeric CD23 composed of a leucine zipper attached to portions of the extracellular domains of CD23
mAb	Monoclonal antibody

MEF	Mouse embryonic fibroblasts
MES	Buffering agent at low pH (5-6)
MIP	Macrophage inflammatory protein
mRNA	Message ribonucleic acid
NF-κB	Nuclear factor kappa B
NHS	*N*-hydroxysuccinimide
NP40	Nonidet-P40
OVA	Ovalbumin
PBMC	Peripheral blood mononuclear cells
PBS	Phosphate buffered saline
Penh	Enhanced pause
qRT-PCR	Real time quantitative Polymerase chain reaction
RAB11	Ras-like GTPases11 – found specifically in the late or recycling endosomes
rADAM10	recombinant A disintegrin and metalloprotease
RPMI 8866	Human lymphoblastoid cell line
RPMI	Roswell Park Memorial Institute
RT-PCR	Reverse transcriptase polymerase chain reaction
RU	Resonance units
sCD23	Soluble CD23
SPR	Surface Plasmon Resonance
STAT	Signal transducer and activator of transcription
Th1	T helper cell type 1

Th2	T helper cell type 2
v/v	volume to volume
WT	Wild Type
YFP	Yellow fluorescent protein

ABSTRACT

ADAM10 EXACERBATION OF ALLERGIC DISEASE IS POTENTIALLY EXPLAINED BY ITS ROLE IN CD23 EXOSOMAL SORTING.

By Joel A. Mathews.

A dissertation submitted in partial fulfillment of the requirements for the degree of Doctor of Philosophy at Virginia Commonwealth University.

Virginia Commonwealth University, 2011

Director: Daniel H. Conrad, Professor, Department of Microbiology and Immunology

CD23, the natural negative regulator of IgE, has been shown to be involved in asthma progression through its regulation of IgE. To investigate if its sheddase, ADAM10, is also involved in asthma progression, three mouse models were utilized; an IgE/mast cell dependent model, an IgE dependent, mast cell independent model and a mast cell and IgE independent model. Experimental asthma was then induced in mice which were selectively deficient for ADAM10 in B cells ($ADAM10^{-/-}$) and compared to WT controls. The $ADAM^{-/-}$ mice had decreased signs of asthma, including eosinophilia, AHR and IgE synthesis in the IgE dependent model compared to LM controls, while with the IgE independent model there was no significant difference. Thus, CD23Tg and $ADAM10^{-/-}$ B cell mice have reduced IgE dependent lung inflammation in mouse models compared to WT controls. As a follow up, ADAM10 was inhibited in WT mice by intranasal administration of an ADAM10 inhibitor, compared to carrier (DMSO) treated mice. As with $ADAM10^{-/-}$ mice, inhibition of ADAM10 was only able to control IgE dependent models. These results thus show that ADAM10 is a possible target in

controlling IgE dependent allergic disease, possibly as blocking ADAM10 would cause an increase in CD23 membrane expression.

To better understand how ADAM10 cleaves CD23 we first sought to confirm previous studies that CD23 is internalized, with the hypothesis that shedding takes place intracellularly, rather than at the cell surface as previously assumed. Indeed, ADAM10 is more highly expressed intracellularly than at the cell surface. At 37 ºC, crosslinking CD23, especially with the anti-stalk mAb 19G5, resulted in extensive CD23 internalization. In addition, the expected increase in soluble CD23 (sCD23) production when 19G5 was added was blocked by the addition of NH_4Cl. NH_4Cl is known to block the progression of the endosomal pathway. These findings thus confirmed our hypothesis that cleavage of CD23 requires internalization and progression through the endosomal pathway before it is released into the extracellular space. We further demonstrated that ADAM10 is not only involved in cleaving CD23, but also in sorting CD23 into exosomes, as B cells lacking ADAM10 do not incorporate CD23 into exosomes. In addition, we found that exosomes secreted from the cell contain full length CD23, thus showing that they could bind IgE/antigen complex and be involved in the known CD23 dependent enhancement of antigen presentation by the injection of IgE/antigen complexes compared to antigen alone. These results also show that the change in ADAM10 expression specifically in a B cell could be involved in enhancement of IgE dependent inflammation.

To determine what signals change ADAM10 expression, ADAM10 promoter studies were initiated. We found that both IL-21 and anti-CD40 increased ADAM10 promoter activity, while IL-4 and IL-13 had no effect. Overall our data show that

increasing ADAM10 activity and expression leads to increased inflammation and IgE and is a possible target in controlling IgE dependent diseases.

Introduction

I. Immunoglobulin E

Asthma and allergies are the most common chronic IgE associated diseases. Asthma attacks are characterized by wheezing, chest tightness, shortness of breath, and coughing while allergy symptoms include itchy eyes, running nose and sneezing. The prevalence of these diseases has dramatically increased over the past twenty years. In 2004, in the United States alone, there were a total of 5.6 million children who had been diagnosed with an atopic disease (1). The cost is even more astounding. In 1994, for example 12 billion dollars representing 1 to 2% of the total health-care budget was spent for allergic disease treatment; these numbers have also continued to swell (2).

The underlying cause of asthma and allergies is an increase in allergen specific IgE. The cross linking of IgE bound to its high affinity receptor (FcεR1) causes the degranulation of both mast cells and basophils. When a person is first exposure to an allergen, the allergen is taken up and processed by cells known as APC including dendritic cells. These cells then migrate to the lymph nodes where they present peptides derived from the allergen in the context of MHC class II to T cells. This presentation plus early IL-4 (basophils?) causes the T cells to differentiate into Th2 cells. These Th2 cells then produce large amounts of IL-13 and IL-4. In parallel the antigen also drains into the lymph node and is recognized by B cells through B cell antigen receptors (BCR). In this Th2 environment the B cells are signaled to class switch to IgE producing plasma cells and the IgE is then bound by mast cells and basophils (3). When the patient undergoes a secondary exposure, IgE bound to FcεR1, on mast cells and/or basophils will be cross linked and cause the degranulation of these cells, releasing the mediators common to

allergies, including histamine, leukotrienes, and prostaglandins. This release is known as the early phase response and occurs within minutes of antigen exposure. These mediators can then bind their receptors on smooth muscle cells, blood vessels and epithelial cells and cause muscle contraction, mucus production and increased vascular permeability. In addition, several hours after allergen exposure mast cells will release newly synthesized cytokines and lipid mediators including IL-8, TNFα and LTB_4, these mediators will cause the recruitment of additional immune cells which will exacerbate the response (4). These cells including eosinophils and Th2 cells (5) and it is this late phase response which is believed to be the cause of the lasting effects of asthma including airway remolding and smooth muscle hyperplasia.

A. Discovery of IgE: Originally known as reagin, the idea that IgE could be causing allergic reactions began to take shape in 1921, in a paper by Prausnitz and Kustner. They showed that sensitization could be transferred by the transmission of serum from an allergic patient to a non-allergic patient (6). This work also established what came to be called the PK test for demonstrating skin-sensitization to allergens in patients. With this discovery it was shown that the protein/reagin that causes allergies is found in human serum and over the next 40 years through a variety of experiments (reviewed in (7)) scientists tried to discover the identity of this protein. With the development of better serum protein fractionation, the Ishizakas in Denver, CO (8) were able to isolate a highly enriched reagin preparation and prepared specific antibody against the purified reagin. Another group in Sweden had discovered a myeloma that did not fit any of the currently known classes of Ig (9). Exchange of reagents allowed identification

of a new Ig class, which was named IgE. Finally in 1968, the World Health Organization recognized that IgE was the fifth class of Ig (10).

B. Class switching to IgE: Class switching in B cells requires two signals, IL-4/IL-13 and CD40 signaling. In the pre-B stage the VDJ regions are rearranged to form a variable region attached to the constant region of either IgM or IgD, and through negative selection self-reacting B cells are deleted. After activation and trafficking to the germinal center B cells go through what is known as class-switch recombination (CSR) where they can switch to IgG, IgE or IgA (or any of their respective subclasses), by splicing out of sections of the genomic DNA. This occurs when certain signals from outside the cell activate a promoter that causes the transcription of a sterile transcript. In the case of IgE this signal is IL-4 or IL-13 signaling through Stat6 as well as NF-κB activated by CD40. The sterile transcript includes the 140 bp Iε exons along with Cε1-Cε4 of which part is known as the Sε region. This Sε region forms a DNA-RNA hybrid creating a stable "R loop" structure. The transcript binds to the G-rich strand, leaving the C-rich strand as a single strand, which then allows AID to bind and mutate sections of the gene. The activation of B cells is required for AID to be expressed. Once AID is active it attacks the C-rich strand changing the C to U. Then through a process involving Uracil glycosylase and other enzymes, the section between the end of the variable region and the start of the IgE constant region is spliced out (reviewed in (11)).

In addition to CD40, IL-4 and IL-13 there are other cytokines that either increase or decrease the synthesis of IgE, through a variety of mechanisms. These include IFN-γ and α (12), TGF-β (13) and IL-12 (14) which all have an inhibitory effect, while IL-21 (15), IL-10 (16), IL-5 (17), IL-7 (18), IL-6 (19) all increase IgE synthesis.

C. Anti-IgE and other asthma treatments: Multiple strategies have been tried to combat the effects of allergens. The most common allergy drugs are either antihistamines or leukotriene antagonists, such as Benadryl or Singulair respectively (4). The newest approach is the use of a humanized anti-IgE antibody known clinically as Omalizumab (Xolair®). This strategy attempts to block IgE from binding to its receptor on mast cells/basophils. Studies of FcεR1 seem to suggest that it is being produced constitutively and that with the addition of IgE it controls the loss of FcεR1 from the cell surface. Thus with the addition of anti-IgE, not only does it remove free IgE from circulation, but with the decrease in IgE, there is also a corresponding loss of surface bound FcεR1 on both mast cells and basophils (20). With this loss, upon allergen exposure there is also decreased degranulation and mediator release. However, this treatment is not perfect as it is extremely costly and requires repeated treatment because the synthesis of IgE is not blocked. In addition, anti-IgE therapy is only approved for those whose levels of IgE fall in the 30 and 700 IU/ml range (21) possibly because when levels of IgE are to high, the anti-IgE therapy cannot decrease the free IgE to the required levels. Very little (250 ng/ml) IgE is needed to upregulate FcεR1 surface expression and it is this down regulation of the receptor that seems to make anti-IgE therapy so effective (22). Thus, this clearly shows the need for a more cost effective therapy to reduce IgE serum levels, possibly through decreasing its synthesis.

II. CD23

A. Discovery or CD23: In 1975 while searching for proteins that bound immunoglobulin on different cell types, Lawrence *et al.* discovered that lymphocytes could bind IgE (23). Through further studies, the lymphocyte receptor was shown to have

Figure 1: Structure of CD23 and ADAM10 – Structure of CD23 (A) Schematic (24), (B) ribbon (24). (C) Structure of ADAM10 ribbon (25) and (D) schematic.

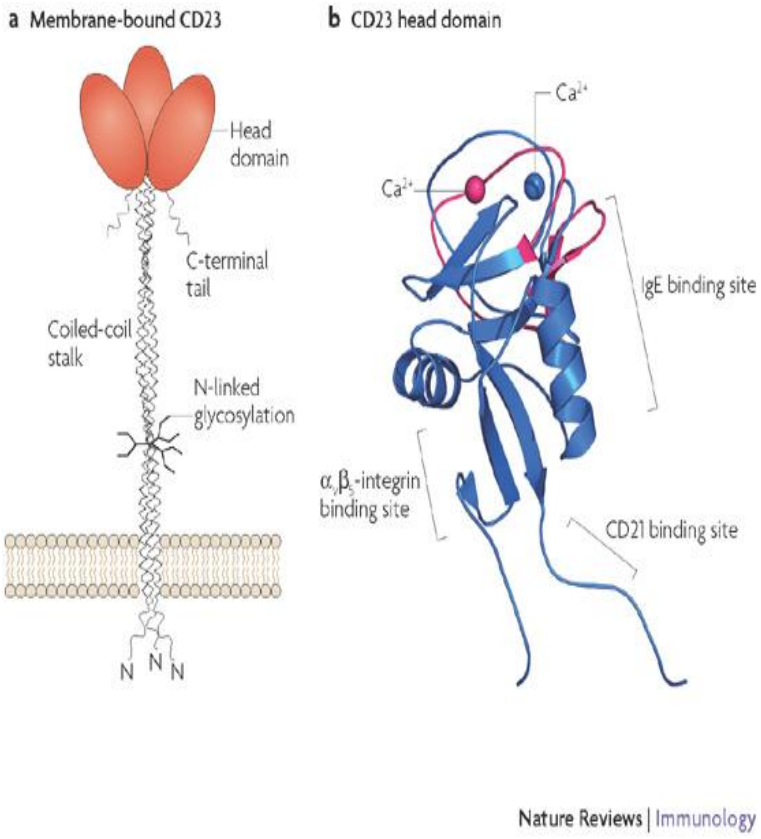

C.

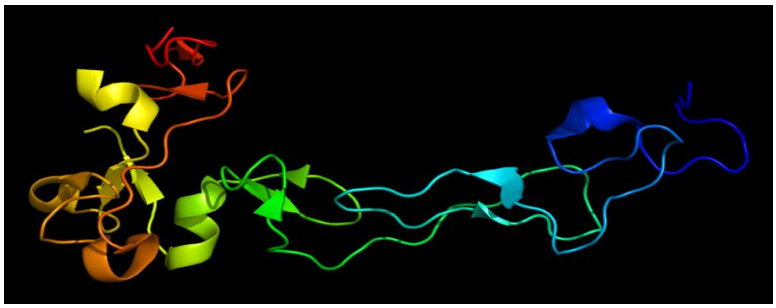

D.

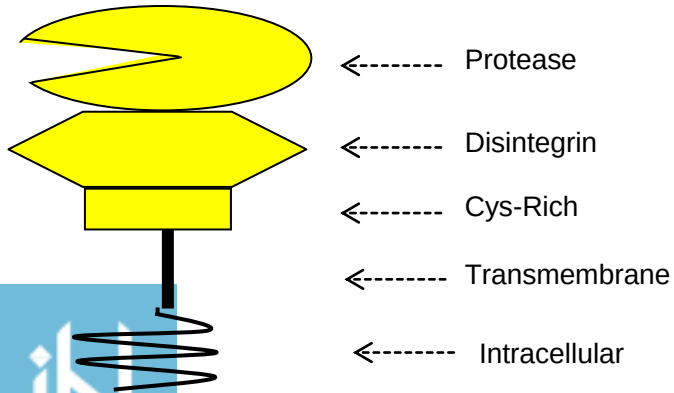

a lower affinity then the FcεRI found on mast cells and basophils and was thus named the low affinity receptor for IgE or FcεRII (reviewed in (26)). Shortly thereafter, while studying Epstein Barr Virus (EBV) transformed B cells (27) and a protein was found to be increased following transformation and was called CD23. A second group also found this same protein and called it BLAST-2, they found it was a marker of cell activation in B cells (28). Later exchange of monoclonal antibodies confirmed that all three were the same protein (29) and thus showed that CD23 was the low affinity receptor of IgE, FcεRII. Cloning of CD23 was accomplished by three independent groups (30-32). This demonstrated that CD23 was unlike other Ig receptors as it is not a member of the Ig superfamily, but requires calcium to bind IgE and is a member of the calcium-dependent (C-type) animal lectin family (33). A quite similar structure was also found for mouse CD23 (33).

B. Expression, structure and Regulation: CD23 (Shown in Figure 1a and b) is a type II transmembrane glycoprotein and has two isoforms, which result from alternative splicing and are known as CD23a and CD23b. In mice CD23a is expressed on follicular Dendritic cells (FDC) and B cells, while CD23b is found on FDC, gut epithelial cells and IL-4 activated B cells. In humans, CD23a is found only on B cells while CD23b is found on a large variety of cells, including IL-4 activated B cells, as well as monocytes, eosinophils and Langerhans (34). In addition to having different cellular distribution, CD23a and b are also proposed to have different functions as CD23a mediates endocytosis of IgE-complexes and CD23b mediates phagocytosis of IgE-complexes (35;36).

CD23 contains two important extracellular regions; the lectin head and the coiled-coiled stalk. The stalk region of CD23 contains a tropomyosin-like, periodic heptad repeat as well as a leucine zipper, allowing it to form a trimerized coiled-coiled stalk at the cell surface (37). The lectin heads have been shown to bind to the dimeric Cε3 domains of IgE in a calcium dependent manner (38) at a ratio of 2:1 lectin heads to IgE (39). CD23 has a dual affinity for IgE; a high affinity (4-10 x 10^7 M^{-1}) , which is when CD23 is held in a stabilized trimer, and it is as a trimer that CD23 has the ability to regulate the synthesis of IgE (40). CD23 when just a monomer has a much lower affinity (4-10 x 10^6 M^{-1}) (34). The leucine zipper portion of the stalk is essential for holding CD23 in a trimer and positioning the lectin heads in the correct conformation (41). CD23 is often referred to by its stability, stabilizing antibodies decrease cleavage, destabilizing antibodies increase cleavage. When CD23 is destabilized, with an anti-stalk mAb, it was found that although the lectin heads are not in close proximity the cytoplasmic tails are still held together. This suggests that CD23 is pre-associated as a trimer at the cell surface and although the trimer can be destabilized, the N-terminus domain stays associated under all conditions (40).

CD23 expression is also regulated by the addition of cytokines and its ligand. High levels of IgE correlate with increased CD23 surface levels (42), however this is not due to changes in mRNA levels or protein synthesis, but decreased cleavage (43). Cytokines however, do change CD23s synthesis, with both IL-4 and IL-13 increasing CD23 levels in the human system (44). The finding that CD23 and its ligand IgE are increased by IL-4 supports the notion that CD23 is a natural negative regulator of IgE production. In addition, LPS and CD40 signaling also increases its expression (45). In

contrast to IL-4, IFN-γ downregulates both CD23a and b on B cells while have the opposite effect on FDC (46). As will be discussed later, this trend seems to show that CD23 is potentially involved in enhancing the initial IgE response, but then negatively regulates later responses.

C. Cleavage. Shortly after its discovery CD23 was also shown to be found in the supernatants of lymphocytes and to retain its IgE binding ability (39). This soluble fraction was termed soluble CD23 (sCD23). As a membrane bound form CD23 in mice is 45 kD and in human 48 kD. After cleavage sCD23 fragments of 37 and 28 kD and 37, 33, 25 and 12 in humans and mice systems respectively are found in the extracellular space (reviewed in (34)). These fragments contain varying amounts of the stalk and thus are mostly found as monomers and have a low affinity in the ($\sim 10^{-6}$) range for IgE. Through the use of a variety of inhibitors it was shown that CD23 was cleaved primarily by a membrane-anchored metalloprotease of approximately 62 kD (47). Eventually in 2006 this protease was identified as a disintegrin and metalloprotease 10 (ADAM10) (48;49) and later confirmed by knockout studies in 2010 (50). These studies found that ADAM10 was responsible for the initially cleavage and that other soluble proteases are responsible for the further fragmentation (48). This work thus suggests that blocking ADAM10 could potentially decrease IgE synthesis.

D. Involvement in IgE regulation/asthma. Studies with CD23 knockout ($CD23^{-/-}$) mice had seeming conflicting results. The first CD23 deficient mouse was produced on a mixed background with $CD23^{-/-}$ embryonic stem cells from a 129 mouse being injected into a C57BL/6 mouse. These mice had normal immune development and were found to have no increase in antigen specific IgE after immunization with an

antigen/adjuvant (51). A second mouse created on a pure C57BL/6 background found a different phenotype as the mice had a two-fold increase in basal level of serum IgE compared to wild type (WT) (52). In addition, when the $CD23^{-/-}$ mice on a pure C57BL/6 background were subjected to a mouse asthma model they had increased eosinophilia, airway hyperresponsiveness and antigen specific IgE levels compared to WT (53). The disparity between these reports is potentially explained by the difference in mouse background because 129 mice are known to have high levels of IgE (54). Additionally, several CD23 transgenic (CD23Tg) mice have also been reported. The first report discussed their findings using two separate transgenic mice strains, where CD23 or sCD23 were overexpressed using the Thy1 promoter on T-cells. In the study with sCD23 they found that, although sCD23 levels were elevated (only relative measurements were used), IgE levels were unchanged compared to WT. This suggested that, at least in the mouse, sCD23 has no effect on IgE (55). However, this finding could be attributed to either inadequate production of sCD23 or because it was not produced in the correct environment. With mouse that had overexpression of membrane bound CD23 the authors found no decrease in basal level IgE, however a reduction in IgE levels in response to an antigen/adjuvant challenge was observed (55). A second CD23Tg mouse was also created with expression being controlled by the major histocompatibility complex (MHC) class I promoter combined with the Ig enhancer; founders were selected that maximally overexpressed CD23 on B cells. In this study, the authors found a decrease in IgE as well as IgG1, at both basal level and following antigen/adjuvant challenge, compared to WT (56). These mice also had a decrease in other atopic signs including eosinophilia and

Figure 2 – Model of CD23 regulation of IgE. This model as proposed by Hannah Gould (24). In (A) she shows potentially how sCD23 can increase IgE production. However, with increased IgE, it will bind CD23 on the cell surface preventing its cleavage and negatively regulate further IgE production. (B) Shows that with large amounts of sCD23 all the membrane IgE and CD21 on the cell surface would be cross linked and lead to increased IgE production. (C) Shows the overall model that with CD23 binding of IgE or an anti-lectin mAb, synthesis of IgE is negatively regulated, while with the cleavage of CD23 this regulation is lost.

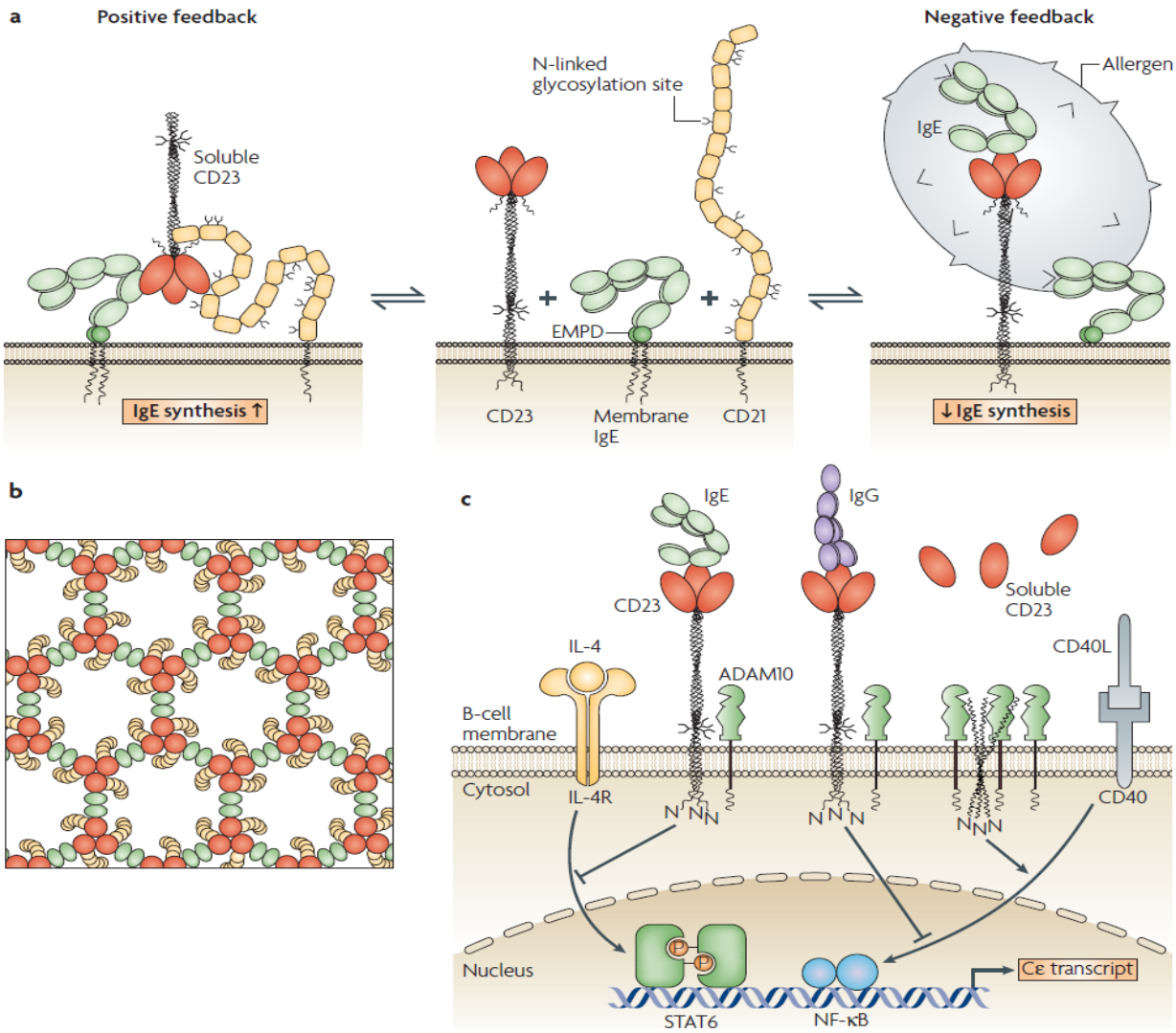

airway hyperresponsiveness following asthma induction (53). These mouse strains clearly show that CD23 regulates IgE synthesis in the context of asthma and that stabilization is a possible target for therapy. However, in a clinical trial in allergy patients who were injected with a humanized anti-CD23 (Lumiliximab), no change in allergy symptoms were seen. Lumiliximab caused only a 40% drop in serum IgE (57), which is not sufficient for clinical efficacy. But this trial did show that CD23 could be targeted to make other therapies more effective. Of note, lumiliximab is currently being tried as an add-on therapy in B cell chronic Lymphocytic Leukemia (58) and was well tolerated and in initial trials seemed to have some efficacy.

Overall a model that focuses on how CD23 controls IgE production in the human system has been proposed by Hannah Gould and is shown in Figure 2 (24). She proposes that when sCD23 is released from the cell while still a trimer it can cross-link CD21 and membrane bound IgE. This cross-linking serves as a positive feedback and leads to increased IgE production. Conversely as IgE levels increase, it will bind to membrane bound CD23, preventing its cleavage. Additionally this CD23 bound IgE can be cross-linked to membrane bound IgE by antigen and this cross-linking will then negatively regulate further production of IgE. Although this model works for findings in the human system, it is not supported by findings in the mouse system, where CD23 lacks the ability to bind CD21. Herein we suggest a different model.

E. Involvement in antigen processing and presentation: The concept that the aggregation of antibodies can increase uptake and processing of antigen has been known for over a century (59). In connection with this, if antigen bound to an antibody is injected *in vivo* there is over a 1000-fold increase in antigen specific antibody response

(reviewed in (60)). This is also true for IgE and is completely dependent on CD23 expression, as this enhancement is not seen in mice treated with anti-lectin mAbs or mice deficient in CD23 (61). Gustavsson *et al*. additionally showed that this effect is specifically caused by B cell CD23 as $CD23^{-/-}$ mice that where injected with bone marrow derived from WTs still display the enhancement (62). In addition, Getahun *et al.* have also shown that when mice are injected with IgE-antigen complexes there is also an increase in antigen specific T cell proliferation (63). In combination with studies in $CD23^{-/-}$ mice these studies demonstrate that CD23 could potentially be involved in enhancing the initial response, but later after IgE reaches a certain threshold it serves to decrease the production.

III. ADAM10

A. Discovery of ADAM10: ADAM10 (Shown in Figure 1c and d) is a member of a large family of proteases which presently includes 40 members (http://people.virginia .edu/~jw7g/Table_of_the_ ADAMs.html). These proteases are similar to MMP and ADAMTS, but differ in that ADAM family members perform their function while being membrane bound. ADAM10 was first discovered in 1996 in *Drosophila*, because of its importance in development, through mutation studies and was named *kuzbanian* (*kuz)* (64). ADAM10 was also found to be important in the mammalian system as mice deficient of ADAM10 die *in utero* at E9.5 (65). This is because of ADAM10 importance in notch signaling. ADAM10 is also involved in T cell (66) as well as MZ B cell development (50).

B. Structure: ADAM10 is a multidomain transmembrane protein containing the following domains protease, disintegrin and cysteine-rich (67). Through use of recombinant molecules missing the protease domain, the major site of substrate interaction was found to be in the disintegrin and cysteine-rich domains (25). Janes *et al.* (25) additionally found that the disintegrin domain is very similar in structure to two other proteins, disintegrins trimestatin and blood coagulation inhibitor from snake venom. The cysteine-rich domain is unique as it contains a novel α/β fold. They additionally showed that the two domains are tightly packed together and held together by disulfide bonds. The cysteine-rich domain was named because of its high concentration of cysteine amino acids and the spacing of these domains in ADAM10 was found to be similar to ADAM17, which might partially explain why these two proteases have overlapping in substrate specificities; however the spacing of the cysteines is different from all other mammalian ADAMs including 9, 12 and 15. Finally Janes *et al.* showed that the cysteine-rich domain contains a surface pocket made up of acidic resides and that when these resides are mutated, ADAM10 loses its substrate-recognition ability (25).

C. Substrates: ADAM10 has been discovered to cleave many proteins and a list can be found in a recent review (68). Some that will be mentioned later are C44 (69), L1 (70), EGF (71), CD23 (48;49) and Notch. As mentioned earlier, when ADAM10 is genetically deleted mice die *in utero* at E9.5. This is attributed to the loss of Notch signaling. Notch is the best characterized of all ADAM10 substrates. As Gibb *et al.* (50) recently reported this signaling is also important in B cell development. There have been four different Notch proteins discovered, but only Notch 1 and 2 have known biological activity. These proteins interact with their ligands, including Delta 1 and Jagged, in both

cis and trans, with cis interaction being inhibiting, while trans interaction is activating. When Notch and its ligand interact it causes a change in conformation and allows ADAM10 to interact and cleave at the S2 cleavage site. This cleavage further changes the conformation of Notch and allows γ-secretase to interact and cleave Notch at the S3 site. This cleaves the intracellular domain known as NICD, which is released and translocates to the nucleus where it acts as a transcription factor. Such genes affected include CD21 in B cells, Hes5, and Deltex-1 (reviewed in (72))

D. Exosomes: The cleavage of plasma membrane bound proteins and their subsequent release from the cell is described as ectodomain shedding. Historically, this was believed to be a cell surface process. However, recently a second mechanism was discovered, involving the release of proteins after their internalization and subsequent trafficking through the endosomal pathway to multivesicular bodies (MVB) (73). In the MVB, the proteins can interact with their sheddase and be cleaved and released or be sorted into exosomes and released as full length proteins. Exosomes are small, 30-100 nm, membrane containing vesicles that are released by a wide variety of cells. As they have high expression of major histocompatibility complexes (MHC) molecules they have been investigated as cell free transporters of cancer antigens in cancer immunotherapy treatments (74). Exosomes released from B cells have also been extensively studied. B cell derived exosomes express integrins (75), which allow them to bind to the cell surface of other cells including T cells. Also due to their expression of MHC molecules they can present antigen to T cells. They have also been shown to transport antigens, including peptides derived from allergen between APCs (reviewed in (76)). B cell exosome secretion is also increased upon activation with CD40L (77) and interaction with T cells

(78). However, the secretion of exosomes by cells and the mechanism that controls the sorting of proteins into exosomes are still poorly understood.

Initially ADAM10 dependent cleavage was believed to take place at the cell surface; however, high levels of ADAM10 are observed in the Golgi and the endosomal regions of the cell. Indeed, two ADAM10 substrates, CD44 and the adhesion molecule L1 (CD171), were recently shown to be released in from the cell in the context of exosomes (79). This indicates an alternative mechanism for ADAM10 substrate trafficking and cleavage.

E. Involvement of ADAM10 and other metalloproteases in asthma: In a pilot study in 2004, twelve atopic asthmatic subjects were injected with 5 mg of the broad spectrum inhibitor Marimastat twice daily for 3 weeks followed by a 6 week washout period (80). Marimastat was shown to decrease hyperresponsiveness as well as sputum inflammatory cells compared to placebo. In addition, using animals where MMPs have been knockout, several MMP have been shown to be involved in experimental asthma progression (reviewed in (81)). These studies highlight the role of proteolysis in asthma. Although, ADAM10 has never been studied for its ability to regulate the progression of asthma, it has been found to be highly expressed in the lungs of asthmatics (82) as well as to be increased at the mRNA level after the induction of a mid-length experimental asthma model (83). These studies thus show that ADAM10 potentially could be involved in asthma as well.

F. Regulation of ADAM10 activity: ADAM10 is first expressed as a zymogen, and its prodomain is then removed by a furin protease while in the Golgi and results in an active protein (84). After activation, ADAM10 can be regulated in a variety of ways (A)

by tissue inhibitors of metalloproteases (TIMP) including TIMP1 and TIMP3 (85). (B) ADAM10 activity is increased by the influx of calcium into the cell (modeled by the use of ionomycin). This increased activity is dependent on ADAM10's intracellular domain, since removal of this domain blocked the calcium effect (86). However, the change induced by calcium did not change the cellular distribution of ADAM10 or increase the removal of the prodomain. Calcium is thought to modify the conformation of the intracellular domain thereby increasing substrate binding and cleavage (86). (C) Activation of the ADAM10 promoter. This has already been demonstrated with retinoic acid (108). Future studies may demonstrate other agents that modify ADAM10 expression in this manner.

IV. Dissertation objectives: In two separate reports it was shown that ADAM10 is the sheddase of CD23 (48;49). In addition for many years there has a theory regarding the stability of CD23. This is based on the observation that antibodies against the stalk region increase cleavage of CD23 and IgE production (42;87), while antibodies against the lectin head region of CD23 decrease cleavage and IgE production (42). In addition, it has been shown through the use of $CD23^{-/-}$ mice, as well as the injection of anti-lectin antibodies and CD23Tg, that increased CD23 correlates with decreased signs of experimental asthma in IgE dependent models (53). The first part of this dissertation is dedicated to determining whether ADAM10 has a role in experimental allergic asthma, using a B cell specific ADAM10 knockout and the administration of ADAM10 inhibitors directly to the lung.

In addition, although CD23 is known to be cleaved by ADAM10, nothing is known about how they interact or where in the cell the interaction of ADAM10 and CD23 takes place. In the second part of this dissertation, we sought to answer this question, and determine how stability affects the interaction. In connection with this we sought to determine what signals increase ADAM10 expression. Finally in connection with our findings in mice we sought to determine the effect of ADAM10 activity on IgE production and B cell proliferation through the use of siRNA and ADAM10 selective inhibitors.

Material and methods:

I. Reagents, antibodies, mice.

FITC-rat anti-mouse CD23 (clone B3B4), an anti-lectin mAb, was obtained from BD PharMingen (San Diego, CA). Rat anti-mouse CD23 (clone 2H10) (40), an anti-CD23 lectin mAb, 19G5 (40), an anti-CD23 stalk mAb and C0H2, a rat IgG2, used as an isotype control mAb, were all purified from tissue culture supernatant as previously described (88). Monoclonal mouse IgE (mIgE-DNP) (89) from H1-DNP-ε-26 was purified from tissue culture supernatant as described previously (40). JW8 (humanized IgE anti-NIP) was purified from culture supernatant. Rabbit anti-ADAM10 was obtained from Chemicon (Billerica, MA). Rabbit anti human CD23 was created in our lab by injecting recombinant trimeric human CD23 (lz-CD23) (90) containing the extracellular region of human CD23 into rabbits. The antibodies were then purified on a Protein G sepharose (Sigma) column. Mouse *lz*-CD23 (extracellular CD23 held in a trimer by the addition of a leucine zipper motif) and fragments, and yellow fluorescent protein (YFP) tagged mouse CD23 were created as previously described (40;90). The ADAM10 hydroxamate inhibitors, INC008765 ((1R,3S,4S)-3-(hydroxycarbamoyl)-4-(4-phenylpiperidine-1-carbonyl) cyclohexyl pyrrolidine-1-carboxylate) (Figure 3a) and INC009588 (91), were synthesized by the Incyte Corporation (Wilmington, DE). These inhibitors are selective for ADAM10 as they require at least 5 fold higher concentrations to inhibit MMP12 and at least 20 fold to inhibit any other enzymes including ADAM17 (91). GI254023X ((2R,3S)-3-(Formyl-hydroxyamino)-2-(3-phenyl-1-propyl) butanoic

Figure 3: Chemical structure of inhibitors. (A) Structure of Incyte ADAM10 inhibitor (INC008765). (B) Structure of Glaxo ADAM10 inhibitor (92)

A.

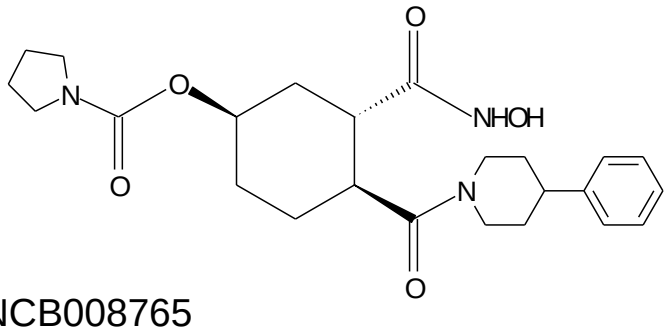

INCB008765

B.

Chiral

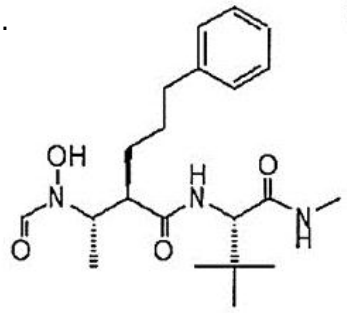

GI254023X

acid [(1S)-2,2-dimethyl-1-methylcarbamoyl-1-propyl] amide) (92) is shown in Figure 3b and was provided by Neal Broadway at GlaxoSmithKline (Stevenage SG1 2NY, UK) and will be referred to as Glaxo ADAM10 inhibitor in the paper. Both the Glaxo and Incyte inhibitors are competitive inhibitors and bind the active site of ADAM10, thus blocking its ability to cleave its substrates including CD23 (49), it is also believed at least for the Glaxo ADAM10 inhibitor that the phenyl group can also bind the S1' pocket of ADAM10. This pocket is believed to constitute a large portion of the protease's substrate recognition domain. INC000129, Incyte ADAM17 inhibitor was also used to show the inhibitors were selective for ADAM10.

HA-mADAM10-pcDNA3.1 (86) was a gift from Carl Blobel at Cornell University. HA-hADAM10-pUK-BK-C (92) was a gift from Uwe Konietzko at the University of Zurich. Dominant Negative ADAM10 lacks its Metalloproteinase domain and consists of the leader sequence and part of the prodomain linked to the disintegrin, cysteine-rich, transmembrane, and cytoplasmic domains and was produced as described (93) and inserted into p-Tracer. Rabbit anti-HA was purchased from Novus Biologicals (Littleton, CO). Goat anti-Rabbit-HRP was obtained from Southern Biotech (Birmingham, Alabama). A humanized anti-CD23 lectin (IDEC-152) (94) was a gift from Marylin Kehry at Biogen-Idec (San Diego, CA). Ez-link-sulfo-NHS-biotin (NHS-biotin) was purchased from Pierce (Rockford, IL). Anti-H2-I/Adβ (5K43) was purchased from Santa Cruz biotech (Santa Cruz, CA). Mouse IL-4 was a gift from Bill Paul (NIH). Rabbit anti-calnexin (BD) (marker of endoplasmic reticulum), goat anti-EEA1 (Santa Cruz) (marker of early endosome), Rabbit anti-Rab11 (Invitrogen) (marker of recycling endosome/MVB), and Mouse anti-LAMP1 (marker of lysosome) (University of Iowa

Hybridoma bank) were all gifts from Dr. Jason Carylon (VCU). DyLight 649-Donkey anti-Rabbit IgG and DyLight 649-Goat anti-mouse IgG were purchased from BioLegend (San Diego) and APC-Rabbit anti-Goat IgG is from BD. PE-Goat anti-rabbit IgG and FITC-Goat anti-rat IgG were also purchased from BioLegend. Recombinant mouse ADAM10 (rADAM10) was purchased from R&D Bioscience (Minneapolis, MN). Chicken Ovalbumin (OVA) and Imject Alum Adjuvant were purchased from Sigma (St. Louis, MO) and Pierce (Rockford, IL), respectively. DNP-Ova was prepared by as explained previously (95).

CD23 transgenics were described previously (56) and have been backcrossed 12 generation onto a BALB/C background. Littermates negative for the transgene were used as controls. CD19-Cre+/-ADAM10fl/fl mice on a C57BL/6 background (50) were described previously, and were also used as a source of ADAM10 deficient B cells and will be referred to as ADAM10-/- throughout this paper, littermates that were negative for Cre expression were used as WT controls. Female C57BL/6J and BALB/C mice were purchased from Jackson Laboratory (Bar Harbor, ME) and used in the inhibitor studies. Female mice ages 8-12 weeks were used in the experiments. All mouse protocols were approved by the Virginia Commonwealth University Institutional Animal Care and Use committee.

II. Mouse Asthma inductions.

Experimental asthma was induced using three different models, two IgE dependent models and one IgE/mast cell independent model. The first model (Figure 4a) was previously described (96) and was shown to be dependent on both mast cells and IgE using W/Wsh and FcεRI mice respectively and will be referred to as model A. The mice

Figure 4. Mouse asthma models. (A) Mast cell/IgE dependent model. This model is a modified model developed by the Dr. Stephen Galli laboratory of their original model published in (97) used in Figures 15-17 and is called Model A in text. Mice were injected IP with OVA on days 1, 3, 5 and 7. Then on days 22, 25 and 28 mice were challenged IN with OVA and sacrificed on day 29. (B) Mast cell/IgE independent model. This model was used in Figure 18 and 19 and is called Model C in text. Mice were injected with OVA/Alum on days 1 and 8. Then ever day from 14-10 mice were challenged by giving aerosolized OVA (1% in PBS) for 45 minutes. Then on day 21 mice were sacrificed.

A. Model A

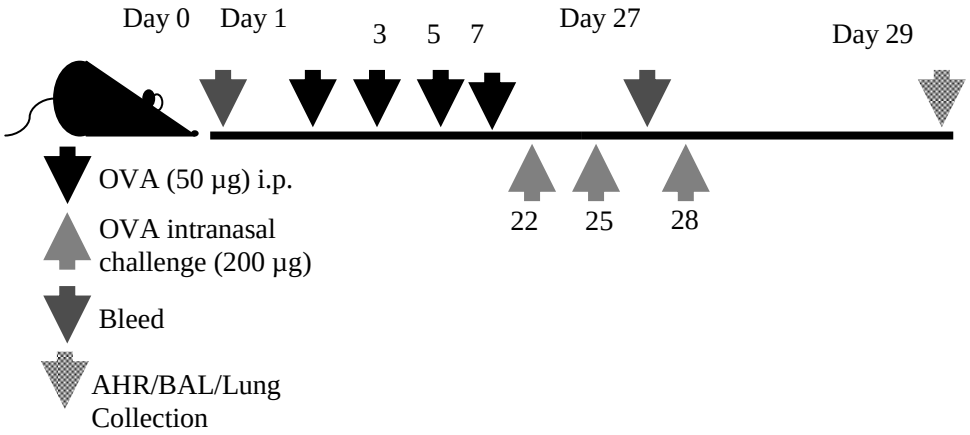

B. Model C

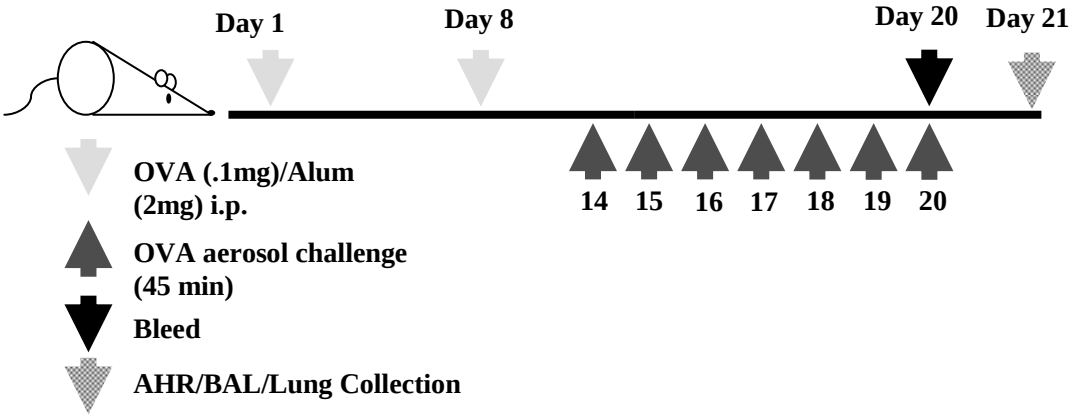

Figure 5: IgE dependent and mast cell independent mouse asthma model. This model was used in Figures 20 and 21 and will be called Model B in the text. Adopted from (98). Mice were injected IP on days 0 and 14 with OVA/Alum. Mice were then challenged with aerosolized OVA (1% in PBS) on days 19, 22 and 27. Mice were then sacrificed on day 29.

Model B

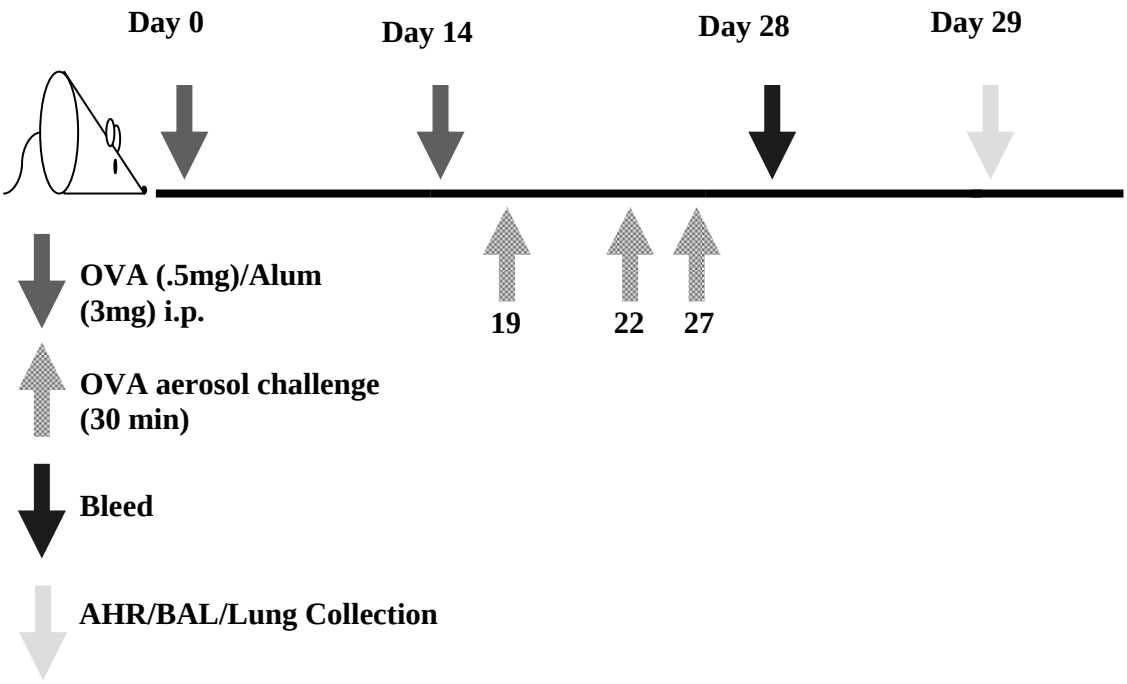

were initially bleed on day 0 to determine baseline IgE levels, mice were sensitized by the intraperitoneal injection of 50 µg of OVA in 100 µl of (0.15 M) saline on days 1,3,5 and 9. Then 15 days later the mice were challenged intranasally with 200 µg of OVA in 20 µl of PBS and again on day 25 and 28 (Shown in Figure 4a). Finally 18 hours after the final OVA challenge, airway resistance was measured using the Flexivent system (Scireq, Montreal, Canada). Briefly, mice were anesthetized by intraperitoneal (IP) injection of 206.7 mg/kg of ketamine (Bulter Schein, Middletown, PA) and 41.7 mg/kg of xylazine. Tracheotomy was performed by inserting a 20 gauge blunt end cannula (Ellsworth Adhesives, Germantown, WI) into the trachea and tied to ensure there were no leaks. Following cannulation, mice were paralyzed with an intraperitoneal injection of 0.5 mg decamethonium bromide (Sigma). Mice were ventilated with a Flexivent small animal ventilator at a frequency of 2 breaths per second and a tidal volume of 2×10^{-7} m^3 and positive end-expiratory pressure of 3 cm H_2O. Measurements were started once breathing was completely by mechanical ventilation. Following measurement of baseline lung function, mice were exposed to a PBS aerosol followed by aerosols containing increased doses (10, 25, 50 mg/ml) of Acetyl-β-methylcholine chloride (Methacholine) (Sigma) when C57/B6 mice were used or (2.5, 5, 10 mg/ml) when BALB/C mice were used. Aerosols were generated by the means of an ultrasonic nebulizer and were delivered to the inspiratory line of the Flexivent. Each aerosol was delivered for 10 sec and measurements were made over 3 minute intervals following each aerosol. The total lung airway resistance was recorded as the maximum resistance after each methacholine exposure. Additionally Newtonian resistance (Rn), tissue damping (G) and tissue elastance (H) were all measured at a dose of baseline (PBS) and 50 mg/ml of

methacholine by averaging the three highest values at each point and is expressed as the change from baseline for each value.

Following the Flexivent analysis, bronchoalveolar lavage fluid (BALF) was collected by lavaging the lungs with 1 ml PBS (1% BSA in PBS) using the same cannula associated with the Flexivent. The BALF was centrifuged and supernatant fluids were saved for further analysis. Pelleted cells were resuspended in 100 µl PBS, counted, cytospun onto slides and stained with Diff-Quik (Siemens Healthcare Diagnostics, Deerfield, IL). Percentages were determined by counting of at least 100 leukocyte cells per cytospin.

In addition, cardiac puncture was performed to collect serum for total IgE, OVA-specific IgE and OVA-specific IgG1 measurements. The heart was then perfused with 10 ml of PBS to flush the lungs of blood. The right lope of the lungs was removed for mRNA analysis. Finally the rest of the lungs and heart were removed and fixed in 10% formalin (Fisher) and stored at 4°C until paraffin sections were prepared by the Anatomic pathology research service at VCU. 5 µm sections were then prepared and stained with hemotoxin and eosin (H&E). A Nikon eclipse with a SPOT Flex Shifting Pixel Color Mosaic (Diagnostic Instrumental inc., Sterling Heights, MI) camera was used to take pictures of the sections.

Experimental asthma was also induced using a second IgE dependent model (Figure 5), which also has been previously described (99), and work independent of mast cells (as when induced in W/Wsh there was no reduction in eosinophils (work performed by Dr. Jill Ford, shown in Figure 14)) and will be referred to as model B. In this model the mice are initially bled and serum collected to establish baseline IgE levels. Then on

day 0 and 14 mice were injected with 500 µg of OVA emulsified in 3 mg Alum. Alum has been shown to make mouse experimental asthma models mast cell independent (96). Mice were then challenged on days 19, 22, and 27 for 30 minutes with aerosolized 1% OVA in PBS using an ultrasonic nebulizer (Medline Industries, Munderlein, IL). Finally on day 29, Airway hyperresponsiveness (AHR) was assessed and BALF and lungs were collected as described above.

Finally experimental asthma was induced in the mice using an IgE/mast cell independent model, Figure 4b and referred to as model C. This model was developed by the VCU pulmonary medicine division and its independence of IgE and mast cells were shown using $IgE^{-/-}$ and W/Wsh mice (work performed by Dr. Jill Ford, shown in Figure 14). Mice again were bled on day 0 and baseline IgE was determined. The mice were then sensitized by the injection of 100 µg of OVA emulsified in 2 mg Alum on days 1 and 8. Mice were then challenged for 45 minutes with 1% OVA aerosolized in PBS using the same ultrasonic nebulizer described above on days 14 – 20. On day 21, AHR was assessed and BALF and lungs were collected as described above.

III. *In vivo* ADAM10 inhibitor asthma studies

As a follow up to the studies with CD23Tg and $ADAM10^{-/-}$ studies, we also used two hydroxamate inhibitors that are very selective for ADAM10 (see discussion under reagents). The inhibitors have limited solubility in water and thus were dissolved in DMSO, at a stock concentration of 20 mg/ml. This mixture was then diluted 1:20 in PBS and 20 µg inhibitor was delivered intranasally, every three days (Figure 6 and 7), using both the IgE/mast cell dependent and IgE/mast cell independent models. Then similar parameters were assessed as explained above.

Figure 6: Inhibitor dosing IgE dependent model. Model used in Figures 22-23 to show that ADAM10 inhibitors could also block induction of asthma, similar to ADAM10$^{-/-}$. Mice were injected IP with OVA alone on days 1, 3, 5, 7, 9, 11 and 13. Then on days 40, 43 and 46 mice were challenged with OVA IN. To inhibit ADAM10 inhibitors were given every three days IN starting on day 1 throughout the entire experiment.

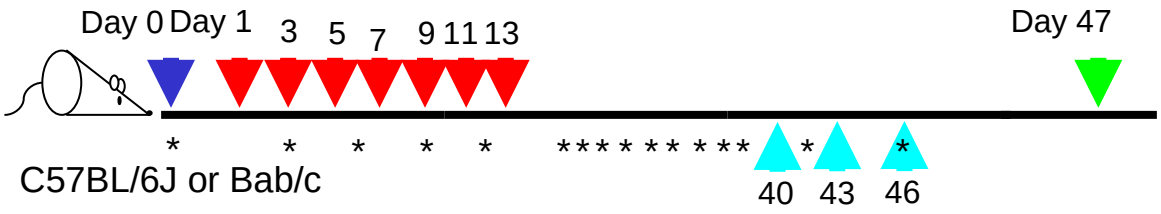

* ADAM10 inhibitor (20 µg)

OVA (10 µg) i.p.

OVA intranasal challenge (20 µg)

Bleed

AHR/BAL/blood/Lung Collection

Figure 7: Inhibitor dosing IgE independent model. Model as explained in Figure 4b used to determine, if inhibiting ADAM10 activity had any effect on IgE independent asthma induction. ADAM10 was inhibited by administering inhibitors of ADAM10 everyday starting on day 1 throughout the entire experiment.

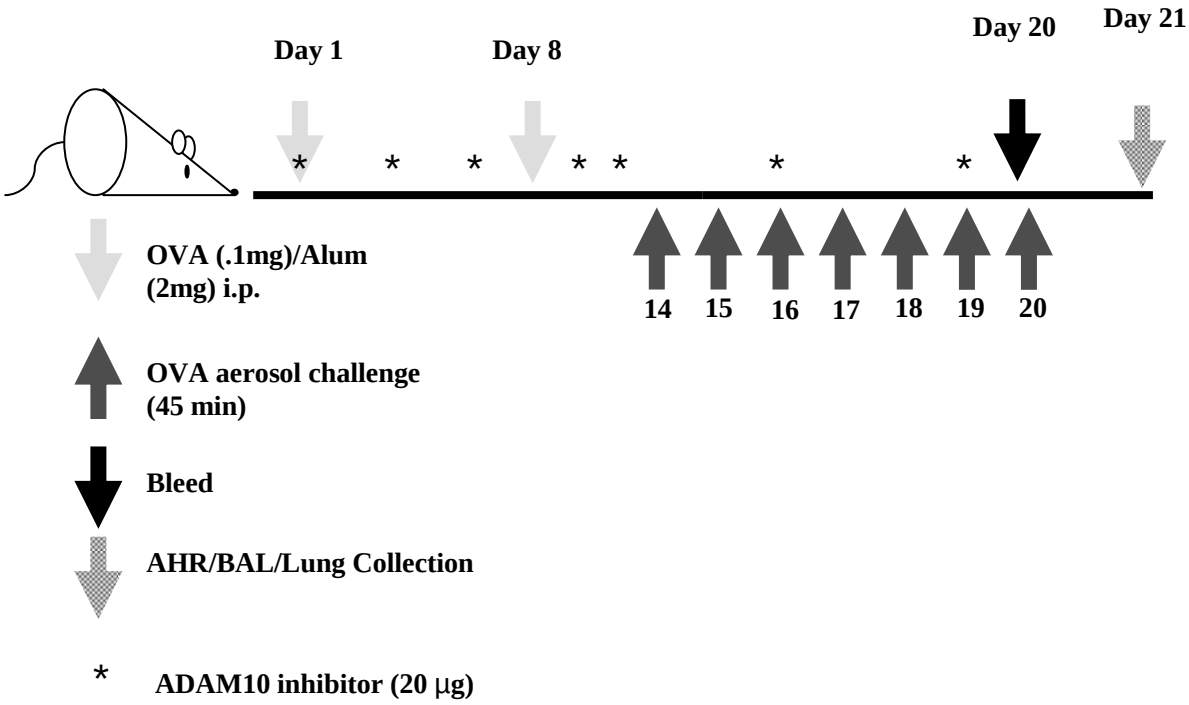

IV. ELISAs/multiplex

Total mouse IgE was measured as previously described (15). For OVA specific IgE, R1E4 (rat anti-mouse IgE) was used as the capture antibody and OVA-DNP-Biotin in combination with Streptavidin-alkaline phosphatase (AP) was used for detection. Mouse IgE anti-DNP was used as a standard. For OVA-specific IgG1, OVA was used to capture the antibody. Samples and standard (serum from a mouse hyper immunized with OVA was used as an internal control) were detected with an AP-goat anti mouse IgG1. Cytokines in the BALF were measured using multiplex kits from Biorad (Hercules, CA) according to the manufacturer's instructions. The liver enzymes aspartate aminotransferase (AST) and alanine aminotransferase (ALT) were measured as previously described (100).

V. qRT-PCR/RT-PCR

Total RNA was extracted from disrupted lung tissue and purified as explained previously (50). Real time quantitative PCR (qRT-PCR) was performed using the SsoFast EvaGreen Supermix (Bio-rad) and the MyQ2 (BioRad). For analysis the following primers were used: GATA3, sense 5' ACCACGGGAGCCAGGTATG-3', antisense 5' CGGAGGGTAAACGGACAGAG–3'(101); T bet - sense 5' TCCCATTCCT GTCCTTCA-3', antisense 5' GCTGCCTTCTGCCTTTC-3'(101); IL-25 sense 5'- GGCATTTCTACTCAGGAACGGA -3', antisense 5'-GGTGGAGAA AGTGCCTGT GC-3' (102); and IL-33 sense 5'-CAGGCCTTCTTCGTCCTTCAC-3' antisense 5'- TCT CCTCCACTAGAGCCAG CTG-3' (102). PCR products were amplified according to manufacture instructions with 18S as an internal control and analyzed with iQ5 real time PCR software (version 2.0). Human ADAM10 levels were

determined using the Taqman system using primers and probes purchased from Applied bioscience (Carlsbad, CA) (Hs02935708_cn), and 18S was again used as an internal control. For RT-PCR human ADAM10 (sense – CATTACACCAAAAACACCA GCGTG, anti-sense – TCCACAC CAAATTTGGGAAACGG) and G3PDH (Ready-made primers®) were purchased from Integrated DNA Technologies (Coralville, IA). PCR was run using AccessQuick™ RT-PCR system (Promega Madison, WI).

VI. Cell culture.

293T cells were a gift from Dan McVicar (National Cancer Institute (Frederick, MD)), and were grown in complete DMEM (10% FBS (Gemini), 100 U/ml penicillin and streptomycin, and 2 mM L-glutamine (all from HyClone, Logan, UT). They were transiently transfected using Fugene 6 with mouse a plasmid under the CMV promoter expressing CD23-YFP (40) to study the effects of CD23 stability on internalization and localization. The 293 variant (293-F) was purchased from Invitrogen (Carlsbad, CA) and grown and transiently transfected with mouse ADAM10-HA contained in pCDNA3.1 according to the manufacturer's protocol. Mouse $CD23^{+}$-CHO ($mCD23^{+}$-CHO) cells, were previously described and grown in DMEM-GS (90) and were used to examine internalization of mouse CD23 as well as exosome formation. RPMI 8866 cells were maintained as described (49). Mouse B cells were isolated by sorting with anti-B220 and stimulated with 10 µg/ml LPS (sigma) and 25 ng/ml IL-4. ADAM10 null Mouse Embryonic Fibroblast (MEF) were a gift from Carl Blobel (Cornell University) (49). These cells were previously selected for stable expression of mouse CD23 with blasticidin ($ADAM10^{-/-}$ require 3 µg/ml, $ADAM10^{+/-}$ 5 µg/ml).

VII. Fluorescence Imaging

mCD23^{+}-CHO cells were plated at a concentration of 2 x 10^{5} cells/ml on glass cover slips previously coated with 0.1 mg/ml poly Lysine (sigma) and allowed to bind. FITC-B3B4 was then added at 4°C and after 30 minutes internalization was initiated by transferring the cells to 37°C for the time indicated. Cells were then fixed with FCM fixation buffer (Santa Cruz Biotechnology) and adhered to microscope slides using Prolong Gold Antifade Reagent (Invitrogen). Imaging was performed under oil immersion at 100X on a Zeiss AxioObserver.Z1 with an integrated MRm Camera and analyzed with Axiovision 4.63 software (Carl Zeiss, Inc. Thornwood, NY). 293T transiently transfected with mouse CD23-YFP were also plated on poly Lysine coated coverslips. After 24 hr the following antibodies were added 19G5 (destabilizing), 2H10 (anti-lectin, stabilizing), IgE, or IgG control and after additional 24 hr incubation, cells were then fixed and imaged and the percentage of cells with internalization was determined by looking at orthogonal views. In addition some cells were also stained with antibodies against specific intracellular compartments, with antibodies against the following antigens: EEA-1 for early endosomes (103), LAMP-1 (104) for lysosomes, Rab11 (105) for recycling endsomes/MVB and calnexin for ER (106). The percentage of cells with co-localization was determined, with a cell being counted as positive if any co-localization in the cell was determined.

VIII. Mouse sCD23 Release Studies

mCD23^{+}-CHO were plated at 1 x 10^{6}/ml in six well plates and allowed to adhere. After incubation for 30 minutes with 10 mM NH_4Cl the cells were incubated with either

Figure 8: Recombinant mutant CD23 fragments used in binding studies. Adapted from (41), used to determine the region of CD23 important for interaction with ADAM10.

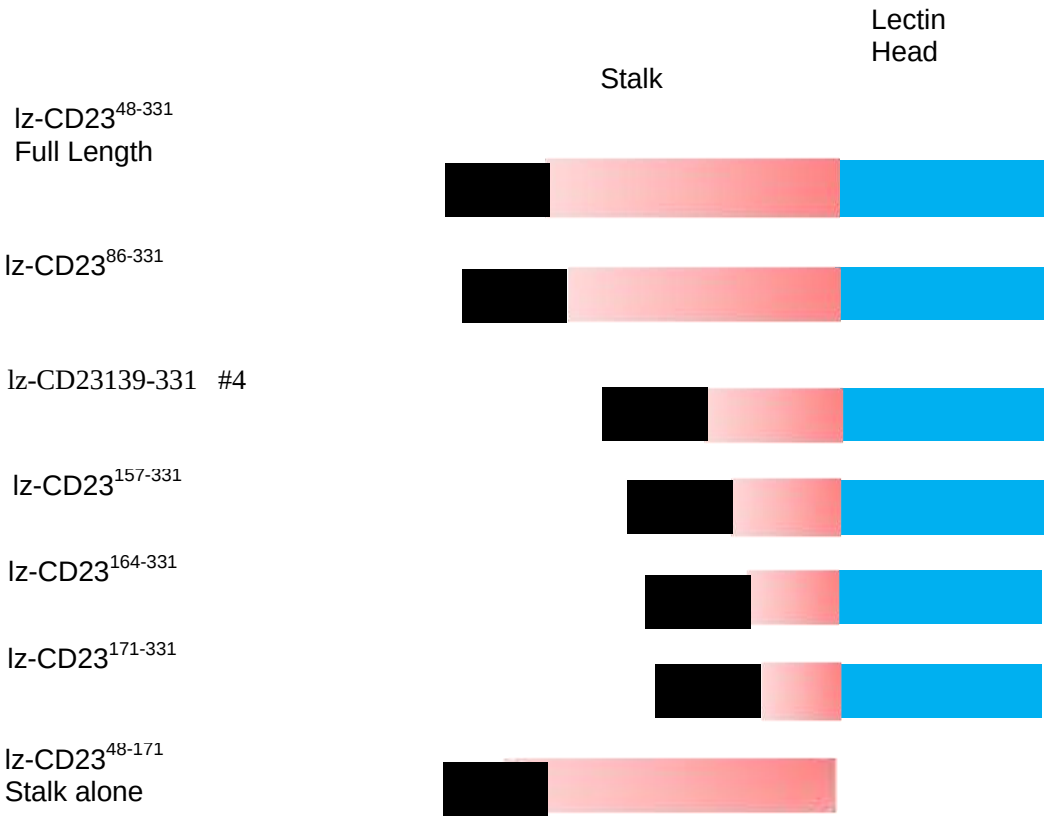

Figure 9: Conformation of 293-F transfection with ADAM10-HA. As a source for ADAM10 protein, 293-F were transfected with PCDNA3.1-ADAM10-HA and expression was confirmed by (A) western blot (anti-HA) and (B) FACS.

A.

B.

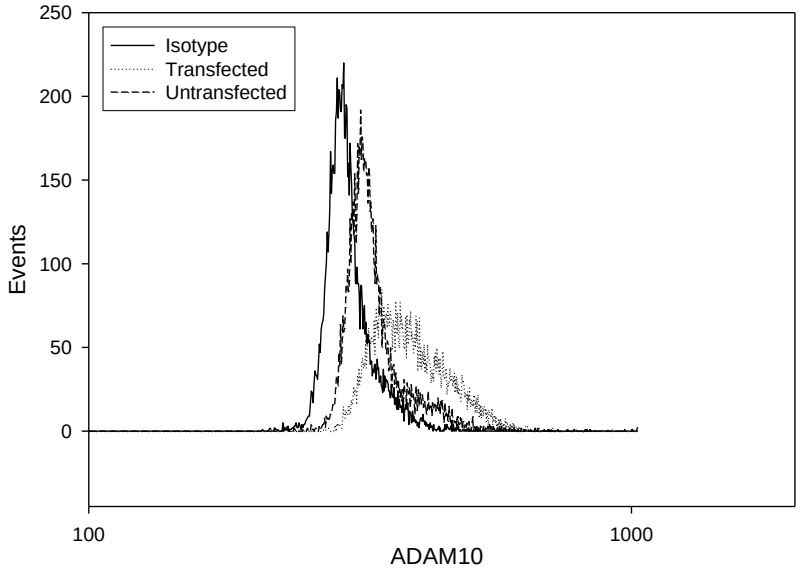

19G5 or IgE for 8 hrs. sCD23 in the supernatants was determined by ELISA (40) with 2H10 (rat anti-mouse CD23 antibody) as the coating antibody and rabbit anti-mouse CD23 for detections. EC-mCD23 (recombinant extracellular mouse CD23) was prepared in our laboratory and used as a standard.

IX. Dot/Western Blots

lz-mCD23 (showed in Figure 8 (41)) starting at 20 µg/200 µl of PBS was serially diluted 1:2 across a Hybrid-Dot Manifold (Life Technologies, Gaithersburg, MD) containing nitrocellulose (Pall Corporation, Pensacola, FL) and excess liquid was removed by applying vacuum. The nitrocellulose containing CD23 was then removed from the apparatus and blocked in 5% milk in 1X HBS and 0.05% Tween-20. Some blots were then incubated with 19G5, IgE or nothing. Following washing, cell lysate from 293-F cells that had been transiently transfected with HA-ADAM10 (transfection was confirmed by Flow Cytometry and western blot (Figure 9)) expression vector two days previously were added and blots were incubated over night at 4°C. ADAM10 binding was then detected using a rabbit anti-ADAM10 and a HRP-goat anti-Rabbit. For mouse and human CD23 dot and western blots, CD23 was detected with either a rabbit anti-human or rabbit anti-mouse CD23 followed by a HRP-goat anti-Rabbit. For ADAM10 and MHC class II blots, the respective proteins were detected using Rabbit anti-ADAM10 and Anti-H2-I/Adβ followed by their respective HRP conjugated secondary antibodies.

X. Immunoprecipitation/Biotinylation

Human CD23 contained in supernatant or exosomes was precipitated with either IDEC-152 in combination with Protein A/G or avidin-agarose and analyzed by western

blot. For biotinylation experiments, RPMI 8866 cell surface proteins were biotinylated as described by the manufacturer (Pierce). Briefly cells were suspended in 1X Hepes Buffered Saline (HBS) containing 50 µg/ml NHS-biotin for 30 minutes at 4°C and then washed three times in 1X Tris Buffered Saline (TBS) to remove unbound biotin. Cells were then grown for 24 hours and exosomes were isolated as described below. Exosomes were lysed for 10 minutes on ice in 1X HBS containing 0.5% NP-40 and a complete protease inhibitor cocktail tablet (Roche). Biotinylated proteins were then isolated with avidin-agarose and analyzed for CD23 by western blot. For mouse CD23 precipitation, 2H10-affi-gel (BioRad) was used, 2H10 was coupled to Affi-gel according to manufacturer's instructions.

XI. Isolation of Exosomes

Exosomes were isolated as previously described (79). The cell sources included RPMI 8866 or mCD23^{+}-CHO cultured overnight or primary mouse B cells cultured for 3 days with IL-4 and LPS. Briefly cells were pelleted by spinning them at 350 x g for 5 minutes and supernatants were harvested. To remove any possible apoptotic bodies the supernatants were spun at 27,000 x g for 20 minutes. Finally exosomes were harvested by spinning at 1 x 10^5 x g for 1 hour; the exosome pellet was resuspended in 5 mls of PBS and pelleted again using ultracentrifugation. Some samples were then suspended in HBS and layered over a discontinuous sucrose gradient using the following concentrations 2, 1.3, 1.16, 0.8, 0.5 and 0.25 M sucrose in HBS at 1 x 10^5 x g for 17 hours. 1 ml fractions were then removed starting at the top and diluted in 4 mls of HBS. Fractions were then by spun at 1 x 10^5 x g for 1 hour to pellet vesicles. Pelleted exosomes were then suspended in equal volume of PBS with SDS and reducing agent and

boiled; the presence of CD23 and ADAM10 were then detected via western blot as described above.

XII. Surface Plasmon Resonance (SPR)

The association of mouse CD23 with rADAM10 was measured by SPR using a Biacore T100 optical biosensor (GE Healthcare, Uppsala, Sweden). Lane one of a CM5 sensor chip (Series S CM5; GE Healthcare) was activated, then blocked with ethanolamine; in the second lane, rADAM10 (10 µg/ml diluted in 0.01M acetate, pH 4.5) was immobilized to an equivalent of 1500 resonance units (RU) and then blocked with ethanolamine. Recombinant *lz*-CD23 (amino acids, 139-331 (90) (Figure 8)) at a flow rate of 30 µl/min was passed over the wells at a concentration of 5-100 µg/ml diluted in either (10 mM Hepes buffered saline, ph 7.4 containing 2 mM CaCl, 1 µl/(100 µl buffer) DMSO (we found it lower the background binding) and 0.05% (v/v) surfactant-P20 or 50 mM MES buffered saline, ph 5.8 containing 2 mM CaCl, 1 µl/(100 µl buffer) DMSO and 0.05% (v/v) surfactant-P20) and binding was recorded. The response from the control lane was subtracted and affinity and Rmax was determined using the biacore evaluation software v1.1 using steady state analysis as well as conformation change analysis. To determine the amount of recombinant CD23 that renatured correctly, binding to IgE-affi-gel was determined as described previously (41) The purified recombinant *lz*-CD23 protein concentration was adjusted by this percentage. Finally to confirm conformation change of the proteins a linked reaction test was run, as explained previously (107). Briefly the same concentration of *lz*-CD23 (50 mg/ml) dissolved in the ph 5.8 buffer was flowed (10 µl/min) over the top of rADAM10 bound chip for different periods of time (175, 500, 750, 1000, 1500 seconds) the off rates of the curves were then compared.

XIII. *in vivo* exosome studies

1 mg of 19G5 (rat IgG2a anti mouse CD23 stalk) or isotype control were injected i.p. into BALB/C mice on days 1 and 3 as previously explained by (87). Then on day 5 mice were cardiac punctured and exosomes were isolated as explained above. In addition in the exosome free fraction, CD23 was immunoprecipitated as explained above and the location of CD23 was determined by western blot.

XIV. Promoter Studies

We received the human ADAM10 promoter construct in pGL3 as a gift from Dr. Claudia Prizen (Institut fur Biochemie, Mainz, Germany) (108) (Figure 10). In initial experiments, RPMI 8866 cells were transfected with both the ADAM10 promoter plasmid plus 10 μg of pGL4.75 (Promega, Madison, WI) which contains the Renilla luciferase gene under the control of the CMV promoter using the Amaxa Nucleofactor I Solution V program X05 (Walkersville, MD). 24 hours later promoter activity was measured at baseline and with the addition of cytokines in a 96 well format using the Topcount Plate Counter (Perkin Elmer, Waltham, MA) using dual-glo (Promega). The following cytokines and or antibodies were tested for their effect on ADAM10 promoter activity; IL-4 (10 ng/ml), IL-13 (10 ng/ml), IL-21 (25 ng/ml), and anti-CD40 (1 μg/ml). The Bay inhibitor (Bay 11-7082) was a kind gift from Dr. Steven Grant (VCU). It specifically inhibits IκB phosphorylation and was used at a concentration of 1 μM.

XV. Creation of stable cell line

To create a stable cell line expressing the ADAM10 promoter controlling the firefly luciferase gene, the ADAM10 promoter and luciferase gene contained in pGL3 were moved to pCDNA3, a vector that contains a neomycin cassette. PGL3 was digested

Figure 10: Plasmids used in promoter studies. (A) Original plasmid used in ADAM10 promoter studies. (B) Plasmid used to create stably expressing cell lines for promoter studies. The plasmid was created by moving the ADAM10 promoter and Luciferase gene from pGL3 to pCDNA3 as explained in the material and methods. It was then (C) linearized and RPMI 8866 cells were transfected and stably expression was selected for with G418.

A.

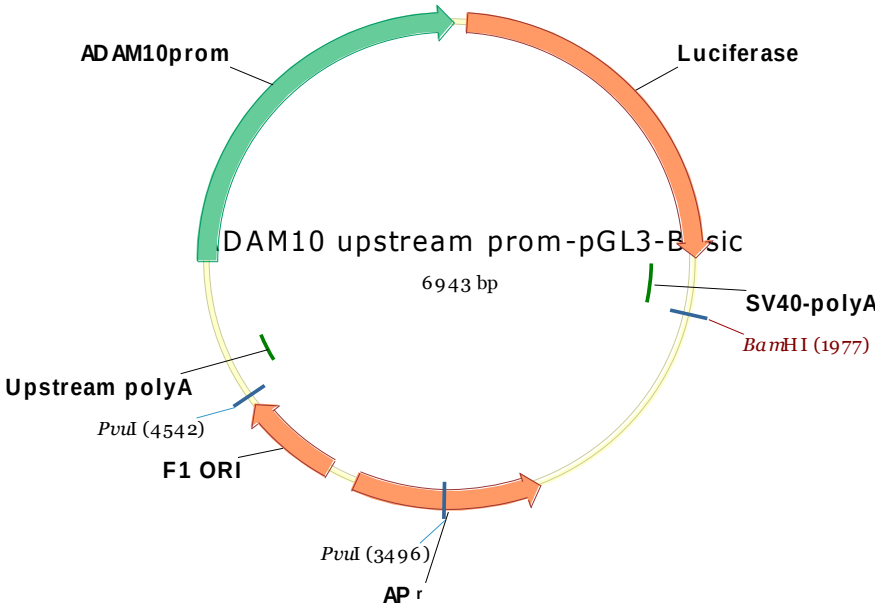

B.

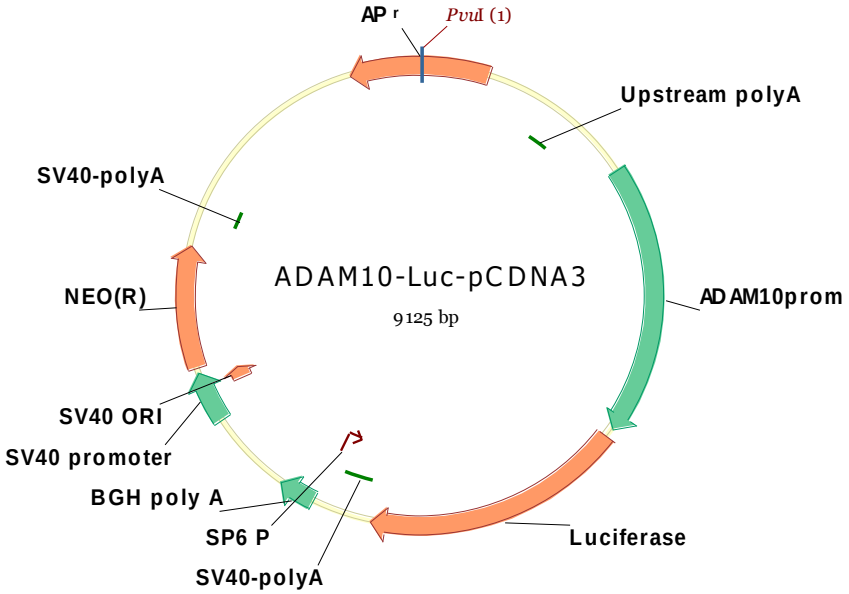

C.

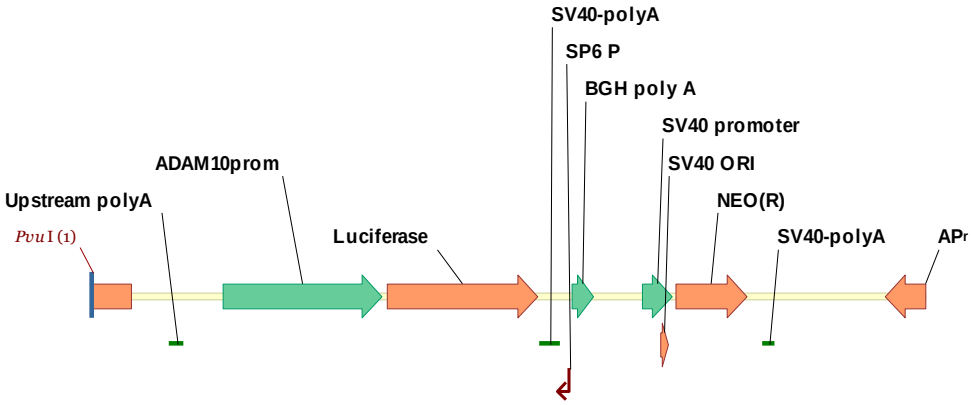

ADAM10-Luc-pCDNA3
9125 bp

with Pvu1 and BamH1 and pCDNA3 was digested with Nru1 and BamH1. The fragments were then separated on a 1% TAE agarose gel and the correct size fragments isolated using a geneclean kit (MP Biomedicals, Solon, OH) and ligated using T4 ligase (New England Bio) (shown in Figure 10). INVaF' chemically competent E. coli were then transformed with the this plasmid and grown up for isolation of the plasmid (correct ligation was tested for by sequencing). Pre-testing RPMI 8866 indentified sensitivity at 400 μg/ml G418 and Jijoye required 700 μg/ml. RPMI 8866 were then transfected with linearized (Figure 10) ADAM10-luc-pCDNA3 and after 24 hours selection for stable lines was begun by adding G418. Three days later cells were plated at 1 cell per well in 96 well plates to select individual clones. The clones were then further tested for luciferase expression using Steady-glo (Promega). The results for two lines are shown in Figure 42. The luciferase activity in subsequent studies was normalized to total protein as measured using Bradford assay, and all data shown was generated using this cell line.

XVI. FACS analysis

It was necessary to determine if the 293-F cells used in the interaction studies above were indeed overexpressing ADAM10. 24 hours after transfection 1 x 10^5 cells were stained with FITC anti-mouse ADAM10 (R&D) and expression was determined using a Coulter FC500 Flow Cytometer and the data was analyzed using the CXP software (Beckman Coulter Fullerton, CA) and compared to untransfected cells.

To test if cytokines as well as activation had an effect on ADAM10 protein levels, flow cytometry was used. 1 x 10^5 RPMI 8866 in 100 μl were blocked with Fc block (Miltenyi, Bergisch Gladbach, Germany) for 15 minutes and then stained with FITC-anti-human ADAM10 (R&D) for 30 minutes at 4°C, and then washed. The cells were then examined

as explained above. Before testing RPMI 8866 were activated with 1 μg/ml of anti-CD40,10 ng/ml IL-4, 25 ng/ml IL-21 or media alone for 24 hours and then tested for ADAM10 levels.

For carboxyfluorescein diacetate succinimidyl ester (CFSE) (molecular probes, Eugene, OR), 5 x 10^6 primary human tonsillar B cells were stained according to manufacturer's recommendations and then one aliquot was analyzed to establish a baseline while the others were cultured with anti-CD40 (1 μg/ml), IL-4 (10 ng/ml) and IL-21 (200 ng/ml) as explained previously (109). After 5 days in culture, cells were then harvested and analyzed using a BD Canto and analyzed using FCS express software V3.

XVII. *in vitro* ADAM10 inhibitor studies

Primary B cells were isolated and stimulated as previously described (15). Briefly, tonsils were obtained by routine tonsillectomies and obtained through the Tissue and Data Acquisition and Analysis Core here at VCU. The tonsils were then disrupted using a Seward Stomacher 80 Biomaster Lab Blender (Brinkmann, Westbury, NY) and a single cell suspension was obtained. Cells were then positive selected using anti-IgD in combination with magnetic beads (Miltenyi). B cells were then plated at 12,500 cells/well in 200 μl of CRPMI (RPMI 1640 containing 10% FBS (Gemini), 100 U/ml penicillin and streptomycin, 1 mM Sodium pyruvate, 10 mM HEPES, 100 mM non-essential amino acids and 2 mM L-glutamine (all from HyClone, Logan, UT) as well as 50 μM 2-mercaptoethanol (Invitrogen, Carlsbad, CA)) plus 10 ng/ml IL-4 (R&D), 1 μg/ml anti-CD40 and 200 ng/ml IL21 and grown at 37°C and 6% CO_2. To determine, the role of ADAM10 in immunoglobulin synthesis, cultures were also treated with either the ADAM10 inhibitor from Glaxo (1.25 μM) or Incyte (INC008765) (10 μM), or with the

carrier (DMSO) as a control. For sCD23, supernatants were isolated after 5 days and for immunoglobulin after 14 days and levels were determined by ELISA as explained below. To determine if the decreased IgE production by the addition of the ADAM10 inhibitor was because of decreased sCD23 it was added back at 2 µg/ml (sCD23 was purified from RPMI 8866 cultures supernatants using IDEC-152 coupled to affi-gel 10 in the presence of 2 µM calcium. sCD23 was then released by the addition of 10 mM EDTA, the concentration was then determined by ELISA and frozen in the -70°C until used). In addition to primary tonsillar B cell cultured, ADAM10 inhibitors were also added to PBMC cultures. PBMC were obtained by from whole blood by Ficoll (BD) density gradient centrifugation and cultured at 300,000 cells/well in CRPMI containing IL-4, IL-21 and anti-CD40 as explained above. All studies were performed in accordance with the Virginia Commonwealth University Institution Review Board.

XVIII. Human Elisa/Elispot

Human IgE, total IgG and total IgM as well as sCD23 were described previously (109).

Human IgE elispots were performed following the basic outline explained in (110) that was adapted to use for IgE. Briefly, tonsillar B cells were isolated and plated (12,000 cells/well) as explained above. Then on day 8 cells were isolated and washed and replated in complete RPMI containing IL-4, IL-21 and anti-CD40 in MultiScreen Filter plates (Millipore, Billerica, MA) pre-coated with mouse anti-human IgE (4.15) (5 µg/ml). Twenty hours later plates were washed and IgE was detected using biotinulated-mouse anti-human IgE (Southern Biotech (clone B3102E8) (1:25,000).

XIX. Proliferation

To determine ADAM10 inhibition effect on proliferation, primary B cells, isolated as explained above, were plated at 100,000 cells per well in 200 µl of CRPMI containing IL-4, IL-21 and anti-CD40. After 96 hours of growth, cells were pulsed with 1 µCi/well of [H^3]-thymidine (Perkin Elmer) for 24 hrs. Thymidine incorporation was then determined by harvesting the plates using a filtermate cell harvester onto GFC plates. Plates were then dried for at least two hours. 25 µl of scintillation fluid was then added and counts were determined using the Topcount Plate Counter (Perkin Elmer, Waltham, MA).

For the siRNA studies, RPMI 8866 were plated at 50,000 cells/well after sorting and immediately pulsed with 1 µCi/well of [H^3]-thymidine for 24 hrs. Plates were then harvested and read as explained above.

XX. ADAM10 siRNA

ADAM10 involvement in proliferation of B cells was tested by transfecting RPMI with a GFP expressing plasmid and pSuper (Oligoengine, Seattle, WA) (a gift from Dr. Carl Blobel at Cornell University (Figure 11)) expressing siRNA for human ADAM10 (sequence GACATTTCAACCTACGAATttcaagagaATTCGTAGGTTGAAATGTC) using the Amaxa kit explained above, the lower case letters are the 9 non-complementary spacer. 24 hours later the cells were sorted for GFP expression using the MoFlo cell sorter (Beckman Coulter) and replated as explained under proliferation. Knockdown of ADAM10 was also examined by RT-PCR as explained above.

XXI. Creation of stable siRNA expressing line

To create a stable knockdown cell line of ADAM10, siRNA for human ADAM10 was moved from pSuper to pSuperior (Oligioengine) as pSuperior contains a Neo cassette

and its expression is run under a tetO system. The tet is expressed by pCDNA6/TR and is turned on by the addition of doxycycline (plasmids shown in Figure 12). The siRNA portion of pSuper was moved by amplifying it via PCR and ligated into pCR2.1 using TA cloning kit (Invitrogen) and finally cloned into pSuperior. Stable expression of pCDNA6/TR is selected for with the addition of blasticidin (Invitrogen) and RPMI 8866 were found to die at 4 μg/ml or more. pCDNA6/TR was first linearized and then transfected into RPMI 8866 cells. After selection siRNA-ADAM10 pSuperior was linearized and transfected into the pCDNA6/TR RPMI 8866 cells and selected for with G418. siRNA was then induced by the addition of doxycycline.

XXII. Statistical analysis

All statistics were done using the student two-tailed T-test. When multiple comparisons were performed Bonferroni correction was also used. All error bars represent standard deviation or standard error (indicated in the Figure legend). Lines in graphs show groups that were compared.

Figure 11: pBasic with ADAM10 siRNA. Plasmid co-transfected, with GFP expressing plasmid, into RPMI 8866. RPMI 8866 were transfected to study ADAM10 role in B cell proliferation.

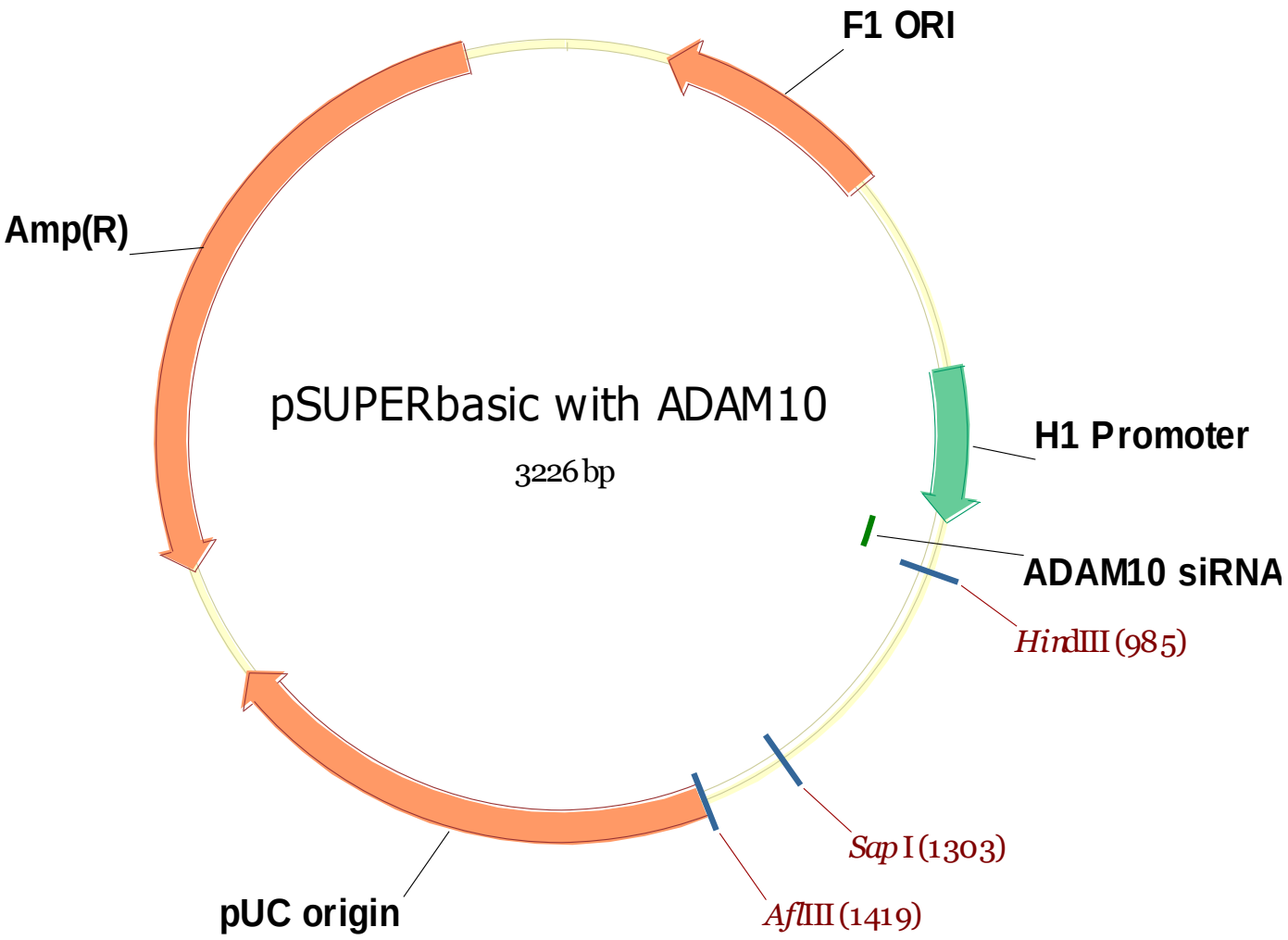

Figure 12: Plasmids used to make stable expressing ADAM10 siRNA. siRNA was moved from pSuper shown in Figure 12 to pSuperior by PCR as explained in the material and methods. RPMI 8866 were then transfected first with plasmid in (A). Cells were then selected for resistance to blasticidin. After selection of a single colony, these cells were transfected with the linearized plasmid shown in (B) and selected for G418 resistance.

A.

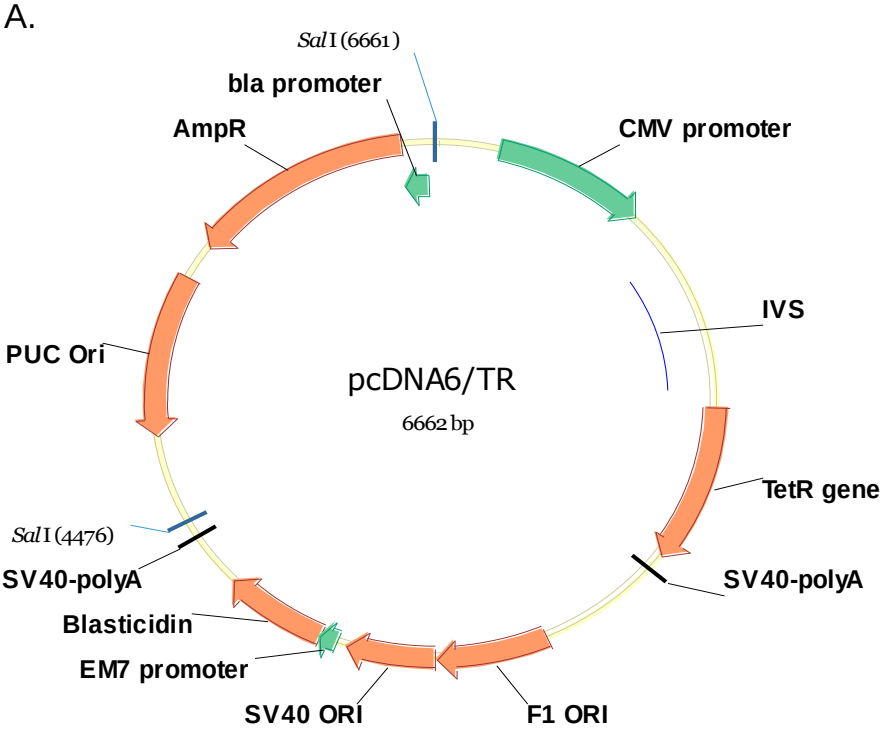

B.

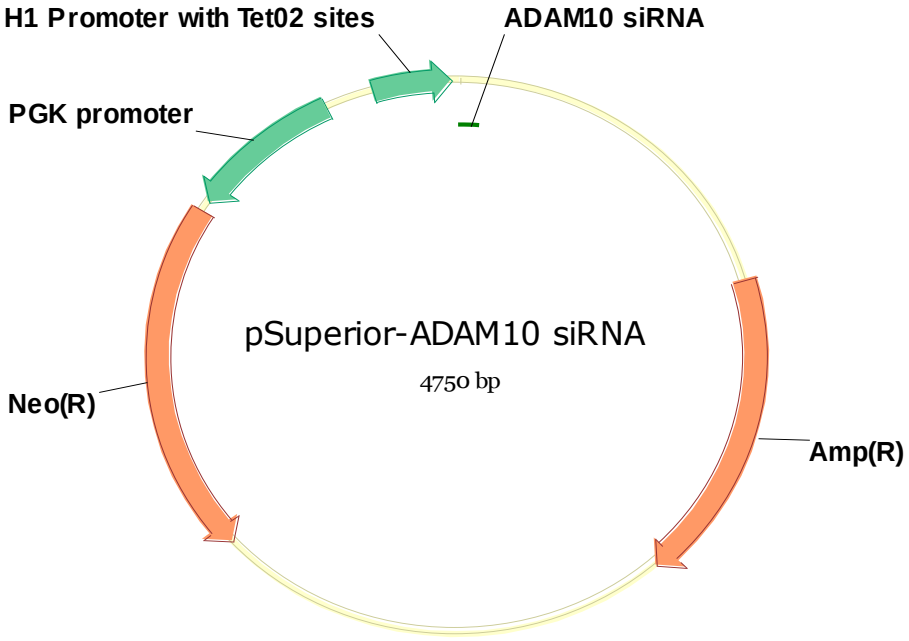

Results

I. ADAM10 activity increases asthma induction in IgE dependent models of experimental asthma, but not IgE independent.

A. ADAM10$^{-/-}$ and CD23Tg mice have decreased signs of allergic lung inflammation in an IgE dependent model. To test the importance of CD23 and ADAM10 in asthma induction we used the murine models of allergic lung inflammation shown in Figure 4 and 5. In agreement with Haczku *et al*. (53), we found that CD23Tg mice (BALB/C background), which have suppressed IgE ((56) and Figure 14b) and have high expression of CD23 on lymphocytes, exhibited decreased eosinophilia compared to LM controls (Figure 14a) when tested in an IgE-dependent asthma model (model A). We also observed decreased levels of the chemokine IL-5 (Figure 14c) which may explain the decreased eosinophilia seen. In contrast to the IgE-dependent model (model A) no differences between CD23Tg and LM controls in BALF eosinophilia was seen when model C was used (Figure 13a, performed by Dr. Jill Ford). In addition, when the CD23Tg mice were crossed onto an IgE$^{-/-}$ background and Model B was used (Figure 13c), there was no further reduction in eosinophils in the BALF. These data indicate that the decrease in asthma severity observed in the CD23Tg occurs primarily because of the decreased IgE in these animals. Given that ADAM10 is the CD23 sheddase and that mice which lack B cell ADAM10 have greatly increased CD23 expression (50), we next tested whether these mice would also have reduced inflammation with model A. Lung AHR in ADAM10$^{-/-}$ mice (C57BL/6 background), as determined by total lung resistance (R_L) (Figure 15a) and forced oscillation technique (Figure 15b) was significantly lower than in the LM sensitized control mice. Figure 16c shows that the ADAM10$^{-/-}$ mice also

Figure 13: Model B is IgE/mast cell independent, Model C is IgE dependent mast cell independent. This work was performed by Dr. Jill Ford and Sarah Norton. To determine if these models were dependent on mast cells or IgE, the BALF eosinophilia was determined after the respective models were induced in $IgE^{-/-}$, W/Wsh or wild type (WT) mice. (A) Model C was induced and equal amounts of eosinophils in the BALF were found in the $IgE^{-/-}$ and (B) W/Wsh and their respective controls. This shows that this model is independent of both IgE and mast cells. n = 9 (C) When model B was induced in $IgE^{-/-}$ and WT there were significantly less eosinophils in the $IgE^{-/-}$ mice compared to their LM controls. (D) However, when WT and W/Wsh eosinophilia were compared after induction of model B equal percentage of eosinophils were found in both mice. n = 8. This shows that for model B it is dependent on IgE, but not on mast cells. A and C additionally, show that the CD23Tg are compared to WT mice after induction of these two models, they are only able to control models that are dependent on IgE.

Model C

Model B

A.

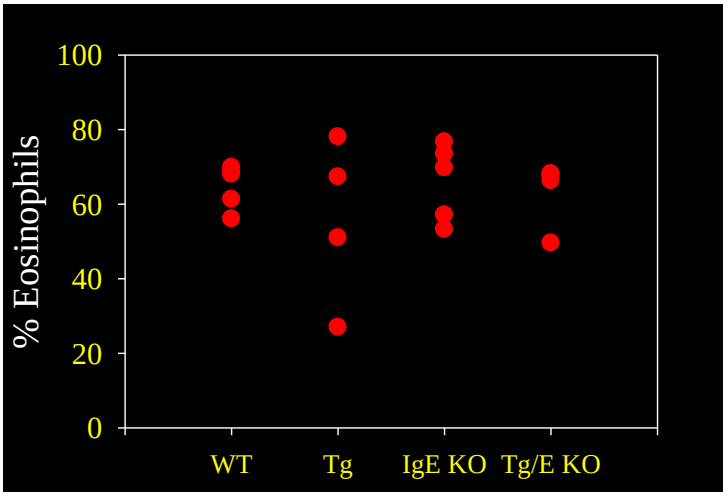

C.

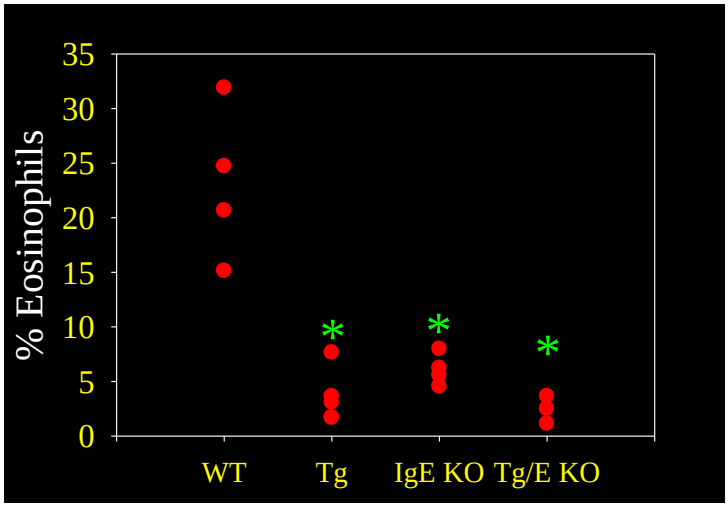

B.

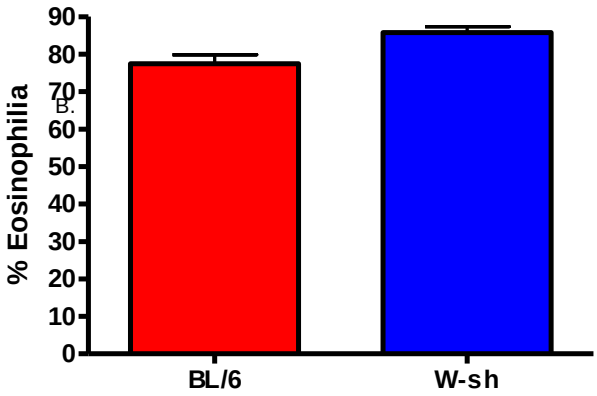

D.

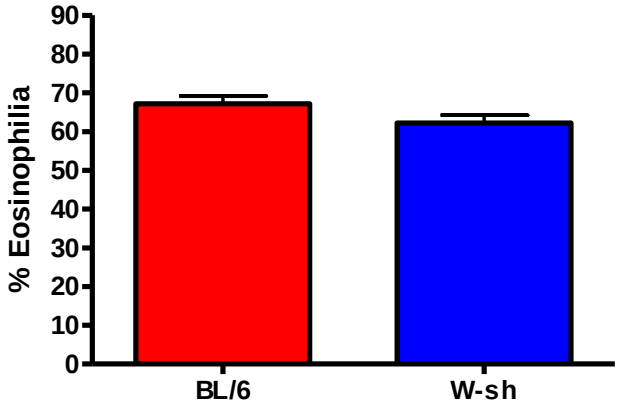

Figure 14. Overexpression of CD23 in CD23Tg can control eosinophilia in an IgE dependent model (A) Asthma was induced in BALB/C LM and CD23Tg mice using model A. BALF was collected and the percentages of cells were determined, as indicated in the Materials and methods, by counting at least 100 cells. Shown is the average of four mice. (B) Serum total IgE was measured by ELISA, shown is the average of 4 mice per group. (C) The cytokines in the BALF of the mice used in A were determined using multiplex kits according to the manufactures' instructions, shown is the average of 4 mice per group. * = P value <.05 and ** = P value <.01. Error bars represent standard error.

A.

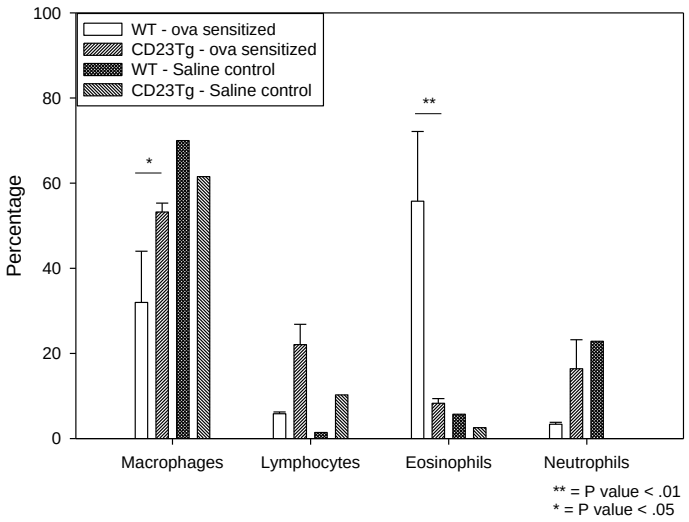

B.

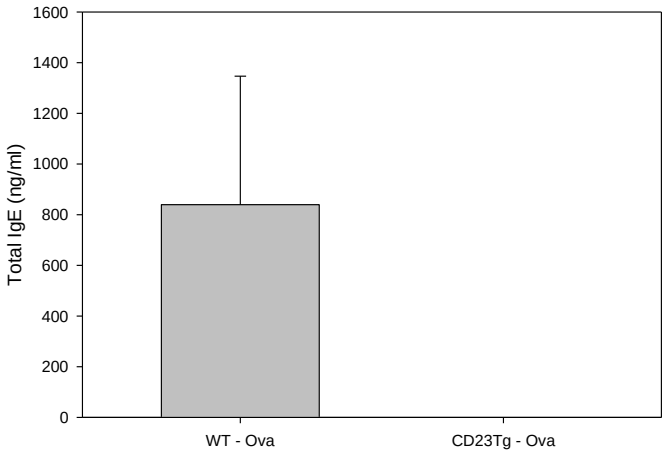

C.

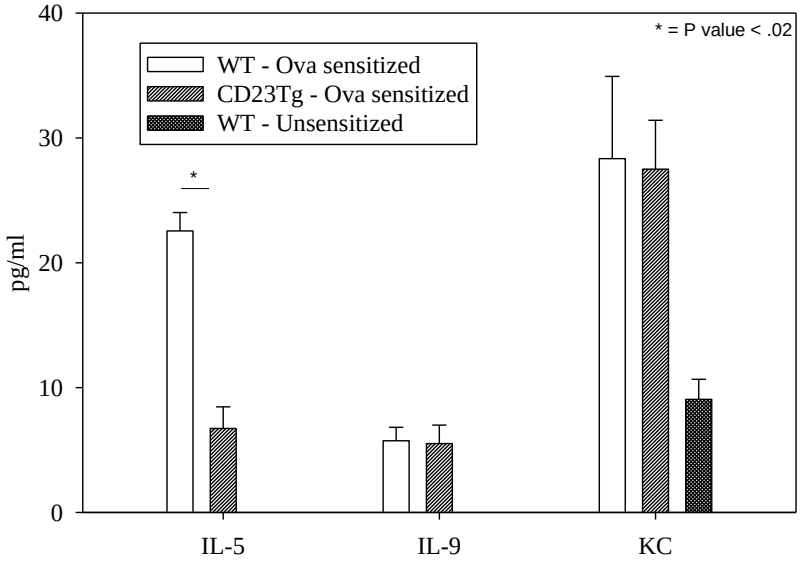

Figure 15 – Conditional removal of ADAM10 decreases the severity of disease in a IgE/mast cell dependent model (A) Mice were sensitized and challenged using model A (mice are on a C57BL/6 background). On day 29 lung function was assessed by measuring total lung resistance as explained in the Material and Methods; shown is the average of at least 4 mice per treated group. Significance is between ADAM10$^{-/-}$ (called A10$^{-/-}$ in figure) and LM. (B) Rn, Tissue Dampening and Elastance were determined at baseline (PBS) and after the addition of 50 mg/ml of methacholine, with the average of the three maximum points at each dose being used for each mouse. Shown is the average of at least 4 mice per group. (C) Cells from the BALF were counted and stained as explained in the Materials and methods. Percentages of cells were then determined in the BALF by counting of at least one hundred cells and numbers presented is the average of at least four mice. (D) The levels of OVA specific IgE in the serum were determined by ELISA, shown is the average of at least five animals. (E) Cytokine levels in the BALF were determined by multiplex analysis, shown is the average of at least four animals (same key as in C). * = P value <.05, ** = P value <.01 and *** = P value < .001. Error bars represent standard error.

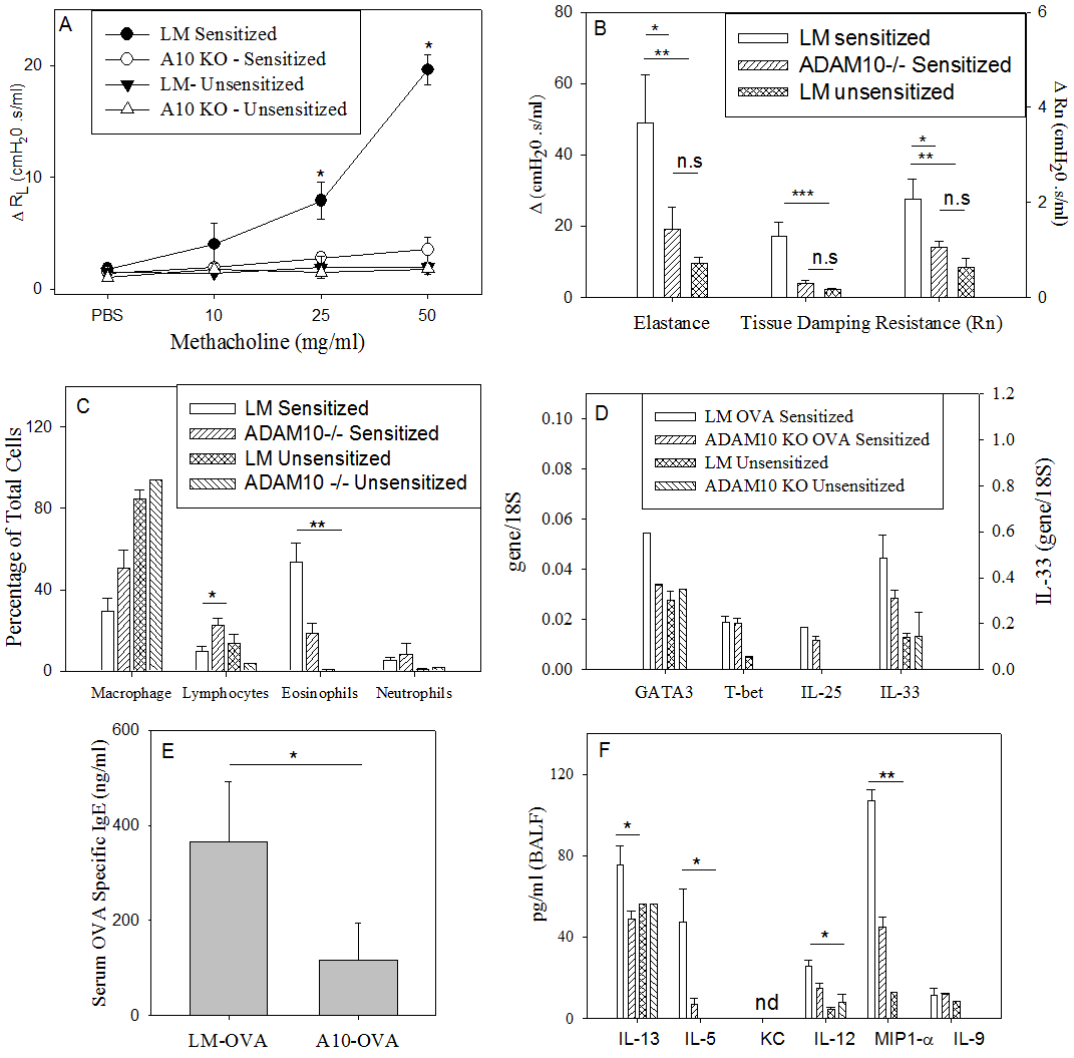

had significantly reduced eosinophilia in the BALF compared to LM sensitized controls. Percentages of other cell types in the ADAM10$^{-/-}$ mice closely resembled the unsensitized animals. ADAM10$^{-/-}$ mice also had reduced serum antigen-specific IgE levels (Figure 15e). In addition, although the mRNA levels for GATA3 and Tbet were not changed compared to LM (Figure 15d) there was a significant decreases in both Th1 and Th2 cytokines (Figure 15f). To determine if the ADAM10$^{-/-}$ had decreased tissue inflammation as well, lungs were sectioned and stained with H&E as explained in the Materials and methods. As shown in Figure 16, the ADAM$^{-/-}$ also had decreased inflammation and eosinophil infiltration. In contrast, when asthma was induced with model C, the ADAM10$^{-/-}$ (Figure 17 and 18) like the CD23Tg (Figure 13a) was not significantly different from the LM sensitized animals with respect to AHR (Figure 17a) or BALF eosinophilia (Figure 17b, c). However, the Th1 cytokines IL-12 and MIP1-α were still significantly decreased in the IgE independent model, when comparing the OVA sensitized ADAM10$^{-/-}$ mice to LM controls (Figure 17d). Overall these data show that increasing CD23 by inhibiting ADAM10 on B cells has the potential for strongly inhibiting the IgE dependent, but not the IgE independent lung inflammatory response by reducing IgE levels.

As the ADAM10$^{-/-}$ had decreased eosiniophilia and other signs of asthma when model A was used, we sought next to determine if was because of decreased IgE binding of and signaling through its high affinity receptor on mast cells or some other mechanism. To do this model B was used which model as shown in Figure 13b and c is dependent of IgE, but not on mast cells. Like with model A, when the ADAM10$^{-/-}$ mice were compared to LM, the signs of experimental asthma were decreased (Figure 19 and

Figure 16: ADAM10$^{-/-}$ mice also have less tissue eosinophilia. Lung sections from mice used in Figure 15 were stained with H&E and shown in the large photomicrographs are 10X and inserts are 100X. (A) ADAM10$^{-/-}$ and (B) LM controls. Shown is a representative photomicrograph of at least 4 mice per group.

A.

ADAM10 KO

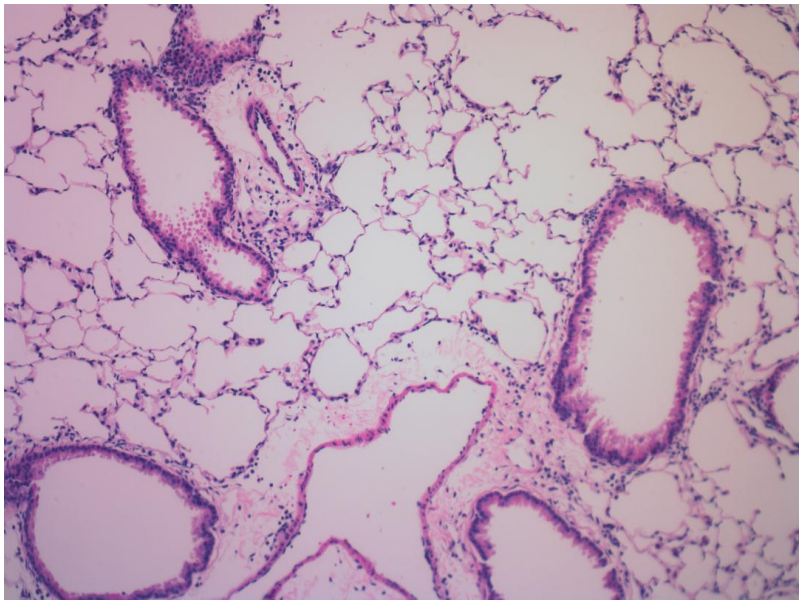

B

Littermate

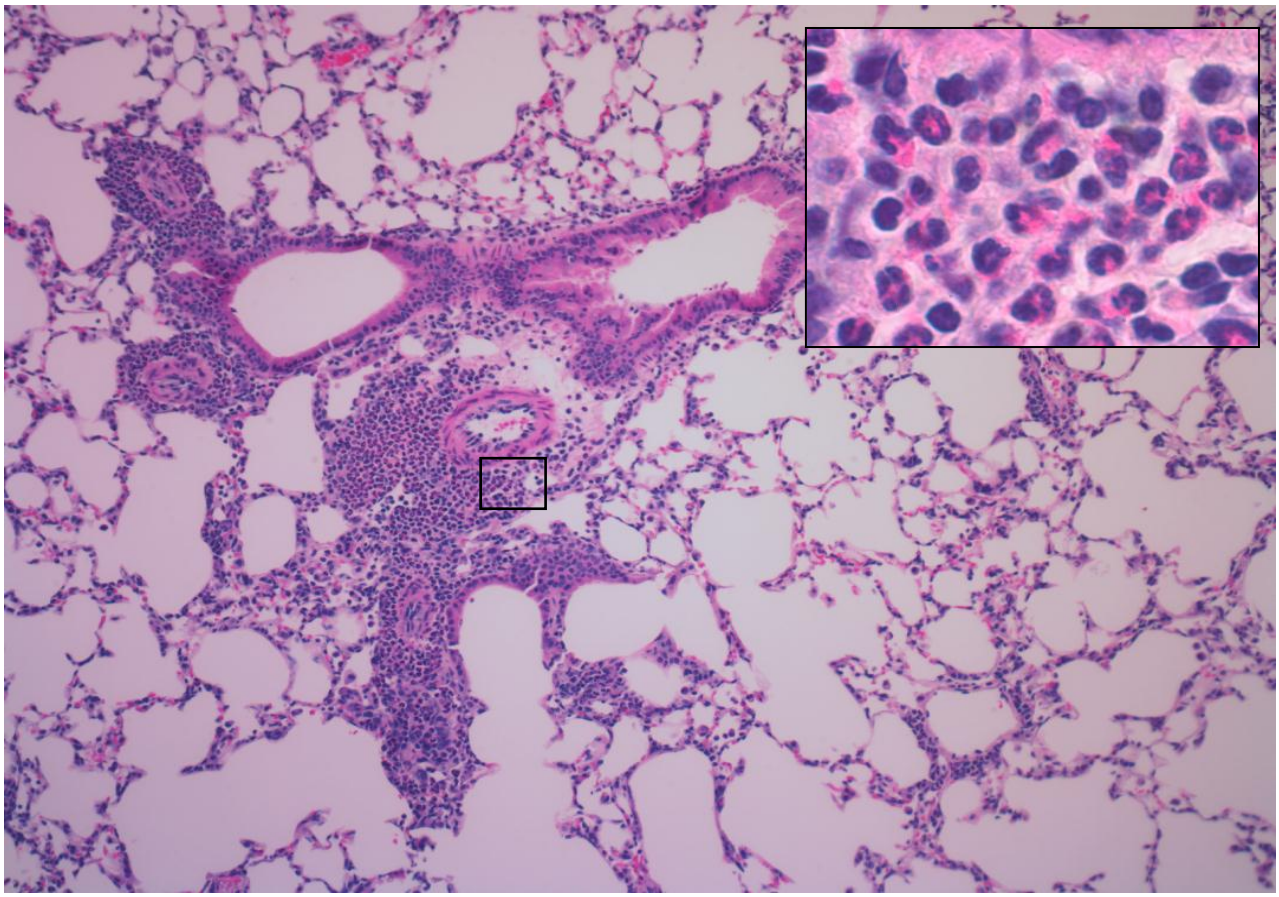

Figure 17: ADAM10 can control only IgE dependent disease. Experimental asthma was induced using Model C (IgE/mast cell independent) in ADAM10$^{-/-}$ (called ADAM10 KO in figure) and LM controls. (A) AHR was measured by R_L. (B) Percentage of cells in the BALF was determined, as explained in Figure 15. (C) Total number of each cell type in the BALF was determined by multiplying the percentage by the total number of cells in the BALF. (D) Cytokines in the BALF was determined by multiplex analysis. (E) OVA-specific IgE found in the serum of the mice at day 29 was determined by ELISA. Shown is the average of at least five mice per group. Error bars represent standard error. * = P value < .05

A.

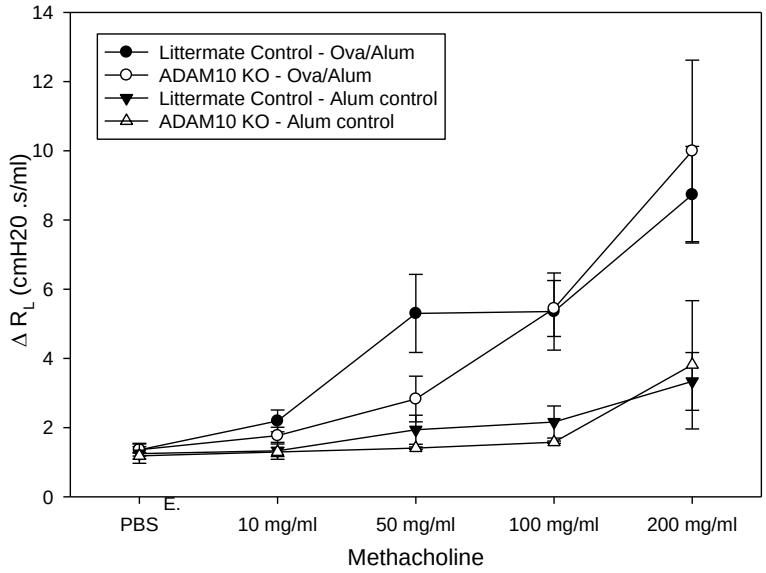

E.

B.

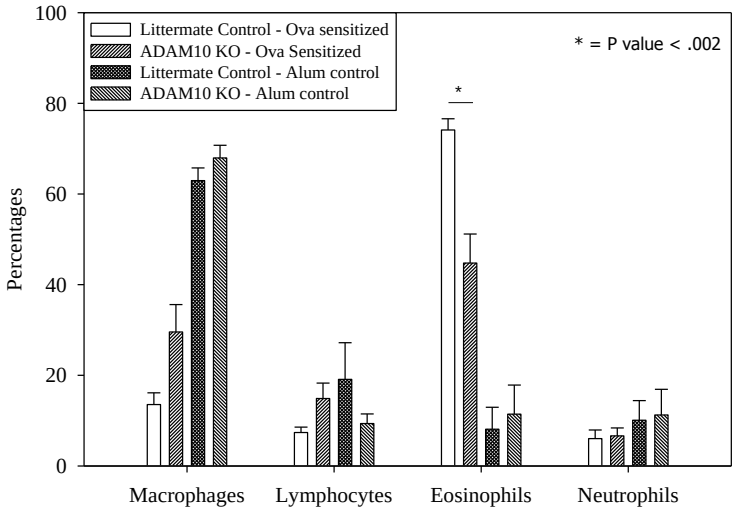

C.

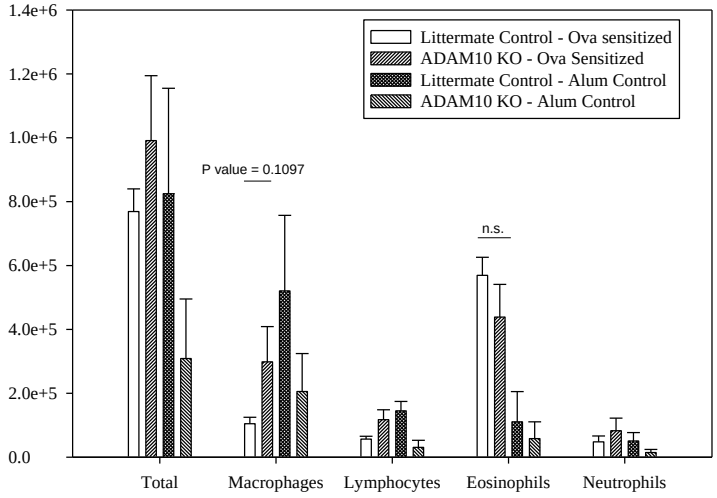

D.

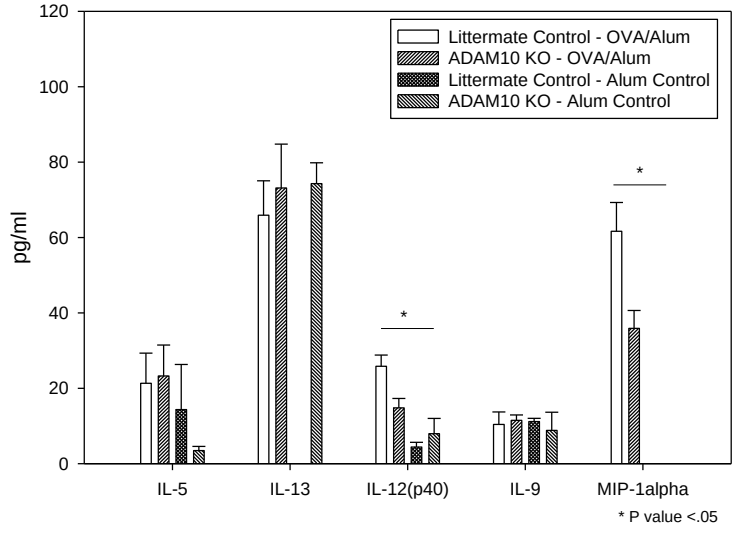

E.

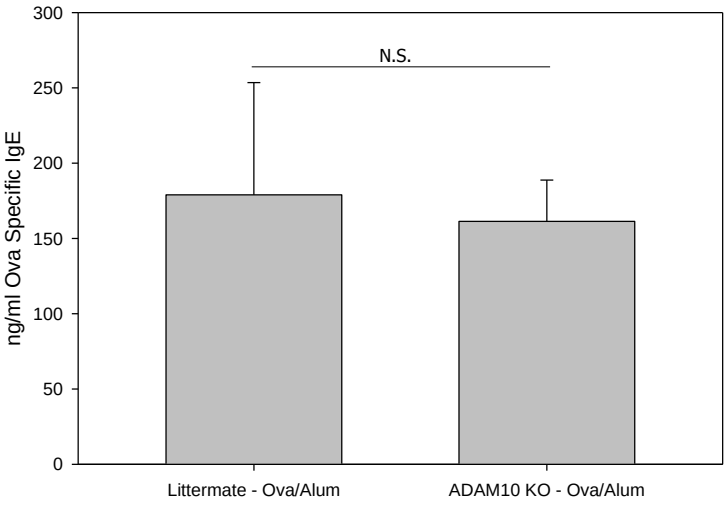

Figure 18: Tissue eosinophilia was normal after IgE independent asthma model induction. Lung sections from mice used in Figure 17 were stained with H&E and shown in the large photomicrographs are 10X and inserts are 100X. (A) ADAM10$^{-/-}$and (B) LM sensitized controls. Shown is a representative picture of at least 4 mice per group.

A.

ADAM10 KO

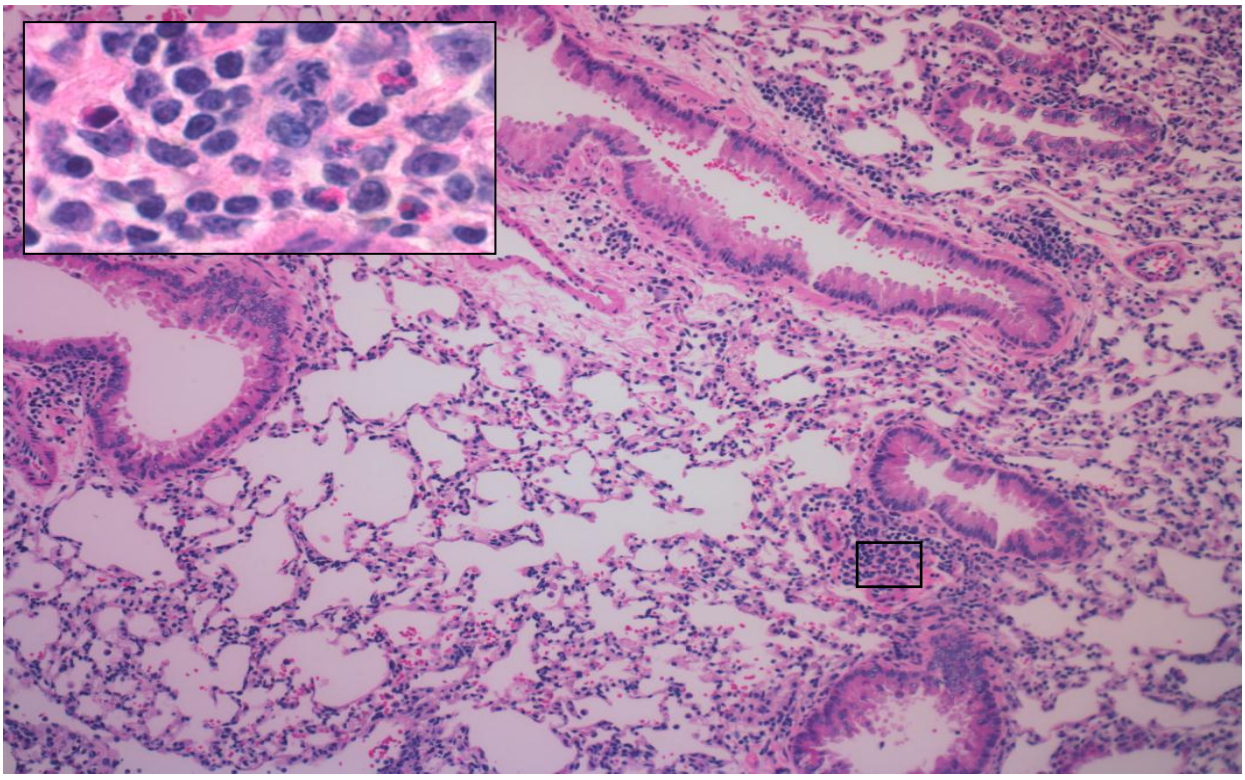

B.

Littermate

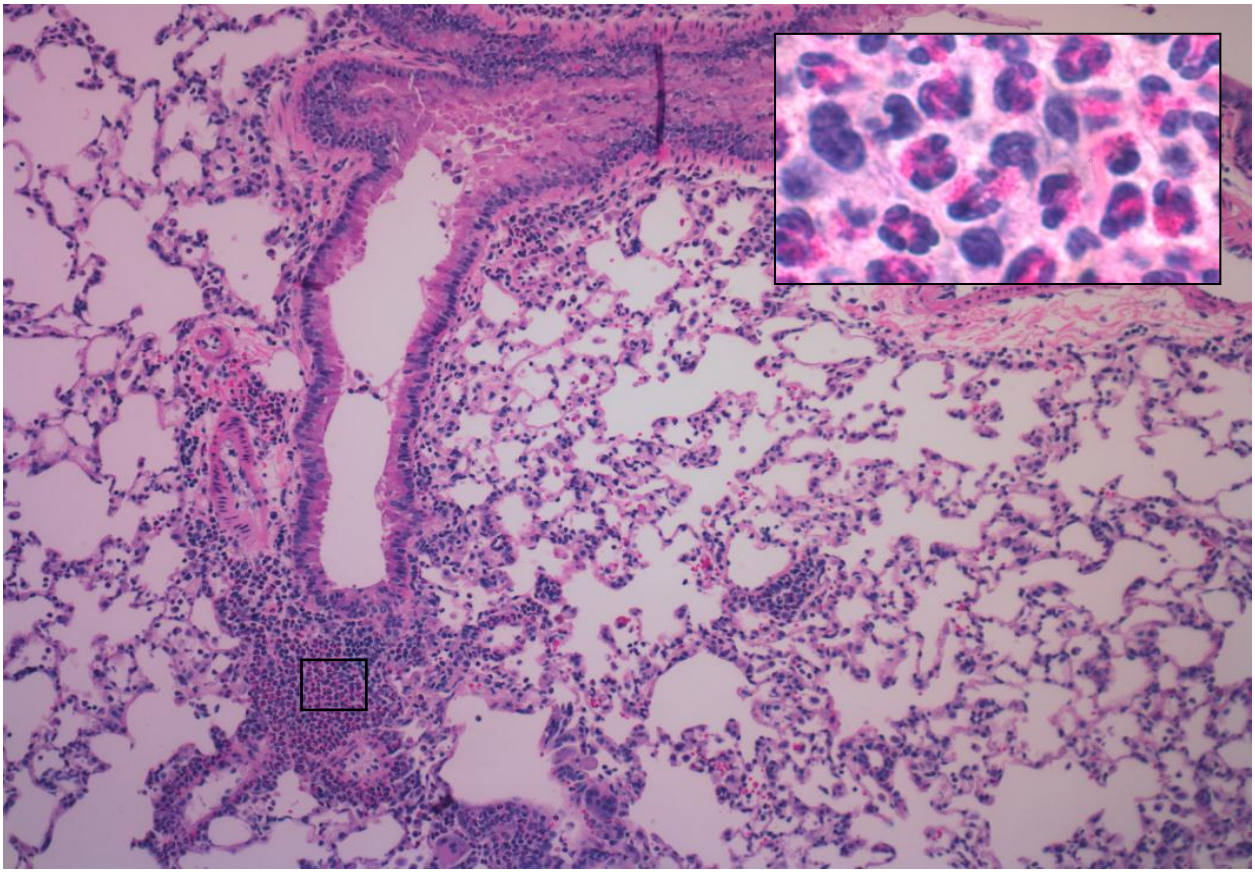

Figure 19: B cell specific ADAM10$^{-/-}$ mice have decreased asthma signs after induction of IgE dependent/mast cell independent model of asthma compared to LM controls. Experimental asthma was induced using Model B (IgE dependent/mast cell independent). (A) AHR was measured by R_L as explained in Figure 15. Comparison is between ADAM10$^{-/-}$(called ADAM10 KO in figure) and LM controls. (B) Percentage of cells in the BALF was determined, as explained in Figure 15. (C) Total number of eosinophils in the BALF (D) OVA-specific IgG found in the serum of the mice at day 29. Shown is the average of at least 5 per group. Error bars represent standard error. * = P value < .05

A.

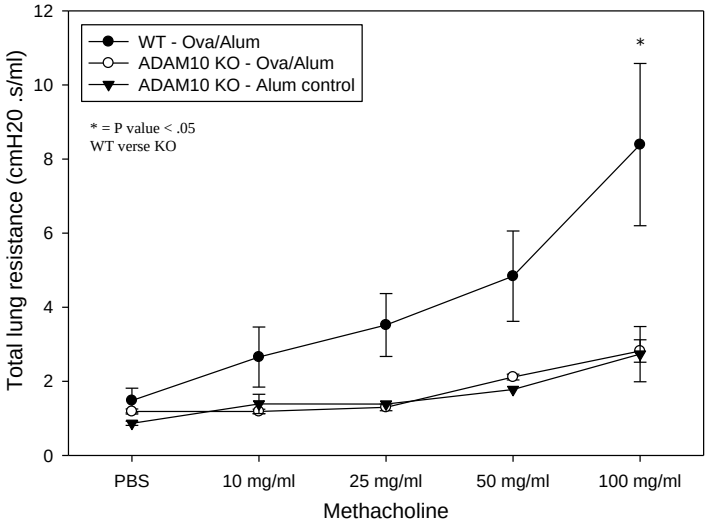

B.

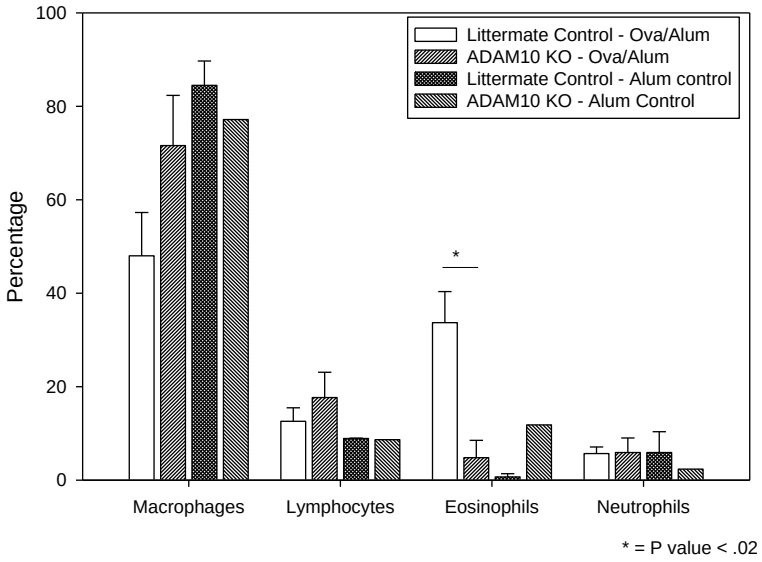

C.

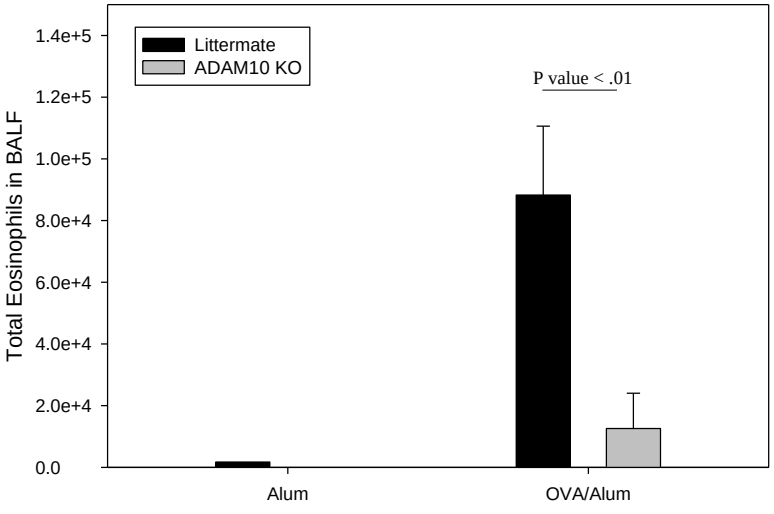

D.

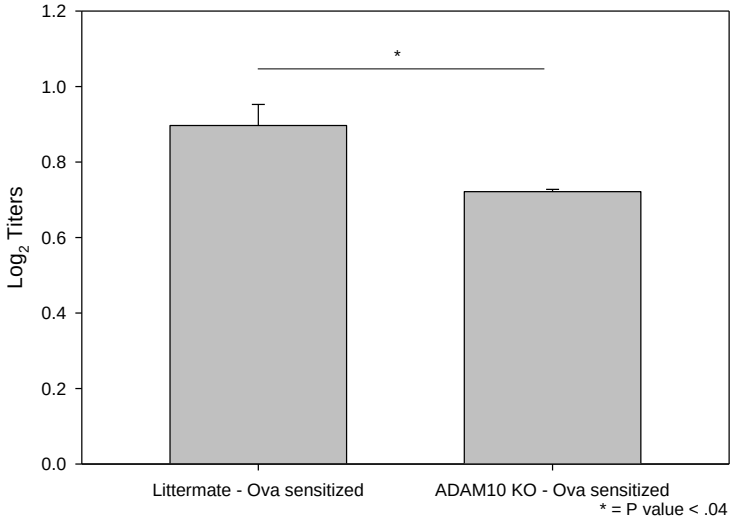

Figure 20: Tissue eosinophilia was also decreased. Lung sections of sensitized mice used in Figure 19 were stained with H&E and shown in the large photomicrographs are 10X and insets are 100X. **(**A) ADAM10$^{-/-}$ and (B) LM sensitized controls. Shown is a representative photomicrograph of at least 4 mice per group.

A.

ADAM10 KO

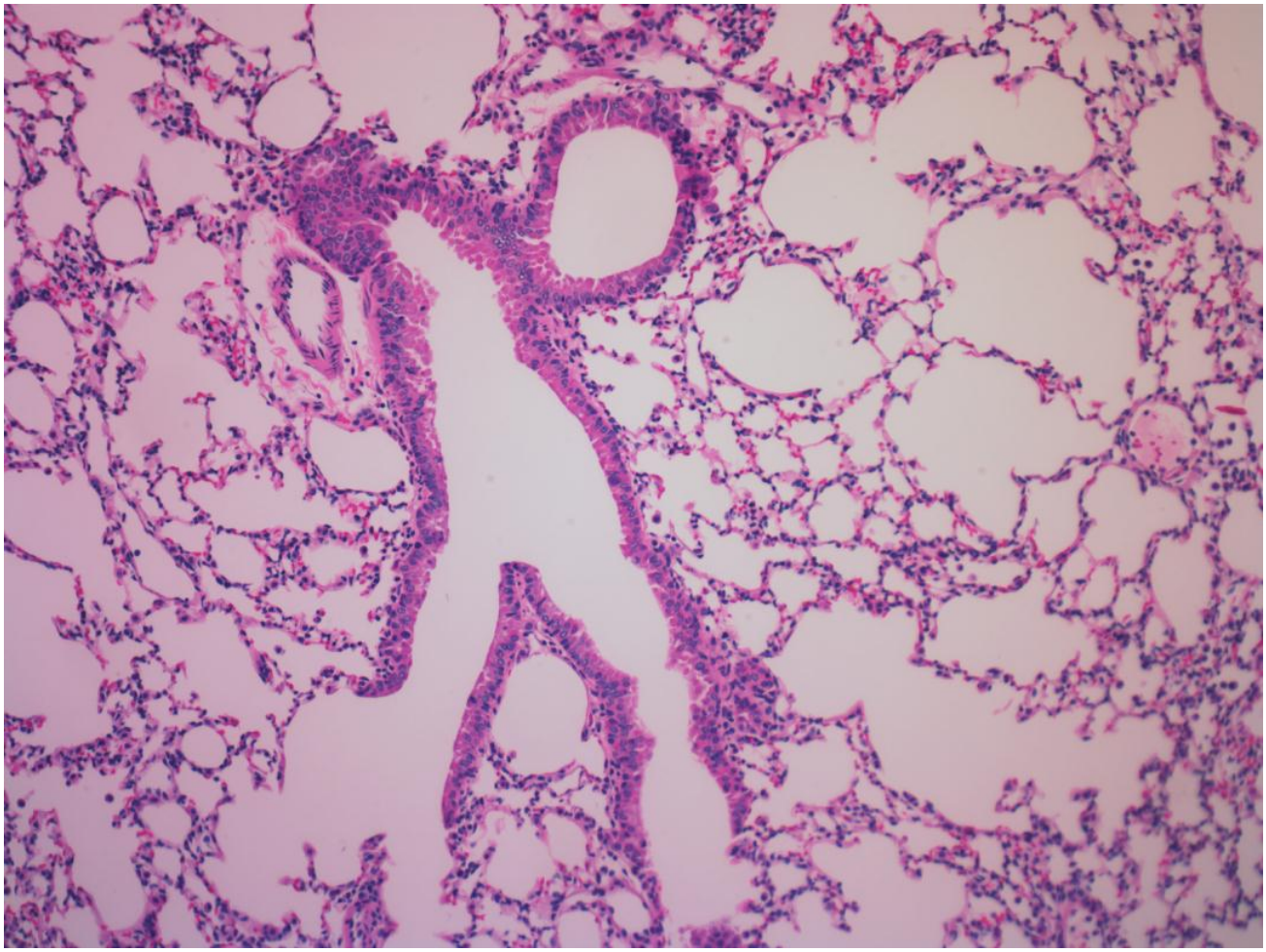

B.

Littermate

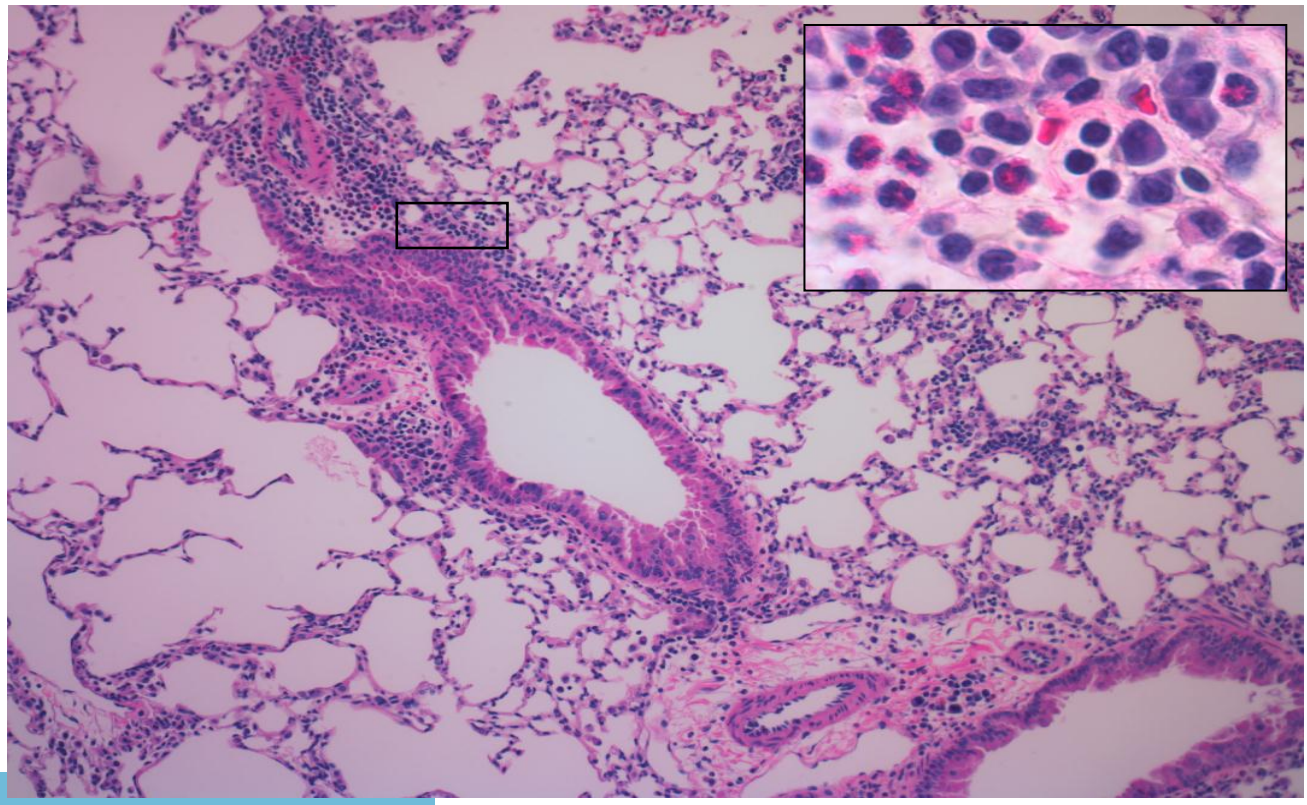

19). This included AHR as shown by R_L (Figure 19a) and eosiniophilia (Figure 19b) as well as lung inflammation (Figure 20). These data additionally show that ADAM10 on B cells is important for the exacerbation of IgE dependent disease, but this exacerbation cannot be explained completely by the decreased IgE signaling and degranulation of mast cells. The nature of other possible IgE dependent mechanisms will be discussed later.

B. ADAM10 inhibition blocks the induction of experimental asthma

Given the above finding that mice lacking B cell ADAM10 have minimal pathology in IgE dependent lung inflammation, we sought to determine if inhibiting ADAM10 activity in WT mice would have the same effect. Experiments were conducted with two hydroxamate inhibitors of ADAM10 (both inhibitors were found to cause a similar decrease in asthma signs, the data from both experiments was thus combined). The inhibitors were dissolved in DMSO and administered intranasally during the induction of the asthma model (Figure 6). The inhibitors were administered intranasally at a concentration of 1 mg/kg (91) (based on a lung volume of 900 µl this is a concentration of 32 µM), a dose based on previous cell based assay performed by Incyte where ADAM10 *in vivo* should selectively be inhibited, in DMSO/PBS every three days throughout the experiment. As a control, the ADAM10 inhibitors were also administered to unsensitized mice and found to have no effect (Figure 21 b, c). Using the IgE-dependent model (model A) we found that the inhibitors significantly decreased the signs of allergic airway inflammation, while having no toxic effects as measured by weight loss or the serum levels of liver enzymes, aspartate aminotransferase and alanine aminotransferase (Table 1). The carrier (5% DMSO in PBS) was well tolerated; responses of the LM controls in Figure 15c were similar to those in DMSO treated mice

(Figure 21c). Thus, any reduction in asthma severity was due to inhibition of ADAM10 activity. We also found that similar to the ADAM10$^{-/-}$ mice (Figure 15), AHR as measured by forced oscillation technique (Figure 21b), as well as R_L (Figure 21a) was decreased by the administration of the ADAM10 inhibitor. The eosinophilia in the BALF was also found to be significantly reduced (Figure 21c). This decrease was even more drastic than in the ADAM10$^{-/-}$ mice, from ~50% to 20% in the ADAM10$^{-/-}$ (Figure 15c) and from ~50% to 5% (Figure 21c) in WT mice treated with the inhibitor. Thus, this suggests that ADAM10 expression by cells, other than B cells, is important in the progression of experimental asthma. The inhibitors may also block ADAM10 activity on epithelial cells, because they can control the allergic response (reviewed in (111)) and have high expression of ADAM10 (82). Although the percentage of macrophages was increased, there were actually only a slight increase of macrophages in the BALF (Figure 21d) compared to DMSO control after inhibitor treatment. To determine if the decrease in AHR and eosinophilia was because of an inhibition of IgE synthesis, as was the case in the ADAM10$^{-/-}$ mice, we measured the levels of total IgE in the serum (Figure 21e), but found it was unchanged from the LM. However, local production of IgE in the BALF was significantly decreased compared to DMSO treated mice (Figure 21f). Hydroxamate inhibitors are known to have a short half-life in serum (112), however as clearly shown by our data when administered intranasally the inhibitory activity is sufficient for at least a 3 day period. The effects on IgE suggest local activity, however, blocking only the local production of IgE is advantageous as it has been shown that local but not systemic, production of IgE (113) is important for disease progression.

Table 1. ADAM10 inhibitors are not toxic to mice. Just prior to measurement of AHR the mice were weighed. Shown is the average of at least 8 mice per group. The serum isolated after sacrifice of three mice of similar treatment were pooled together and then AST and ALT levels were measured in the serum as explained in the material and methods. Shown is the average of at least two different pools. Error represents standard error.

Parameter	DMSO – OVA Sensitized	ADAM10 inh – OVA Sensitized
Weight (time of sacrifice)	20.49 ± 0.5	20.43± 0.28
AST (aspartate aminotransferase)	13.666 ± 6.81	15.558 ± 6.87
ALT (alanine aminotransferase)	2.59 ± 0.93	3.64 ± 0.67

Figure 21 – ADAM10 inhibitor potentially blocks the induction of an IgE/mast cell dependent model through blocking the Th2 response. Asthma was induced using the IgE-dependent model (Model A). 1 mg/kg in a 20:1 mixture of PBS/DMSO of an ADAM10 inhibitor (called A10 inh in the Figure) was injected intranasally every three days throughout the experiment in wild type C57BL/6. The control mice (wild type C57BL/6) received just the PBS/DMSO mixture. (A) On day 47 AHR was measured using total lung resistance (significance is between ADAM10 inhibitor and DMSO treated) and (B) forced oscillation measurements as explained in Fig 15b. Data represents the average of data from at least four sensitized mice and two unsensitized mice. (C) Percentages of BALF cells were determined as in Fig 15c. Shown is the average of at least three animals (same key as B). (D) Total IgE in the serum as determined by ELISA, average of at least four animals. (E) Total IgE in the BALF as determined by ELISA, average of at least three animals. (F) qRT-PCR of total lung RNA was performed using the primers listed in material and methods. Shown is the average of at least five animals. The unsensitized groups were combined, as no difference where seen between them. (G) BALF cytokine levels as determined by multiplex ELISA. Shown is the average of at least five animals per group. Again unsensitized groups were combined. (same key as F). Number above comparison line equals P value, * = P value < .05 and ** = P value <.01. Error bars represent standard error.

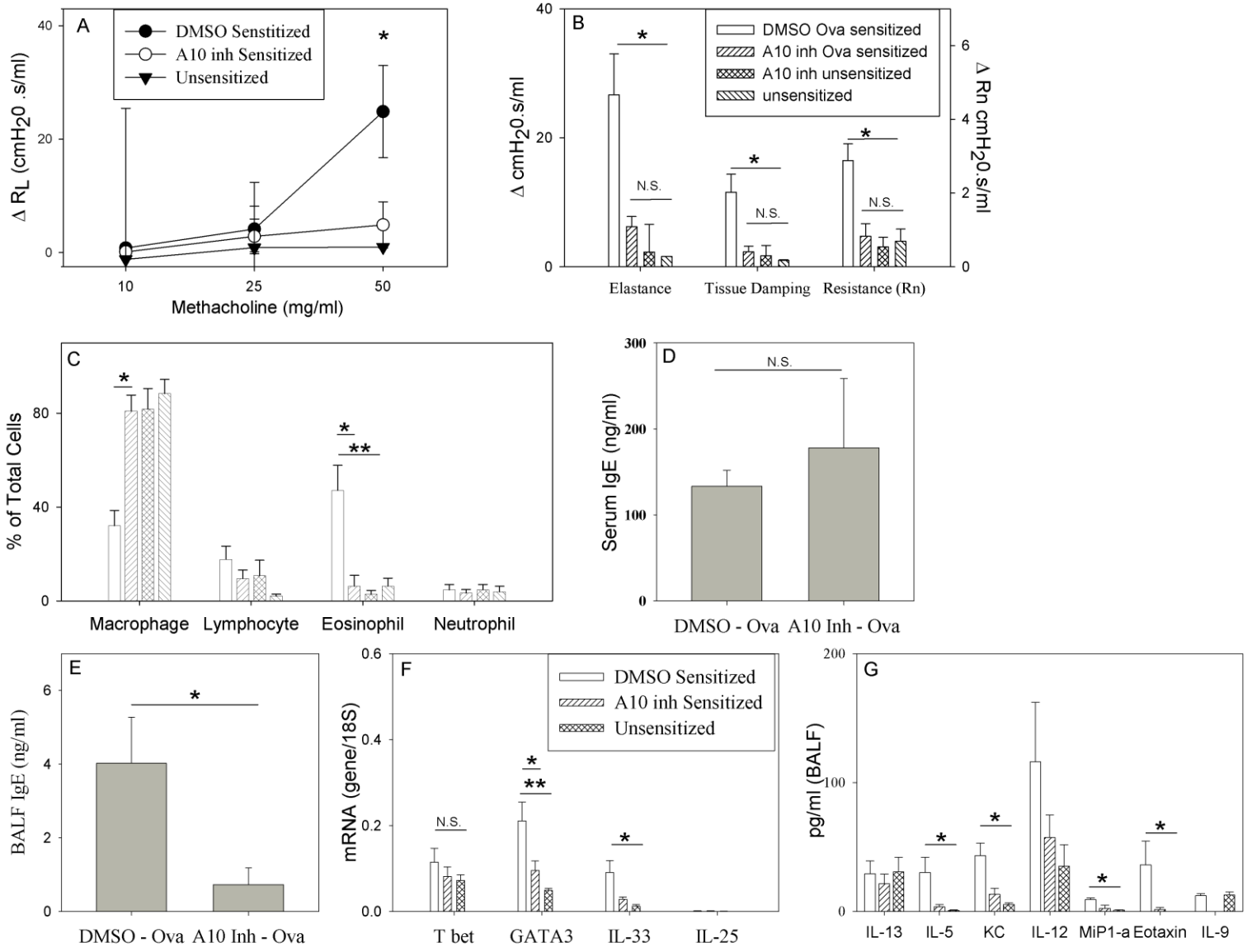

Figure 22: Tissue eosinophilia is decreased by the administration of ADAM10 inhibitor. In order to determine if inhibiting ADAM10 activity similarly suppressed tissue inflammation, lung sections of the mice used in Figure 21 were stained with H&E and shown in the large photomicrographs are 10X and inserts are 100X. (A) ADAM10 inhibitor treated (labeled as AD10) and (B) DMSO treated mice. Shown is a representative photomicrograph of at least seven per group.

A.

AD10 inh

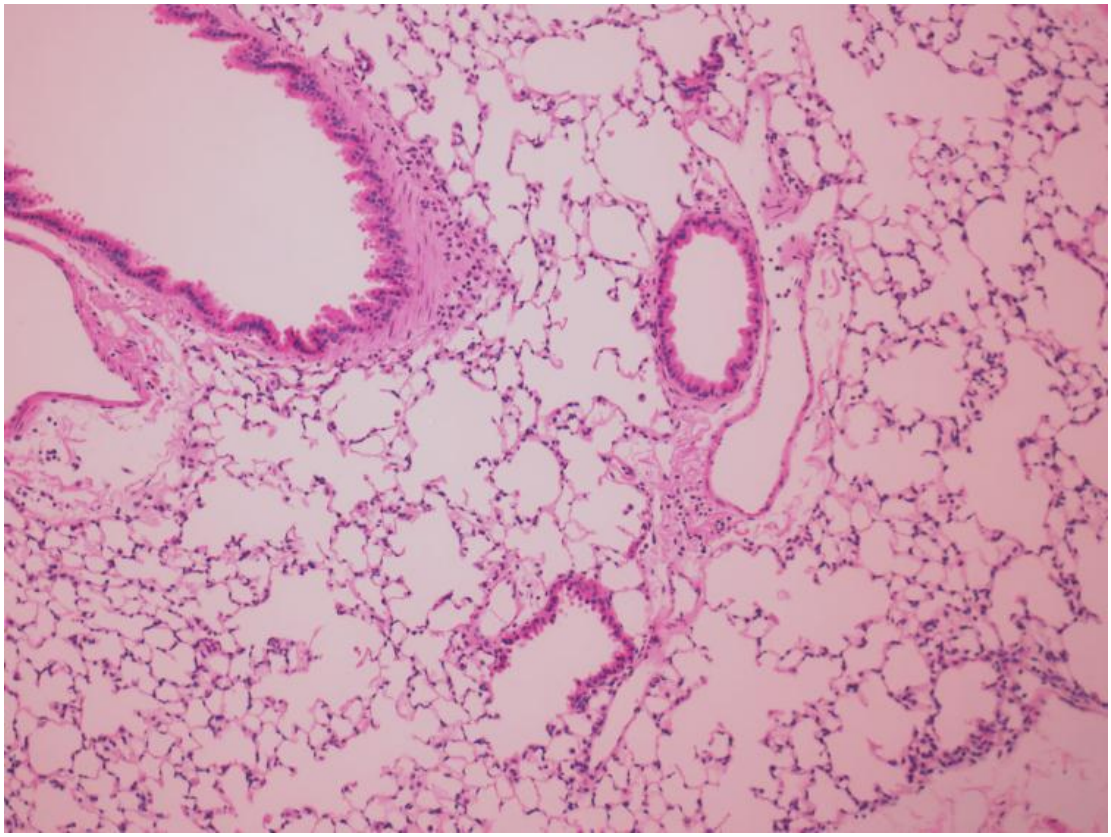

B.

DMSO treated

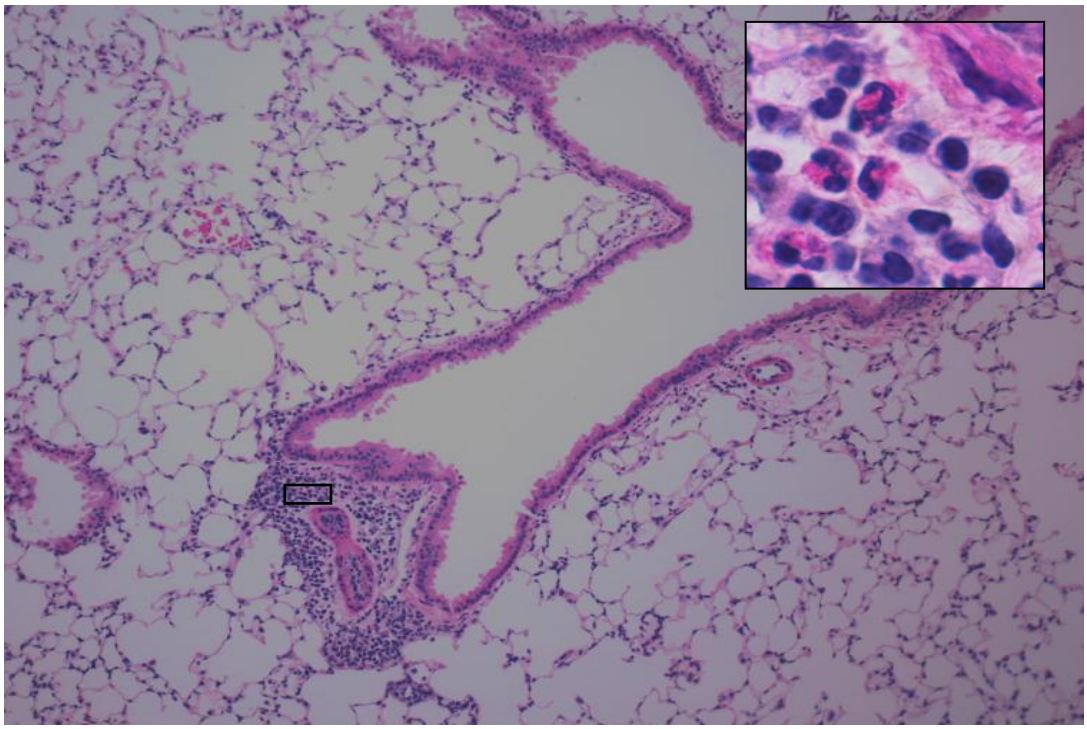

Figure 23: Signs of asthma are decreased when ADAM10 inhibitor is administered during induction of IgE dependent asthma model in BALB/C. To determine if the effects of the ADAM10 inhibitors were just because of the C57BL/6 background, experimental asthma was induced like in figure 19 in BALB/C mice and INC009588 was administered throughout the experiment. (A) AHR as measured by R_L (comparison is between DMSO and ADAM10 inhibitor treated) or (B) Rn, tissue damping and elastance. (C) Percentage of cells in BALF determined as explained in Figure 15c. (D) Cytokines in the BALF. (E) Total IgE in the BALF. (F) Expression of selected genes in the left lobe of the lung determined as explained in figure 19. Shown is the average of at least four mice. Error bars represent standard error. * = P value < .05

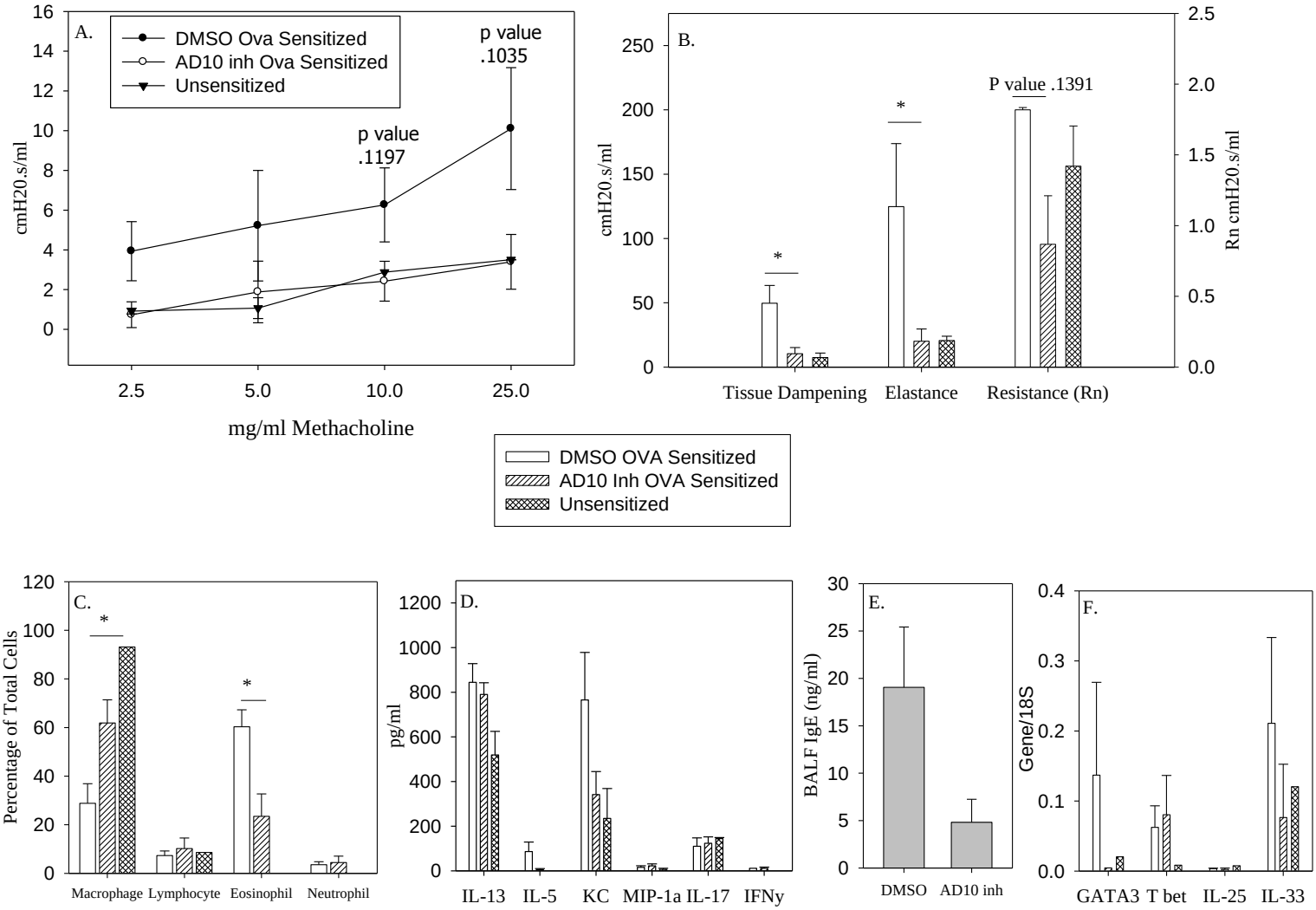

Figure 24: Similar to ADAM10$^{-/-}$ mice the administration of ADAM10 inhibitor cannot decrease asthma signs when an IgE independent model is used. With the ADAM10$^{-/-}$ we found that ADAM10 on B cells was only important in IgE dependent diseases. To determine if the same was true with inhibition of ADAM10 activity experimental asthma was induced using the schedule shown in figure 6. (A) AHR as measured by Rn, G (tissue damping) and H (Elastance). (B) Total cells of each type in the BALF. This was determined by multiplying the percentages of each cell type by the total amount of cells found in the BALF. (C) Percentages of cells in the BALF were determined as explained in figure 16c. (D) Gene expression was determined as explained in Figure 19. (E) Cytokines expression in the BALF was determined as explained in Figure 15. (F) IgE levels in the BALF as determined by ELISA as explained in the materials and methods. Shown is the average of at least six mice. Error bars represent standard error. * = P value <.05, *** = P value < .001.

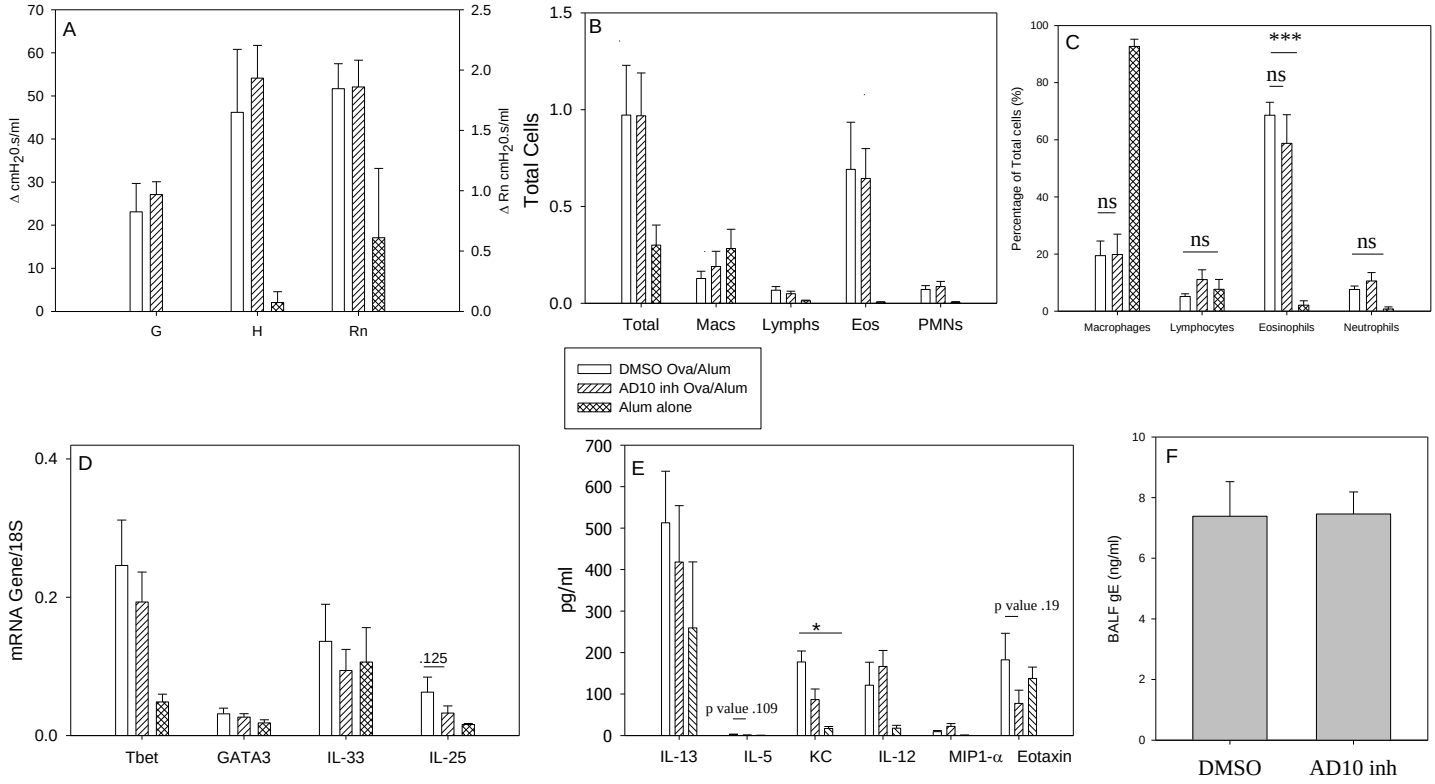

Figure 25: ADAM10 inhibitors have no effect on tissue eosinophilia when IgE independent model is induced. To determine if inhibition of ADAM10 activity had any effect on lung inflammation, lung sections from the mice used in Figure 24 were stained with H&E. Shown in the large photomicrographs are 10X and areas of obvious inflammation as insets at 100X. (A) ADAM10 inhibitor treated and (B) DMSO treated. Shown is a representative photomicrograph of at least 4 mice per group.

A.

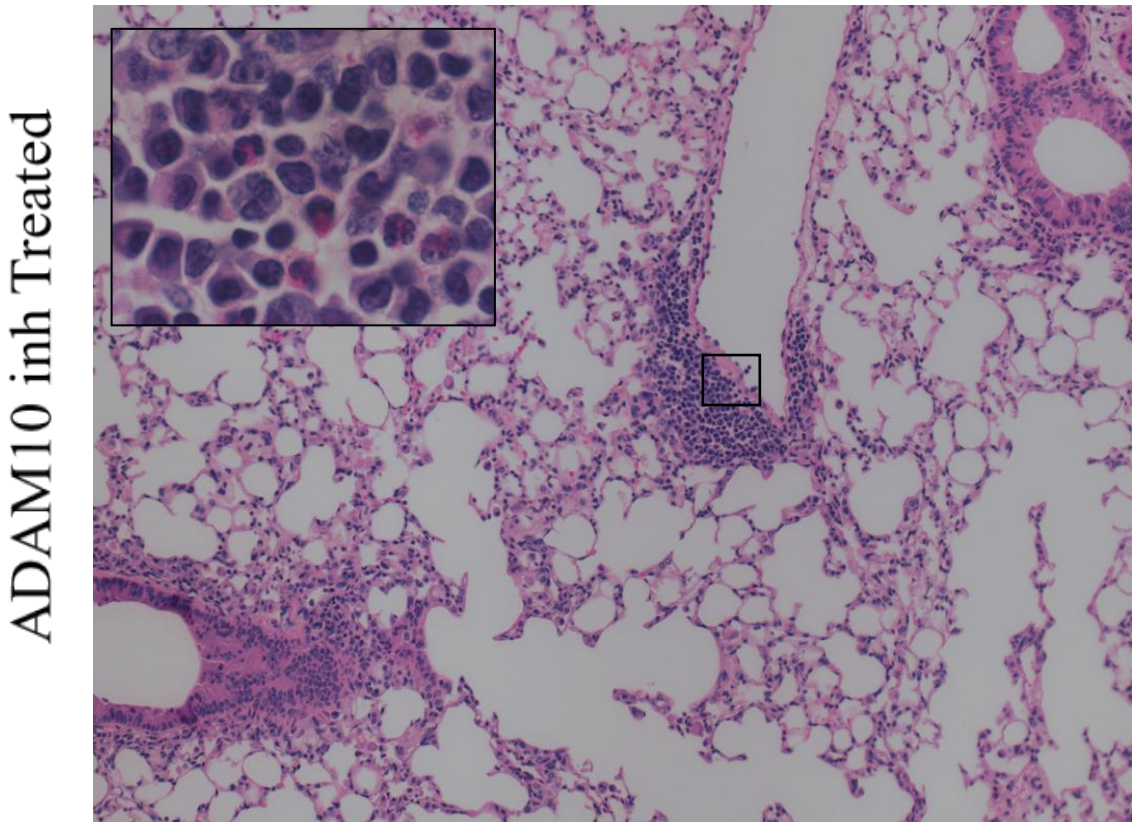

B.

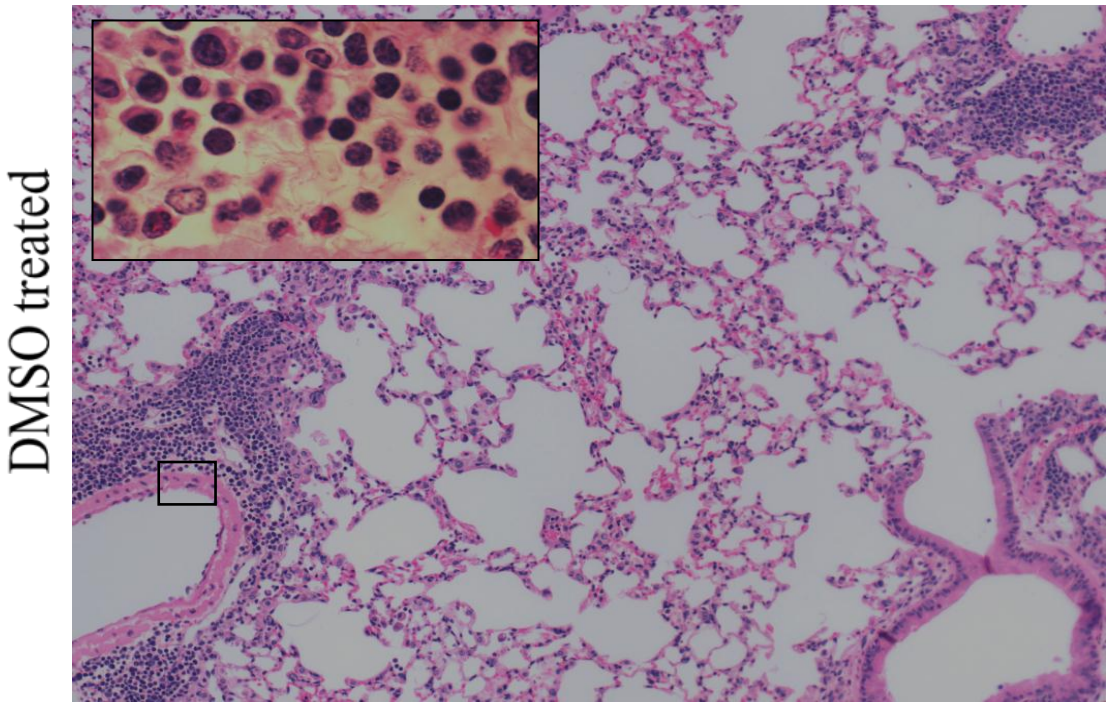

To test if ADAM10 inhibitors have effects beyond that of inhibiting IgE, we isolated total lung mRNA from ADAM10 inhibitor treated and control mice, and used qRT-PCR to measure the levels of several components known to be important in asthma progression, including the Th2 response. In the ADAM10$^{-/-}$ mice we found that the decrease in the levels of serum OVA-specific IgE compared to LM correlated with a decrease in Th2 cytokines (Figure 15f). To determine what effect administration of the inhibitor had on T cell responses, the major T cell transcription factors mRNA levels were measured by qRT-PCR. Analysis demonstrated GATA3 mRNA levels were significantly decreased after ADAM10 inhibitor treatment compared to DMSO treatment, while Tbet mRNA levels were not (Figure 21g). Recently two cytokines, IL-25 and IL-33 (reviewed in (114)), have been implicated in the induction of a Th2 response. While minimal IL-25 mRNA levels were detected, message for IL-33 was significantly decreased in mice treated with the ADAM10 inhibitor. These results further support the hypothesis that ADAM10 on non-B cells is important in the initiation of the Th2 response in the lung. Interestingly, when cytokines were analyzed in the BALF, IL-13 levels were not decreased (Figure 21h) when given the inhibitor, in spite of the known association of IL-13 and AHR (115). Alternative sources of IL-13 production (116), not affected by ADAM10 inhibition, could potentially explain this finding. It is also interesting to speculate that ADAM10 inhibition decreases the ability of IL-13 (115) to act on epithelial cells in the lung as will be discussed later. The decreased eosinophilia (Figure 21c) observed after ADAM10 inhibition can be explained by the strong inhibition of IL-5, the primary chemotactic factor in the recruitment of eosinophils, as well as by significant decreases in eotaxin and KC which are also involved in eosinophil recruitment (Figure

21h). Finally, IL-9 in the BALF was also found to be decreased by the addition of the ADAM10 inhibitor. IL-9 is produced by both Th2 cells as well as the new subclass of T helper cells, Th9, and is known to enhance airway inflammation (117). When lung inflammation was investigated by H&E staining after treatment, it was also found to be decreased in the ADAM10 inhibitor treated mice compared to DMSO (Figure 22). Overall, the multiple changes help explain how the inhibition of ADAM10 suppresses IgE-dependent lung inflammation.

When the ADAM10 inhibitor administration was repeated in BALB/C mice using model A (Figure 23), similar results were seen expect the eosinophilia decrease in the BALF was not as drastic (60% to 23% in the BALB/C compared to 50% to 5% in the C57BL/6 after inhibitor treatment). Finally, when the ADAM10 inhibitor was administered every three days during the induction of model C (IgE independent (Figure 7)), no effect was seen (Figure 24 and 25). Overall these results show that regardless of the mouse background, the administration of an ADAM10 inhibitor is able to block the induction of experimental asthma.

II. ADAM10 is also required for CD23 sorting into B cell derived exosomes.

Considering that inhibiting ADAM10 can decrease the signs of asthma, potentially due to increased CD23 expression, we sought to further understand how ADAM10 cleaves CD23.

Figure 26: CD23 is internalized upon ligand binding. mCD23^{+}-CHO (90) were plated on poly-lysine coated coverslips and allowed to adhere. After staining with a FITC-rat anti-mouse CD23 lectin (B3B4) antibody for 30 min at 4°C, cells were either (B) transferred to 37°C for 30 min or (A) left at 4°C and visualized.

A

4°C

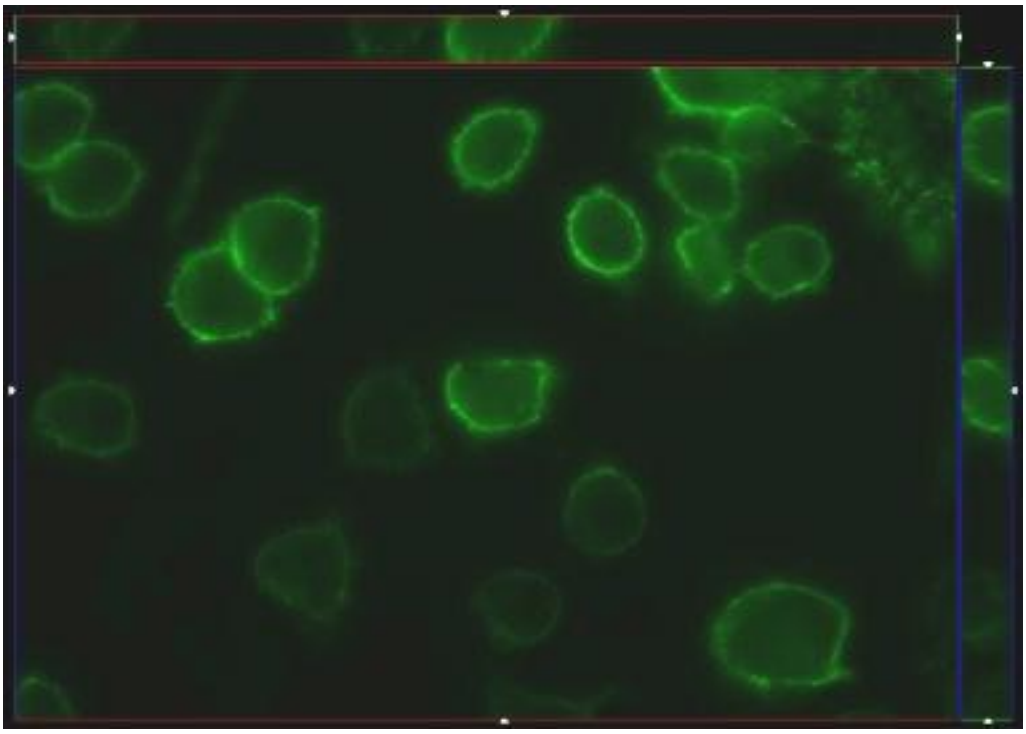

B

Transferred to 37°C

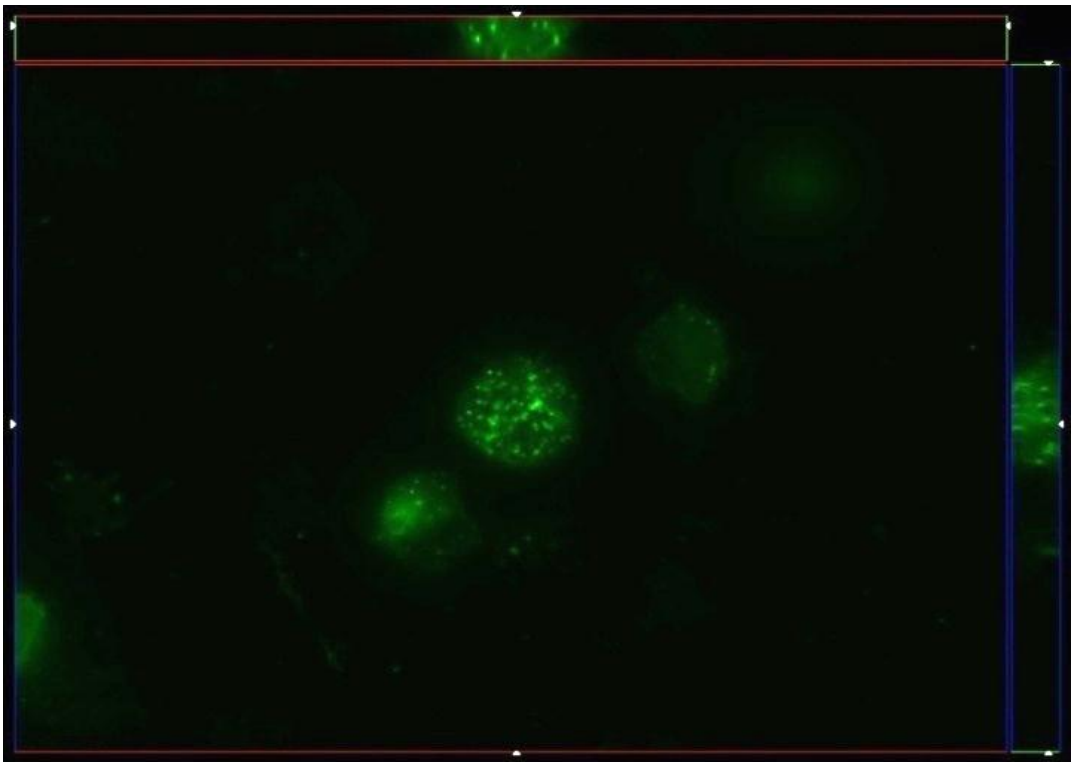

Figure 27: Amount of CD23 internalized is affected by stability. To test if the stability of CD23 affected the amount of internalization a different cell type, HEK 293T transfected with mouse CD23-YFP were plated on coverslips and surface CD23 was either stabilized by the addition of 2H10 (anti-lectin) or IgE or destabilized with 19G5 or left untreated as a control. The percentage of cells where CD23 was internalized (examples are shown in (A) CD23 is cell surface bound or (B) internalized) was calculated after a 24 hr incubation (37°C) with the indicated antibodies. Fig 27A and B data are representative micrographs from 3 experiments of similar design and 27C represents data the averaged. Error bars represent standard deviation. * = P value < .05, ** = P value < .01.

A.

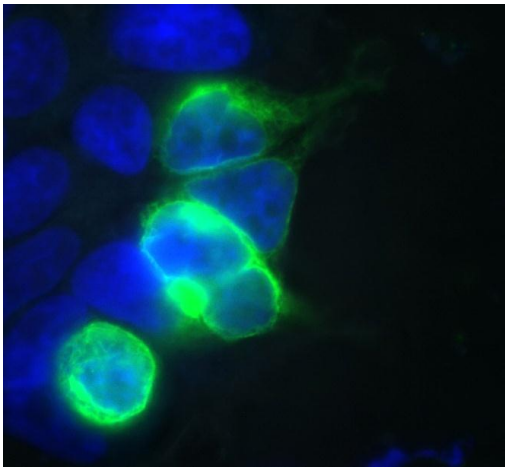

B.

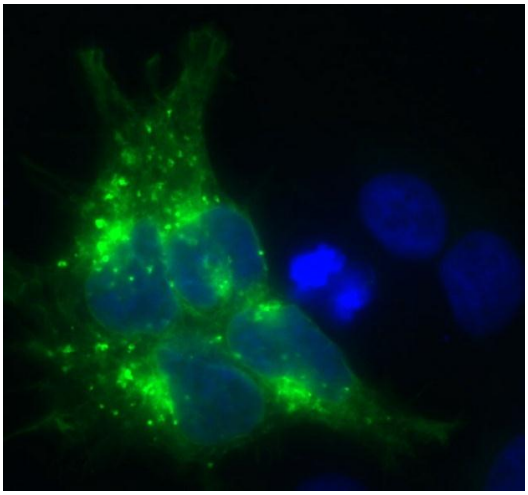

C.

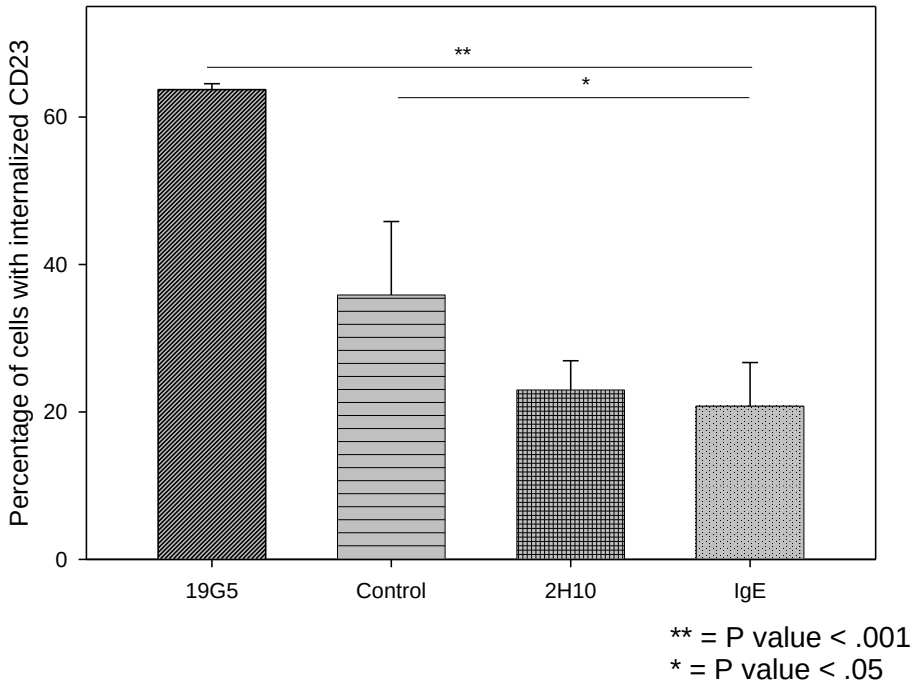

** = P value < .001
* = P value < .05

Table 2: Internalized CD23 localizes to endosome compartments. HEK 293T cells were transiently transfected with CD23-YFP and examined for CD23 internalization after 48 hrs. Cells were then stained with antibodies against different cellular compartments and their respective secondary antibodies. Percentage of cells with co-localization was determined, with a cell being counted as positive if any co-localization was determined. Data shown was the average of three independent experiments. Error represents standard deviation.

Table 2: CD23 localization

Marker	Compartment	% Co-localization with CD23
Calnexin	ER	11.7±0.71
Early endosomal Ag	Endosome	72.1±18.5
LAMP1	Lysosome	21.2±8.8
Rab11	Recycling endosomes/MVB	95.1±4.4

A. Correlation between CD23 internalization and CD23 cleavage - CD23 binding reagents have been defined previously according to whether they decreased or increased CD23 cleavage, these two activities were called stabilizing or destabilizing, respectively (40). To further investigate this phenomena, we first sought to confirm studies (36;118) that showed that anti-CD23 causes ligand internalization. mCD23^{+}-CHO cells were labeled with FITC-anti-CD23 (FITC-B3B4), which is an anti-lectin mAb, transferred to 37°C and internalization was followed (Figure 26b). Examination of orthogonal views demonstrated that the visualized punctate spots were found inside the cell after 30 minutes, while at 4°C (Figure 26a) they were still at the cell surface; thus, showing that CD23 is internalized following anti-lectin binding. To determine if there was a correlation between CD23 cleavage and internalization, 293T cells were transfected with CD23-YFP. Previous studies had shown that stabilizing CD23 with IgE or anti-lectin antibodies decreased CD23 cleavage while destabilizing antibodies increased cleavage (42;87). The CD23-YFP expressing 293T cells were then incubated with the indicated antibodies for 24 hours and examined by immunofluorescence. The percentage of cells with internalized CD23 was then determined and the data is summarized in Figure 27c. Examples of cells with CD23 still at the surface and after internalization are shown in Figure 27a and b respectively as well. We found that significant CD23 internalization occurs naturally even in the absence of ligand, however, anti-stalk mAbs (19G5) increased this internalization while IgE and the anti-lectin (2H10) decreased internalization compared to this control. Of note with anti-lectin mAbs and IgE there still is internalization as shown in Figure 27c it is just decreased as compared to control. As the anti-lectin and IgE were also found to act similarly, only IgE was used for the

remainder of the study. These data suggests that the stability effect on cleavage could be related to internalization. In additional studies, co-staining with antibodies against markers of different subcellular compartments was performed. This data is summarized in Table 2. CD23 co-localization with EEA1 and Rab11 indicating endosomal trafficking and is in agreement with previous work that showed CD23 traffics through the endosomal pathway (36;118).

B. Enhanced internalization correlates with enhanced sCD23 production - Previous studies have shown that subsequent to the internalization of CD23-bound IgE/antigen complexes, some CD23 eventually recycled back to the cell surface (36). Thus to determine if the internalized CD23 as seen in Figure 28 was related to the fragments found in the supernatant or if it is recycled, cells were treated with antibodies that stabilize (IgE) or destabilize (19G5) CD23 +/- NH_4Cl. NH_4Cl prevents the progression of proteins in the endosomal pathway by neutralizing the endosomal pH (119). As shown in Figure 28a, the enhanced CD23 cleavage that is characteristic of the anti-stalk mAb, 19G5 (87), is reversed in the presence of 10 mM NH_4Cl. In contrast, NH_4Cl treatment of $mCD23^+$-CHO where CD23 was stabilized with monomeric IgE had no affect with respect to sCD23 production (Figure 28b). Note also the amount of sCD23 released into the supernatant was significantly lower in cells where CD23 was stabilized compared to cells where CD23 had been destabilized. NH_4Cl treatment brought sCD23 release from cells in which CD23 was destabilized down to levels only 1.5 times (30 ng/ml vs 18 ng/ml) higher than that released from cells where CD23 was stabilized. In addition, this inhibition of enhanced CD23 cleavage is similar to what was seen with an

Figure 28: Intracellular compartments are important for the release of CD23 fragments. sCD23 ELISA of 8 hr cultures supernatant of mCD23^{+}-CHO cells ± 10 mM NH_4Cl treatment. CD23 cleavage was induced by the addition of a destabilizing antibody, 19G5 (A) or inhibited by the addition of IgE (B). (C) Using RPMI 8866, CD23 was destabilized with the addition of 11E10 (rat anti-human CD23 stalk antibody) +/- Chloroquine. sCD23 in the supernatant was then measured by ELISA. (D) Purified IgD+ tonsilor B cells were stimulated with IL-4, IL-21 and anti-CD40 for 8 hrs +/- NH_4Cl. sCD23 in the supernatant was then measured by ELISA. Error bars represent standard deviation. * = P value <. 05

A.

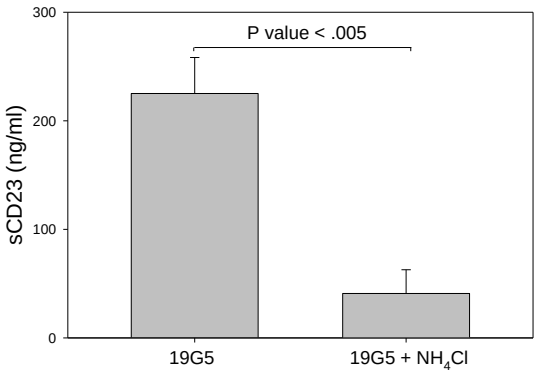

B.

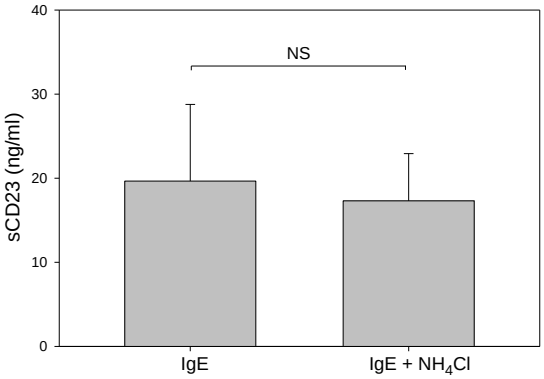

C.

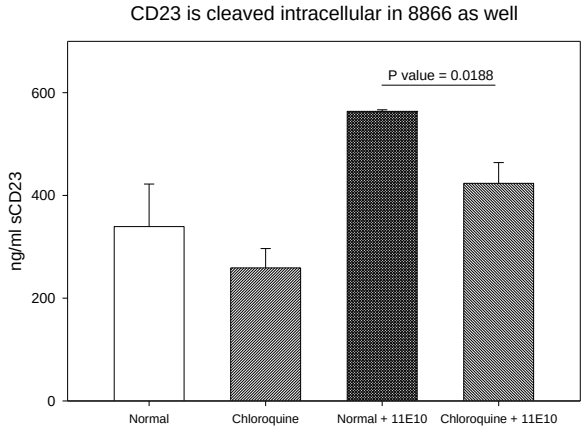

D.

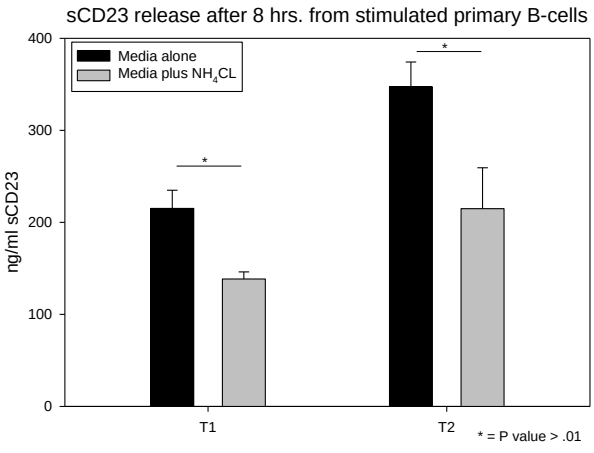

Figure 29: ADAM10 and CD23 interact inside the cell. (A) ADAM10-HA and CD23 doubly transfected HEK 293T cells were grown on coverslips and incubated with rabbit anti-HA (Red) and rat anti-mouse CD23 (Green); after washing detection was with PE-anti-rabbit IgG and FITC anti-rat IgG. (B) CD23 stably transfected MEFs derived from $ADAM10^{-/-}$ embryos (completely knockouts) (14) were stained with FITC-B3B4 and either left at 4°C or transferred to 37°C and examined after 30 min. Each of the above pictures is a representative of at least two independent experiments**.** (C) $CH23^{+}$-CHO cells were stained with an FITC-B3B4 and maintained at 4ºC. In B and C internalization was allowed for 45 minutes at 37 ºC. (D) Preincubated with 10 mM NH_4Cl for 30 minutes before staining and maintained in 10 mM NH_4Cl when transferred back to 37ºC. (E) Cells transferred to 37°C but not incubated with NH_4Cl. Pictures are a representative of three independent experiments. (F) The average number of cells under each condition that had internalized CD23 after 45 minutes. Shown is the average of at least 3 different experiments. Error bars represent standard deviation. ** = P value < .01

A.

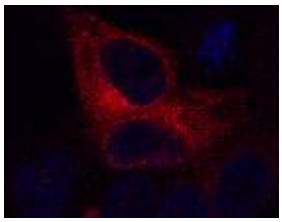

ADAM10

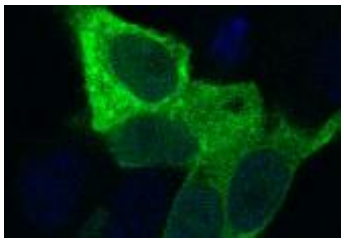

CD23

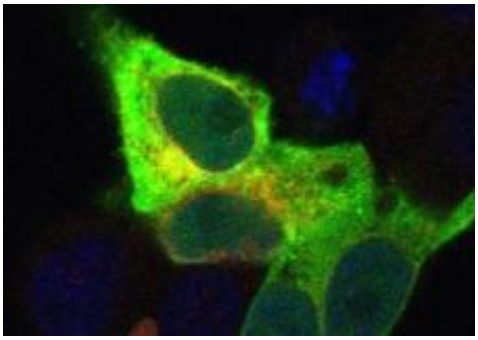

Merge

B

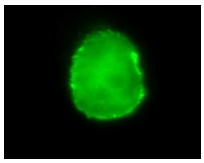

4°C

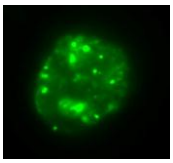

Transferred to 37°C

C

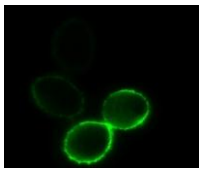

Maintained at 4°C

D

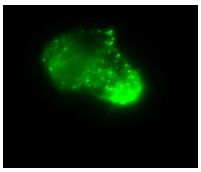

37°C + 10 mM NH_4CL

E

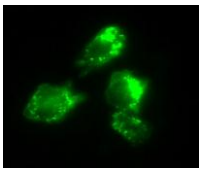

37°C media

F

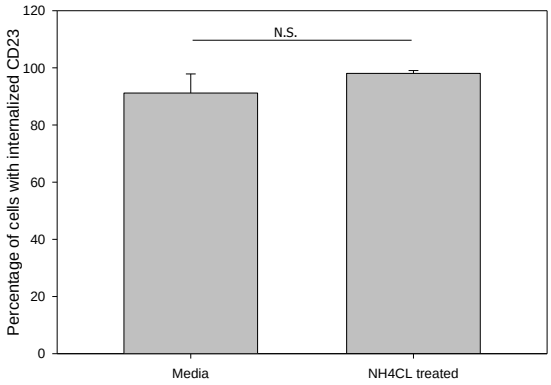

ADAM10 inhibitor (49). A similar trend was also seen in both primary human B cells and RPMI 8866 (Figure 28c and d) in which NH_4Cl caused a 50% drop in sCD23 similar to what was previously found with inhibition of ADAM10 (49). Thus, when internalization was inhibited, as seen with IgE in Figure 28c, the NH_4Cl effect is minimal and the converse is true when internalization is enhanced. To ensure that NH_4Cl was not simply blocking internalization, $mCD23^+$-CHO cells were stained with FITC-anti-CD23 in the presence or absence of NH_4Cl and then internalization was allowed (Figure 29c-e). This shows that NH_4Cl does not block ligand induced internalization and that the effect of NH_4Cl is related to neutralization of the intracellular compartments.

As stated in the introduction, the primary site of CD23 cleavage was thought to be the cell surface. Conversely, our data indicates that a majority of CD23 is internalized before it is released from the cell (Figure 27c). To determine where CD23/ADAM10 co-localization occurred, 293T cells were doubly transfected with ADAM10-HA and CD23. After 24 hrs the cells were co-stained for CD23 and ADAM10 (Figure 29a). CD23 was evident both on the cell surface and inside the cell. In contrast, ADAM10 was mostly intracellular, consistent with other reports (70). Co-localization was also primarily intracellular. This led us to hypothesis that ADAM10 has no role in the internalization of CD23. To confirm our hypothesis that CD23 internalization did not require ADAM10, $CD23^+$-$ADAM10^{-/-}$-MEFs were cultured with FITC-B3B4 as in Figure 27a and b and clear internalization was seen when bound by anti-CD23 (Figure 29b). Overall this figure shows that NH_4Cl blocks intracellular ADAM10 and CD23s interaction, suggesting that low pH might affect their interaction.

Figure 30: Full length CD23 was found in B cell secreted exosomes. Exosomes were isolated by ultracentrifugation as explained in the material and methods from overnight cultures of RPMI 8866 cells, a human B-cell line. (A) Exosomes were then overlaid onto a gradient of 2, 1.3, 1.16, 0.8, 0.5 and 0.25 M sucrose and spun overnight at 1 x 10^5 x g. One ml fractions were collected and added to four ml HBS and again spun for one hour at 1 x 10^5 x g. Pelleted samples were then analyzed by western blot with Rabbit anti-CD23. (B) The blot was stripped and also analyzed for ADAM10 with Rabbit anti-ADAM10. (C) To confirm that CD23 in exosomes was full length, cell lysate from RPMI 8866 were compared to CD23 from exosomes. (D) Exosomes from mouse $CD23^+$-CHO cells where CD23 had been destabilized with 19G5 were isolated, lysed in HBS containing 0.5% NP-40 and protease inhibitors. CD23 was then precipitated with 2H10-affi and visualized by western blot. For comparison, total CD23 was isolated from the same cells by immunoprecipitating $CD23^+$-CHO NP-40 lysates with 2H10-affi. The blots are representative of at least two experiments of similar design.

A.

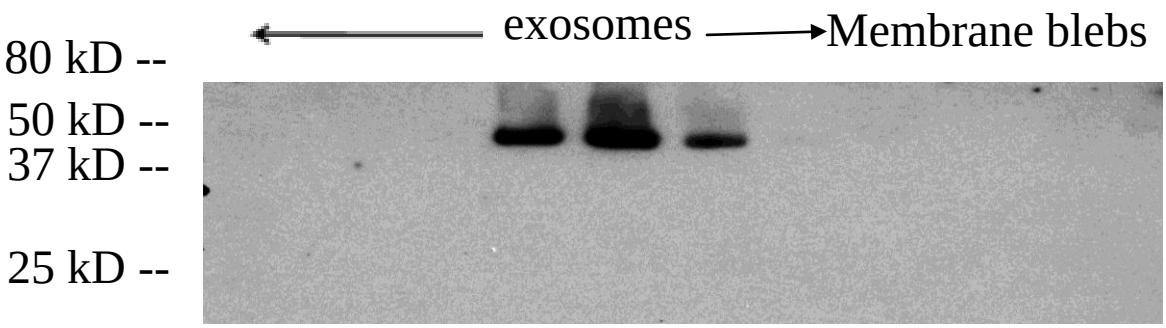

B.

C.

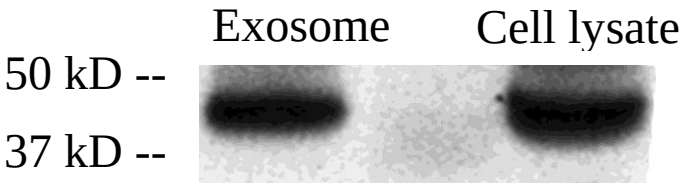

C

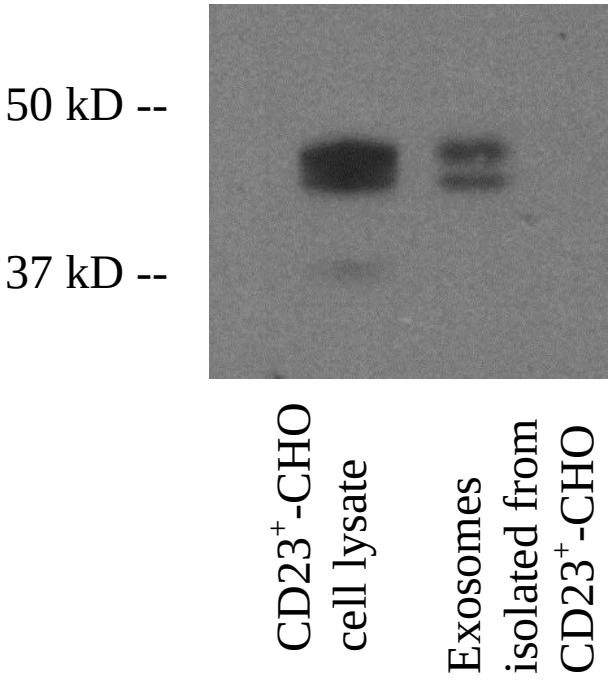

Figure 31: CD23 was cleaved in exosomes in an ADAM10 dependent manner. (A) Exosomes from RPMI 8866 supernatants were isolated and either lysed directly in SDS or resuspended in MES buffered saline (pH 5.8) plus 1% serum and cultured at 37ºC for either 5 or 30 sec. Cultures were then neutralized with tris buffer pH 8.0 and CD23 was immunoprecipitated with IDEC-152 (humanized anti-CD23 lectin), and analyzed for CD23 by western blot. (B) Exosomes were isolated and treated as in a, except this time they were resuspendend in normal RPMI buffer plus serum pH 7.4 and cultured at 37 ºC for 30 minutes, 1 hour and 17 hours. CD23 was then precipitated with IDEC-152 and analyzed for cleavage products by western blot. (C) Exosomes from surface biotinylated RPMI 8866 were isolated and resuspended in media ± 10 µM of ADAM10 inhibitor (INC008765) and incubated at 37ºC for 17 hours. Biotinylated proteins were then precipitated using avidin-agarose and analyzed for CD23 by western blot.

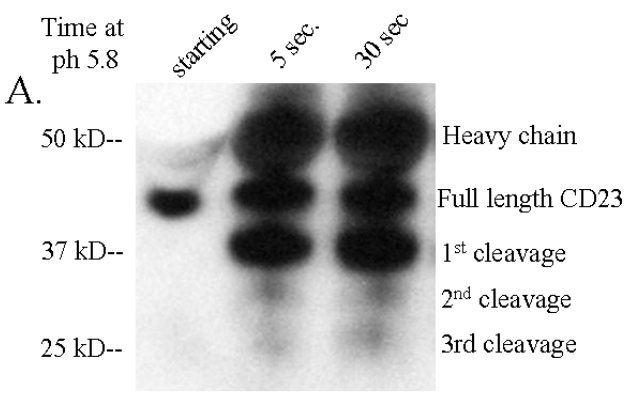

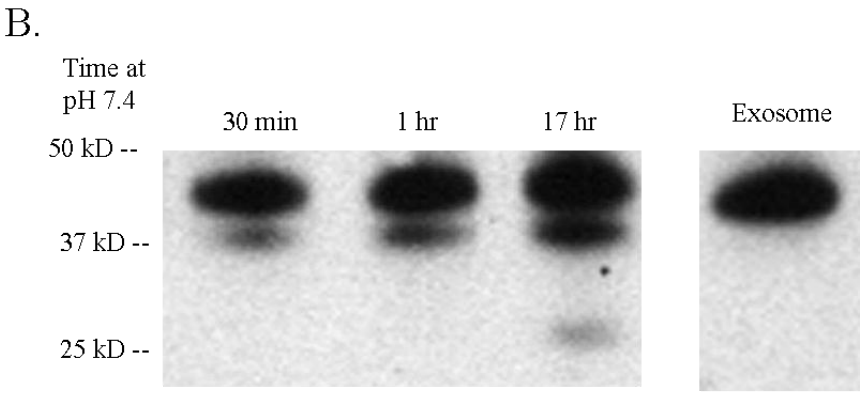

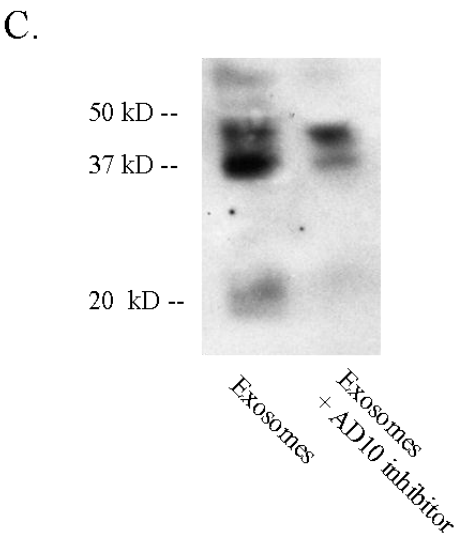

Figure 32: A Large percentage of sCD23 is exosome bound. (A) CD23 from RPMI 8866 cell free supernatant or supernatant where exosomes had been removed were precipitated with IDEC-152 and compared to CD23 from exosomes via western blot. The blots are a representative of at least two independent experiments. (B) $CD23^{+}$-CHO cells were treated with CoH2 (rat IgG control), IgE or 19G5 for 24 hours. Supernatant was then isolated and exosomes were removed, then by ELISA the amount of sCD23 was measured in the supernatant or exosome free supernatant and compared. Shown is the average of three experiments. Error bars represent standard deviation. * = P value < .05

A.

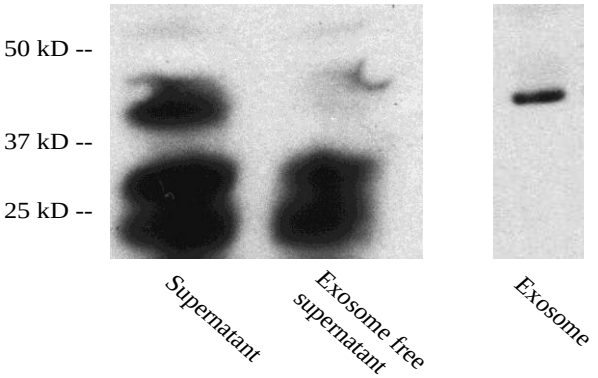

B.

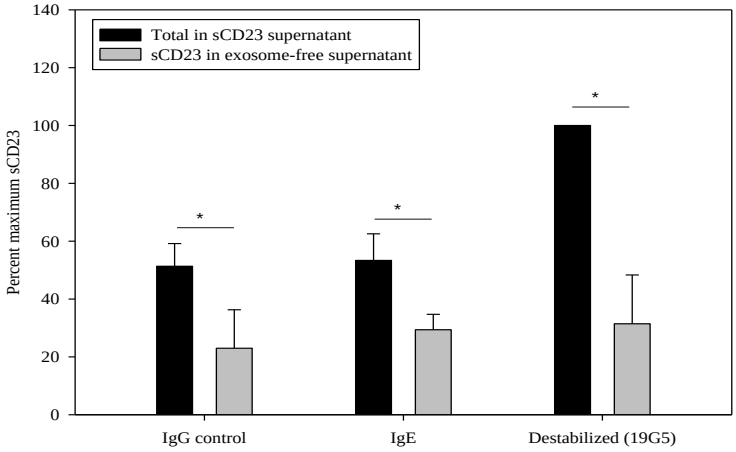

Figure 33: ADAM10 binding of CD23 was essential for sorting into Exosomes. (A) Purified mouse B-cells were isolated by fluorescence activated cell sorting using anti-B220. They were then stimulated with LPS/IL-4 for three days. Exosomes were then isolated from the supernatant and analyzed for CD23 and MHC class II expression. (B) Equal amounts of $mCD23^{+}$-CHO cells were treated overnight with normal IgG or antibodies that either stabilize (IgE) or destabilize (19G5) CD23. Exosomes were then pelleted and analyzed for the amount of CD23 by western blot. Shown is the average relative density of four independent experiments. (C) RPMI 8866 was grown for 24 hours in the presence of 10 µg/ml of either Coh2 or IgE. After 24 hours exosomes were isolated and analyzed by western blot for CD23 presence as explained in the material and methods. Shown is the average of three experiments. (D) $mCD23^{+}$-CHO cells were cultured ± 10 mM NH_4Cl and destabilizing antibody (19G5) overnight; exosomes were then isolated and examined for the presence of CD23 by western blot. Each blot is a representative of at least three independent experiments. Error bars represent standard deviation.

A.

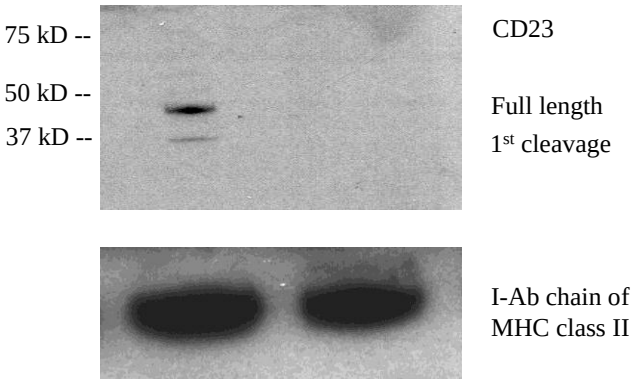

B.

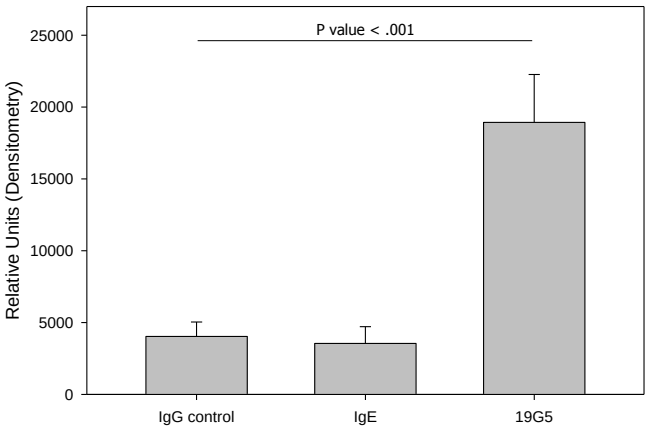

C.

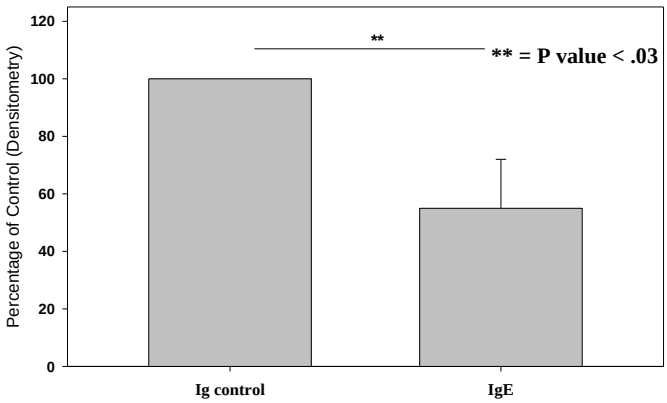

D.

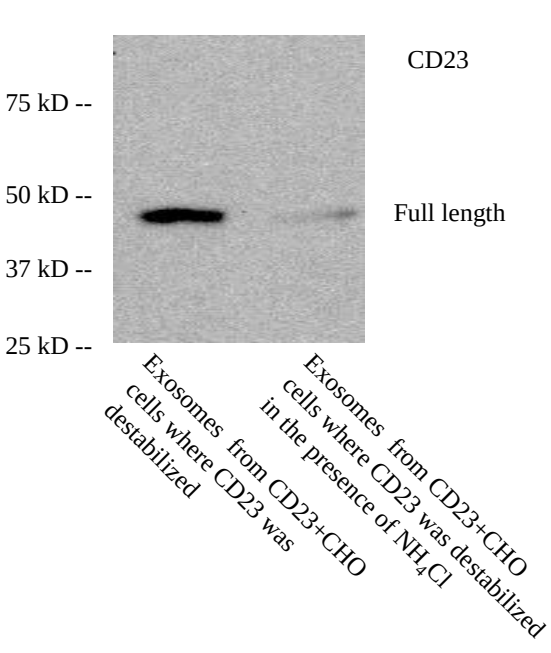

C. Full length CD23 is incorporated into exosomes - Recent reports have shown that multiple surface bound proteins, including MHC class I and II, and the B cell receptor can be internalized and released from cells in the form of exosomes (76). To determine if CD23 was also incorporated and/or released in exosomes, standardized numbers of RPMI 8866 cells were pelleted and exosomes were isolated from the cell free supernatants by ultracentrifugation as indicated in the experimental procedure. The pellet was resuspended and subjected to sucrose density gradient ultra-centrifugation. Fractions were collected and examined by western blot (Figure 30a). CD23 was found localized to the 1.12-1.16 M sucrose region, which is where exosomes are known to be found (70). The 1.3-2 M sucrose region, where membrane blebs localize, did not contain CD23. As exosomes have been shown to express ADAM10 (120), as a positive control the same fractions were also stained with anti-ADAM10 and a 60 kD protein, which corresponds to mature ADAM10, was detected (Figure 30b). Thus, both ADAM10 and CD23 were clearly associated with exosomes. Note that the CD23 is full length in that the molecular weight (mw) is 45 kD the same as that precipitated directly from cell lysates (Figure 30c). This would be expected, since membrane CD23 would be incorporated. Figure 30d represents an experiment where full length mouse CD23, from $CD23^{+}$-CHO cells is also shown to be found in exosomes. For Figure 30d, CD23 internalization was first stimulated by 16 hr culture with the anti-stalk antibody, 19G5. The higher mw of the two bands corresponds to full length CD23 (see Figure 30d) and this band is also seen when examining biotinylated CD23 isolated from cell surface biotinylated cells (not shown). The identity of the lower molecular weight band corresponds to endoH insensitive CD23 (121), and is thus presumably newly synthesized CD23. This band is not seen when

exosomes are isolated from either B cell lines or primary B cells (Figures 30a and 34a) but is only found in transfected cells (Figures 30c and 35) thus is most likely an artifact not seen in primary cells. Note also that CD23 inclusion in exosomes is not just an artifact of transformed cells as CD23 was also found associated with exosomes from primary mouse B cells (Figure 33a), nor is it specific to one species, as CD23 containing exosomes are secreted from both human and mouse B cells.

D. Demonstration of ADAM10 dependent cleavage of exosome CD23 - As the size of CD23 found in exosomes corresponded to full length CD23 (Figure 30c), we examined CD23 cleavage by ADAM10 post exosome incorporation. Exosomes from cultured RPMI 8866 cells were isolated from the supernatant and then resuspended for different periods of time in MES buffered saline (50 mM MES, 100 mM NaCl) (pH 5.8) or RPMI (pH 7.4) containing heat-inactivated fetal calf serum. After neutralization, all samples were kept on ice and CD23 fragments were isolated and examined by Western (Figure 31a and b). The results were quite striking. When the exosomes were resuspended in pH 7.4 there was minimal cleavage, even after overnight culture at 37°C. In contrast, the initial 37 kD cleavage fragment is rapidly apparent if the exosomes are resuspended at pH 5.8, which mimics endosomal conditions. Not all of CD23 is cleaved, which explains why some of CD23 is still released in the context of exosomes. Note also that the primary cleavage fragment observed is the first CD23 fragment reported by others (122). Some additional cleavage to 33 and 25 kD is seen, but this is relatively minimal. Inclusion of ADAM10 inhibitor in the exosome suspension blocked cleavage at pH 7.4 (Figure 31c). The data thus demonstrates that ADAM10 is much more active at endosomal pH and suggests that some CD23 cleavage would take place before the

exosomes are released from the cell. In addition, CD23 fragments were isolated from cell supernatant and exosome free supernatants using anti-CD23, and examined by western. In the exosome free supernatants the primary fragments were the 33 and 25 kD isoforms (Figure 32a), while in the complete cell supernatant a 45 kD isoform was also found. This larger fragment is most likely exosome bound. Finally when the amount of sCD23 found in exosomes versus the exosome free supernatant in $CD23^{+}$-CHO culture were compared the majority was found in the exosome fraction (Figure 32b). These results demonstrate that ADAM10 dependent cleaved fragments of CD23 seen in B cell cultures originates from the cleavage of exosome associated CD23 after intact CD23 was sorted into exosomes. The data further suggest that the later CD23 fragmentation primarily occurred post-exosome release and are probably ADAM10 independent. This hypothesis of the later fragmentation being ADAM10 independent is in agreement with previous findings (48).

E. ADAM10 was essential for sorting of CD23 into exosomes - Previously (50) B cells that lack ADAM10 were shown to have dramatically increased CD23 on the cell surface. In addition, the treatment of these cells with destabilizing antibodies did not cause an increase in cleavage (50) compared to WT. This indicates that ADAM10 might be important not only for cleavage of CD23, but also for sorting CD23 into exosomes. As seen earlier, (Figure 30d), full length mouse CD23 is also included in exosomes. Thus, to test our hypothesis that ADAM10 is required for inclusion in exosomes. B cells from CD19-$cre^{+/-}$-$ADAM10^{flox/flox}$ ($ADAM10^{-/-}$) mice and Cre-negative littermates, used as WT control, were isolated and stimulated with LPS plus IL-4 for three days. Exosomes were then isolated and the presence of CD23 was determined by western blot (Figure

33a). In both cases exosomes were secreted, as seen by the presence of MHC class II, however in the exosomes derived from the ADAM10$^{-/-}$ B cells, CD23 was not present. In addition, Figure 33b demonstrates that enhanced CD23 incorporation into exosomes is observed under destabilizing (19G5) conditions, compared to stabilized (IgE) or control (normal IgG). Additionally, when RPMI 8866 cells were treated with either IgE (JW8) or Ig control (Coh2), IgE decreased the incorporation of CD23 into exosomes (Figure 33c). Finally, CD23 inclusion in exosomes could also be blocked by culturing mCD23^{+}-CHO cells in the presence of NH_4Cl (Figure 33d). Overall, the data of Figure 32 and 33 suggest that CD23 is first incorporated in the MVB into exosomes, and secreted as intact exosome bound CD23. However, at endosomal pH, rapid ADAM10 dependent cleavage occurs. Once released, the initial cleavage is much more gradual, but is still ADAM10 dependent. These results thus showed that ADAM10 is essential for CD23 inclusion in exosomes, most likely through their direct interaction. These results, also demonstrate that a change in internalization of CD23 (see Figure 27c) would be reflected in the amount of CD23 in exosomes.

F. The interaction of ADAM10 and CD23 - We next sought to understand the mechanics of the ADAM10-CD23 interaction. All previously known ligands of CD23, including IgE, CD11, CD18 and CD21, bind CD23 in the lectin head. ADAM10 binds its substrates in a protease independent manner, where binding takes place in the disintegrin or cysteine-rich regions (67). To investigate the binding sites of ADAM10 and CD23 an *in vitro* assay was used where recombinant trimerized mouse CD23 was trapped on nitrocellulose in a dot blot approach. Then after blocking with nonspecific proteins, ADAM10 was allowed to interact. The ADAM10 protein used for binding was

Figure 34: CD23 and ADAM10 binding can be detected by Dot blot (A) *lz*-mouse CD23 starting at 1 mM in PBS was serially diluted 1:2 across the dot blot apparatus and trapped on the nitrocellulose by applying vacuum. Membranes were then removed and blocked in 5% milk in 1X HBS containing 0.05% Tween-20. In the upper western the binding of CD23 is demonstrated. ADAM10 cell lysate from 293-F cells transiently expressing mADAM10-HA was then added to similar CD23 coated membrane and allowed to incubate for 18 hrs at 4°C and then washed. ADAM10 binding was then measured using a Rabbit antibody against the C terminus end of ADAM10 and a HRP-Goat anti-rabbit IgG. In the lower blot, as a negative control BSA starting at 1 mM (shown to bind equally to the blot using Ponceau S staining) was added instead of CD23. (B) *lz*-human CD23 and cell lysates from 293-F expressing human ADAM10 was used as in a, to confirm that CD23 and ADAM10 in the human system also bind. (C) mADAM10-DN was used instead of full length ADAM10 and binding to CD23 was confirmed using the same antibodies as used in A and B. Each blot is a representative of at least three independent experiments.

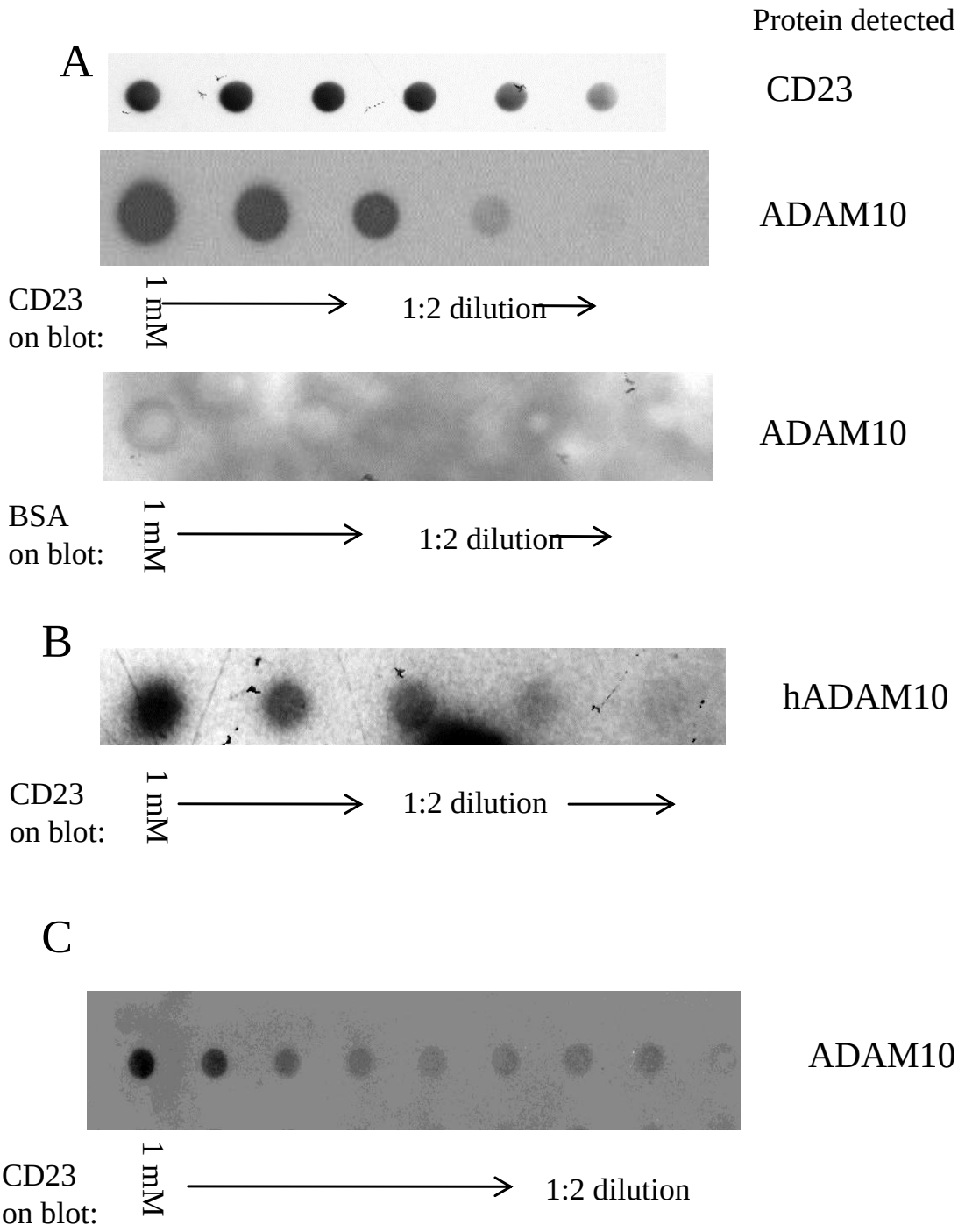

Figure 35: ADAM10 and CD23 co-precipitate from overexpressing cells. 293-F cells were transfected with mouse CD23 and mADAM10-HA. Then 48 hours later cells were lysed in 50 mM MES, 110 mM NaCl pH 5.8 containing protease inhibitors and 0.5% NP40. Cell lysate were spun to remove nuclei, and then split into 3 equal parts for IP and cell lysate. For IP 10 µg/ml of either 2H10 (rat anti-mouse CD23) or Rabbit anti-HA were added to the cell lysate and nutated at 4°C for 30 minutes, protein A/G was then added and nutated for an additional 30 minutes and then washed three times with HBS. Finally precipitated proteins were isolated by boiling the protein A/G bound proteins in SDS buffer and reducing agent for 10 min and resolved on SDS-Page. CD23 and ADAM10 were then detected with Rb anti-CD23 antibody followed by protein A/G-HRP or a mouse anti-HA antibody followed by a Goat anti-Mouse-HRP antibody respectively and compared to unfractionated cell lysate.

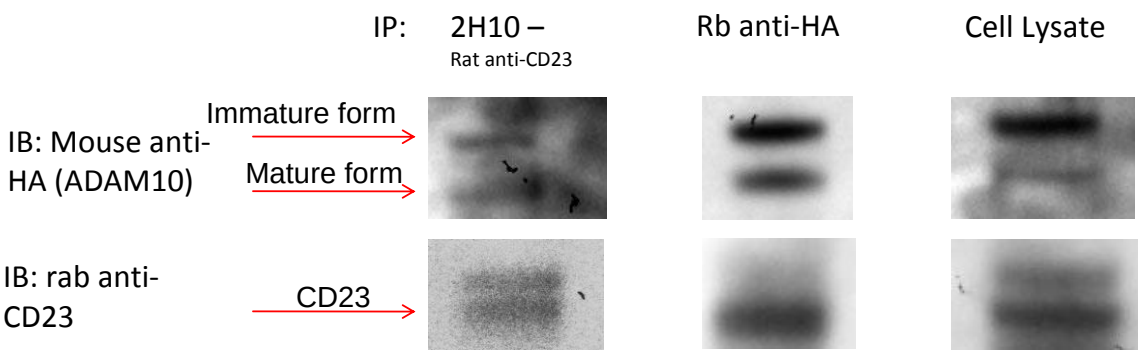

Upper band in CD23 is caused by different glycosylation in HEKs

Figure 36: ADAM10 binds the stalk region of CD23 (A) Mutant forms of CD23 (numbers indicate amino acids included) to determine where ADAM10 bound CD23 were added to the dot blot apparatus as explained in Figure 34 and binding was compared to the full length. (B) Shown is the relative density of the respective spots and is the average of two experiments. (C) Full length CD23 on blot was either stabilized or destabilized by incubation with IgE and 19G5 respectively, prior to the addition of ADAM10 and binding was compared to the untreated control; shown is the average relative density of three independent experiments. Error bars represent standard deviation.

A

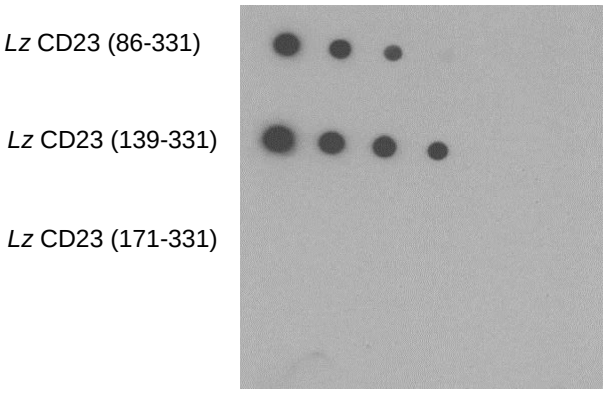

B

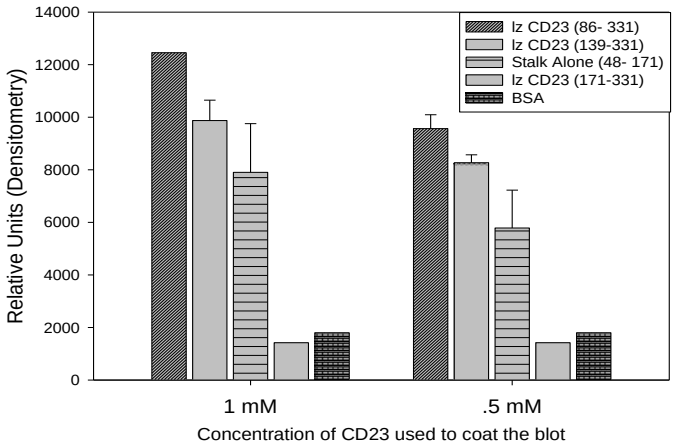

C

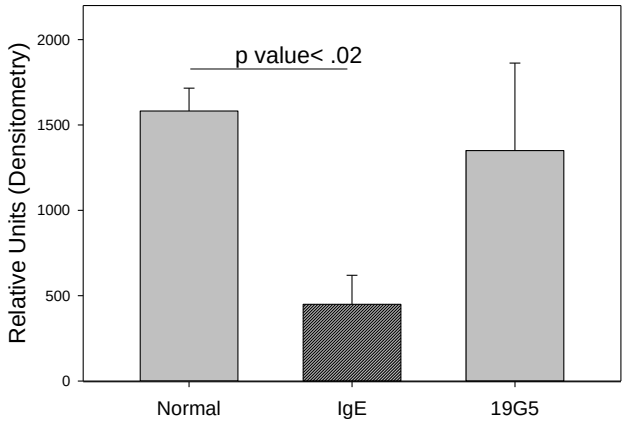

Figure 37: SPR shows ADAM10 and CD23 have a higher rMAX at low pH. (A) Dose response of rCD23 diluted in MES (pH 5.8) binding to rADAM10 bound to the CM5 chip. (B) Comparison of binding of rCD23 and rADAM10 when diluted in either MES (pH 5.8) or HEPES (pH 7.4). Shown is binding when 100 µg/ml of rCD23 was used.

A.

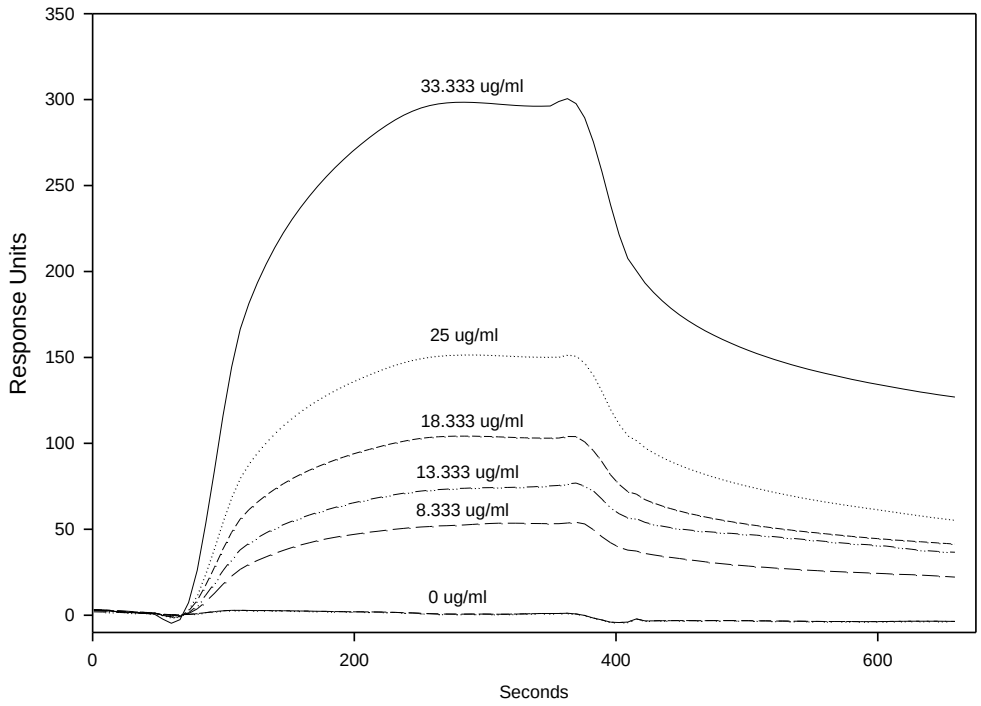

B.

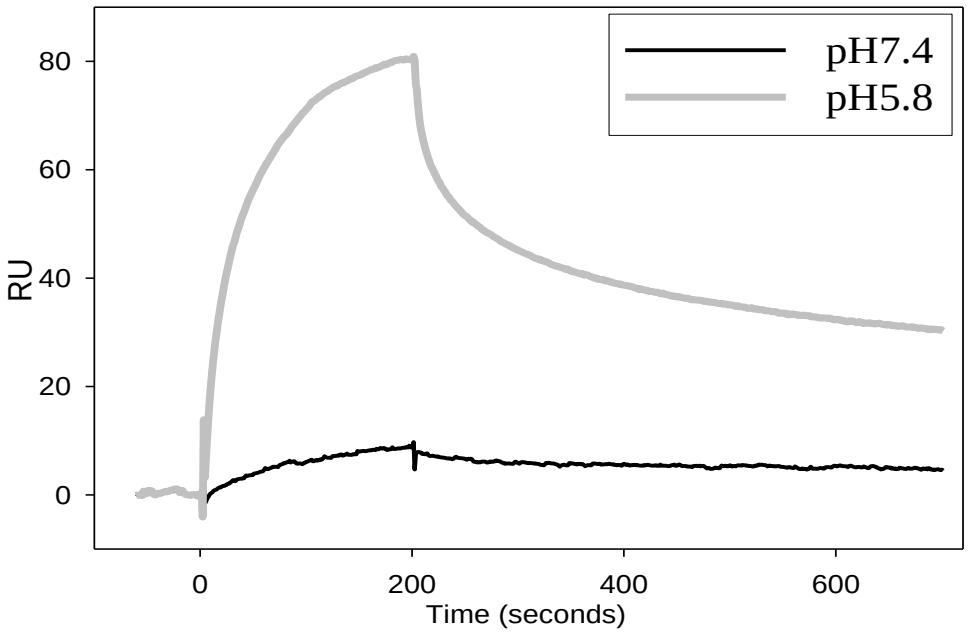

Figure 38: Analysis of SPR. 5-100 µg/ml of rCD23 diluted in either HEPES or MES buffer was flowed over chip bound rADAM10 as explained in Figure 37. Then using the SPR software the affinity and Rmax were determined using either (A) stead state analysis or (B) conformation change analysis. Error represents standard deviation.

`

A.

Steady state analysis

pH	K_a	Rmax
7.4	5.00E+05 ± 1.89E+05	52.6333 ± 8.530208
5.8	6.07E+06 ± 3.85E+06	410.475 ± 44.77292
P value	0.3202395114	0.0011250455

B.

Conformation change analysis

pH	K_a	Rmax
7.4	3.13E+06 ± 2.518E+06	16.14 ± 6.880494
5.8	3.93E+06 ± 4.15E+05	313.9 ± 91.21677
P value	0.700339868	0.008615

Figure 39: Proof of conformation change. To confirm that a conformation change was taking place between CD23 and ADAM10, 50 µg/ml diluted in MES (pH 5.8) and was flowed over rADAM10 for different periods of time (175, 500, 750, 1000, 1500 seconds). Off rates were then compared. (A) Dissociation curves (B) Dissociation rates. n=1

A.

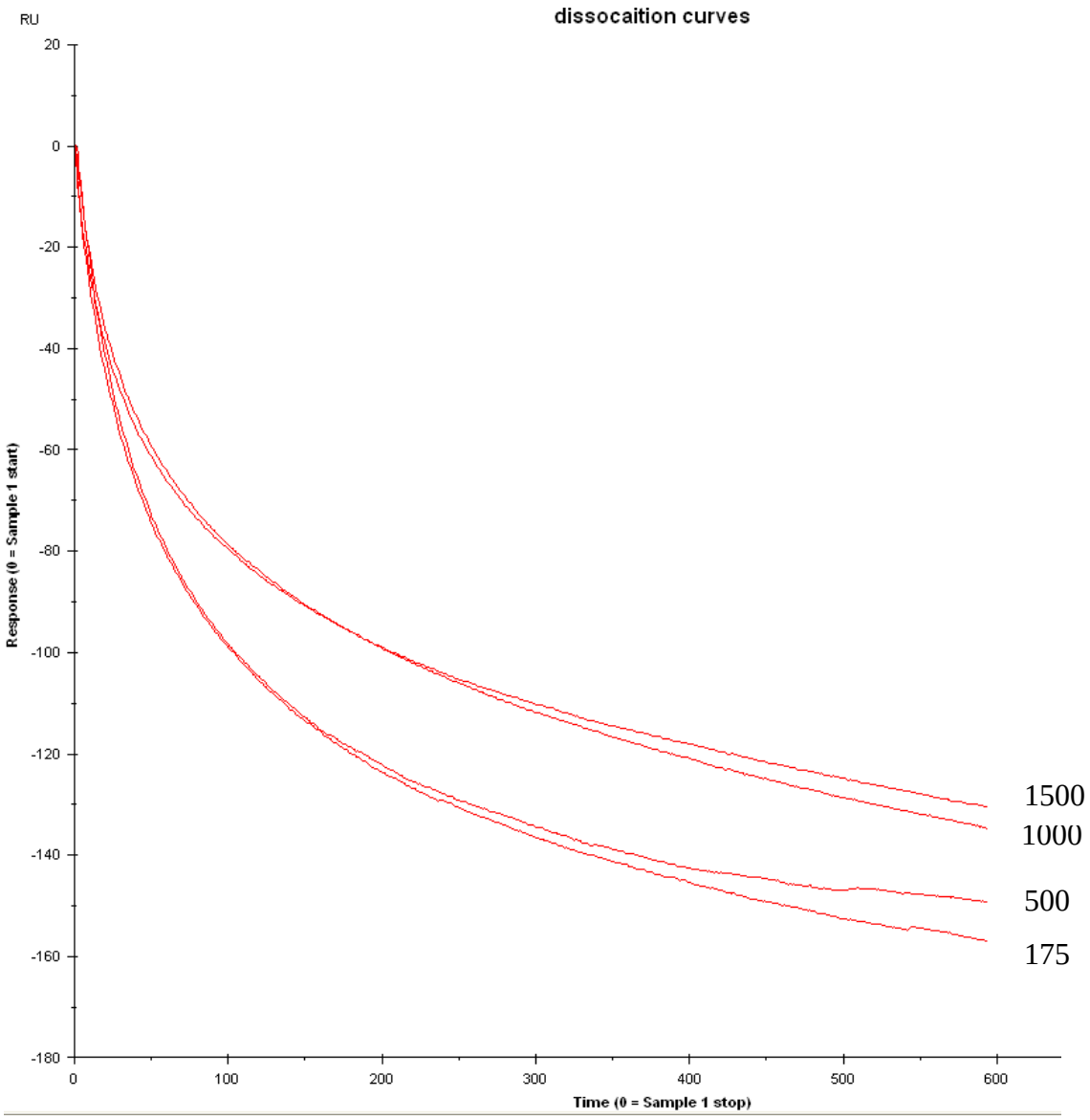

B.

Dissociation rate (Kd)	Injection time (s)
.002134	175
.001648	500
.001492	750
.001307	1000
.001381	1500

from the cell lysate of 293F cells overexpressing ADAM10. After washing, bound ADAM10 was detected using anti-ADAM10. Using this approach we first demonstrated that the CD23-ADAM10 interaction could be determined in this manner (Figure 33a), and confirmed previous data ((48) and Figure 35), that found that CD23 and ADAM10 were co-precipitated in overexpressing cells. Using the dot blot approach we also showed that human CD23 and ADAM10 also interact (Figure 34b). Next, to determine the regions of ADAM10 and CD23 important in binding, mutant recombinant fragments of ADAM10 and CD23 (where either the lectin head or sections of the stalk region of CD23 were removed) were used in the dot blot approach. For ADAM10 lysate from cells over-expressing DN-ADAM10 (123) was used and showed that ADAM10 binds CD23 in a protease independent manner (Figure 34c). For CD23 the mutant recombinants (shown in Figure 8) binding of ADAM10 were compared to full length CD23 (Figure 36a and b). The samples tested were *lz*-CD23$^{86-331}$, which represents full length trimeric CD23 (41); *lz*-CD23$^{139-331}$, which was the mutant form that still contained the ADAM10 cleavage site and still interacted normally with IgE (41); CD23$^{48-171}$, which is the stalk region alone; and *lz*-CD23$^{171-331}$, which lack the ADAM10 cleavage site and no longer interacts with IgE (41). In contrast to IgE and other CD23 binding partners that require the lectin head for binding, the CD23 stalk alone bound ADAM10; showing that ADAM10 binds in the stalk region of CD23. Data from the other mutant fragments showed that this binding takes place between amino acids 139-171 of CD23. These data help explain earlier studies that indicated that polyclonal rabbit anti-stalk blocked CD23 cleavage (40). This demonstrated that ADAM10 binds CD23 similar to how it does its other substrates, namely in a protease domain independent manner.

The dot blot approach was also used to determine if destabilizing (19G5) or stabilizing IgE reagents would influence the interaction of ADAM10 and CD23. As is seen in Figure 36c, 19G5 did not alter the level of interaction, further supporting the concept that "destabilization" really reflects increased internalization. Intriguingly, IgE did partially block the interaction of ADAM10 and CD23. This suggests that IgE inhibits CD23 cleavage in a dual manner, both by keeping CD23 at the cell surface (Figure 27c) and blocking ADAM10 interaction directly (Figure 36c).

To extend and confirm the interaction data SPR analysis was used. Recombinant ADAM10 was immobilized on a CM5 chip and allowed to interact with recombinant CD23. The soluble CD23 that was used was *lz*-CD23$^{139–331}$, which was shown previously to be the minimal amount of stalk to refold in a trimeric form capable of interacting with IgE (41). In addition, this was the minimal amount of stalk needed for ADAM10 binding (Figure 36b). As ADAM10 dependent CD23 cleavage was enhanced at endosomal pH (Figure 31a), CD23 was dissolved in either pH 5.8 (the pH of MVB (119)) or extracellular expected pH of 7.4. A dose response was seen for binding of CD23 and ADAM10 (Figure 37a). Steady state affinity measurements were not significantly different when comparing the values obtained at either pH (Figure 38a); however, the Rmax value was about an order of magnitude higher at pH 5.8. An example sensogram comparison at the two pH values is shown in Figure 37b. The large increase in Rmax indicates that the sites of interaction in CD23 and ADAM10 are more accessible at the lower pH, while the similar affinities indicate that once accessible, the binding strengths are not significantly different.

To attempt to determine the type of interaction that occurs between CD23 and ADAM10, several different models were used including 1:1, bivalent and conformation change binding. Conformation change was determined to have the best fit as determined by the Chi-squared value. To confirm that at the lower pH, CD23 and ADAM10 are truly undergoing a conformation change, and cause the higher Rmax, previously a method was developed by Lipschultz and Smith-Gill (107). They showed that proteins can interact in two states, either the state where conformation change has not taken place or after conformation change takes place. This change in conformation can be seen as a change in off-rate over time. Thus the same concentration of CD23 can be flowed across rADAM10 for increasing time periods and the off-rates can then be compared to determine if a conformation change is taking place. As shown in Figure 39a, this is exactly what we found. When the off rate was determined using the biacore software (Figure 39b) there was about a 35% change in off-rate when more of the proteins were interacting after conformation change. When the affinity and Rmax were then analyzed with conformation change analysis, we found similar results about the CD23 and ADAM10 interaction as we did with steady state analysis (Figure 38b) that lower the pH increased the Rmax but not the affinity.

G. Function of CD23 in Exosomes: Previously Ford *et al.* (87) showed that the injection of 19G5 into mice increased the cleavage of CD23 and IgE synthesis when given in combination with antigen. As we have showed in Figure 27c and 33b, 19G5 causes increased production of sCD23 by increasing the internalization and thus inclusion in exosomes. We thus hypothesized that the mode of action of 19G5 worked *in vivo* is to increase the levels of CD23+-exosome in serum. These exosomes could then bind the

Figure 40: CD23 is not contained in exosomes 5 days after 19G5 injection *in vivo*. As previously shown in (87) when 19G5 is injected in mice there is a large increase in sCD23. To determine if this sCD23 was mostly exosome bound as we found *in vitro,* 19G5 was injected IP into WT BALB/C mice on days 0 and 2 then 3 days after the final injection mice were sacrificed and cardiac punctured. The exosome fraction from the serum was then isolated and compared to the non-exosome fraction for CD23 expression by western blot. 19G5 was injected into two different animals and both are shown.

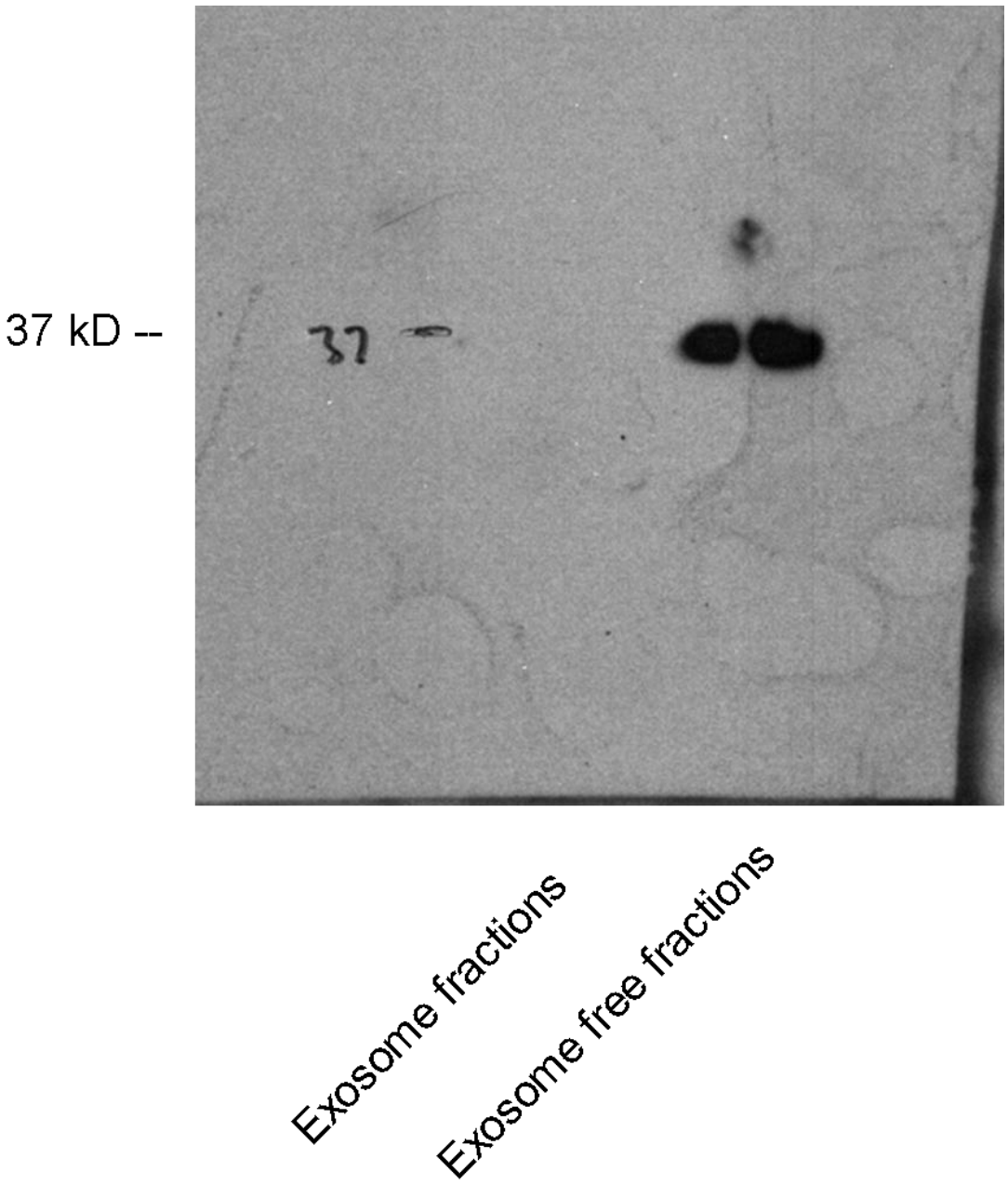

minimal IgE bound to antigen; these exosomes would then be taken up by dendritic cells and increase antigen presentation, leading to increased T cell response, cytokine production and IgE synthesis. To test this BALB/C mice were injected with 19G5 on days 1 and 3 and then on day 5 mice were bled and serum was collected. The serum was then fractionated into exosome and exosome-free fractions and CD23 was purified and analyzed by western blot. Unfortunately, all of the CD23 was found in the exosome-free fraction (Figure 40). This could be because by day 5 all of the exosomes had either been phagocytosed or cleaved by serum proteases.

III. Cytokine increase of ADAM10 could potentially be affecting IgE production.

In the above two sections, we have shown that inhibiting ADAM10 blocks IgE dependent disease potentially in two ways. First off, as cell surface bound CD23 is increased there is a corresponding decrease in IgE. Secondly, as ADAM10 is required for sorting CD23 into exosomes, which are potentially involved in increasing immune reactions, inhibition of ADAM10 would decrease inflammation. As stated earlier, ADAM10 is also known to be increased in the context of inflammation (83). These data thus show that increases ADAM10 levels could potentially also increase the inflammatory response, and thus shows that understanding what effects the expression of ADAM10 is important.

A. Effects of cytokines on ADAM10 expression. Previously Prinzen *et al.* (108) has shown that retinoic acid can increase the activity of the ADAM10 promoter. In B cells it is known that activation increases CD23 expression, then after class switching there is a loss of CD23 from the cell surface (124). We would thus hypothesize that ADAM10 levels might follow the same expression pattern. Using bioinformatics, we

Figure 41: Confirmation that clone #4 has highest Luciferase activity. After transfection of RPMI 8866 and drug selection, cells were plated at a single cell/well. Then multiple clones were screened for their expression of Luciferase activity, shown are two of these clones.

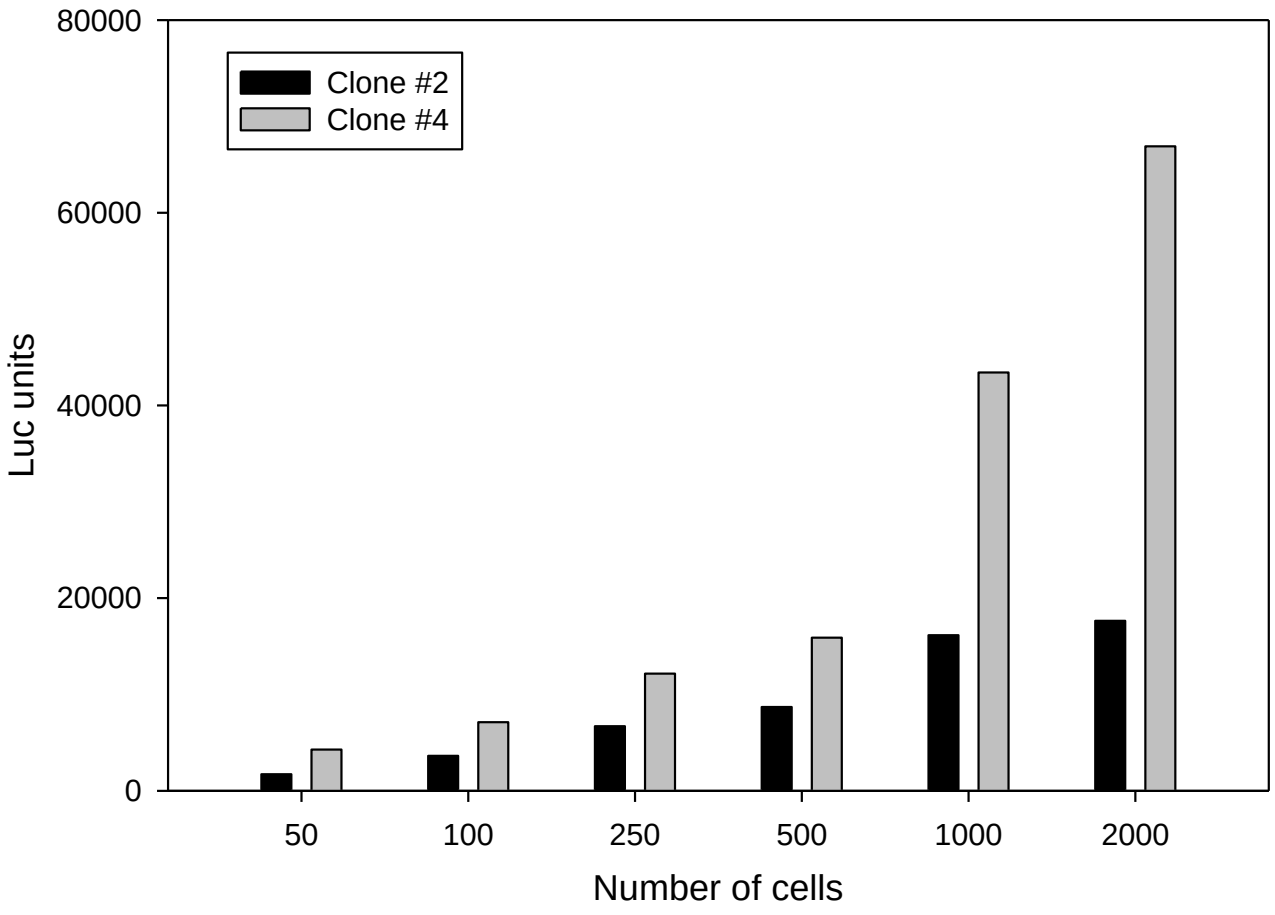

Figure 42: IL-4 only transiently changes ADAM10 expression and promoter activity. RPMI 8866 stably expressing the Luciferase gene under the control of the human ADAM10 promoter were stimulated with (A) 10 ng/ml of IL-4 and promoter activity was compared and normalized to unstimulated cells (shown is only the activity after stimulation with IL-4). (B) Promoter activity was determined after stimulation with 10 ng/ml of IL-13. Shown is only curve that has been normalized to promoter activity in unstimulated cells. (C) Primary B cells were stimulated with IL-4 alone and mRNA was isolated at different time points and compared to unstimulated cells using qRT-PCR as explained in the material and methods. Error bars represent standard deviation.

A.

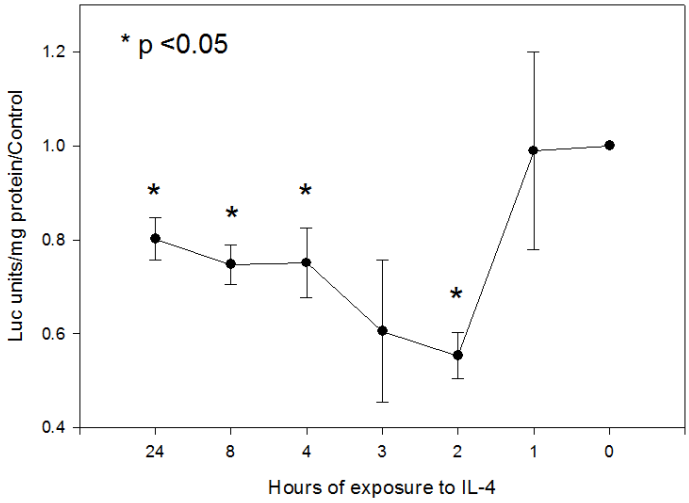

B.

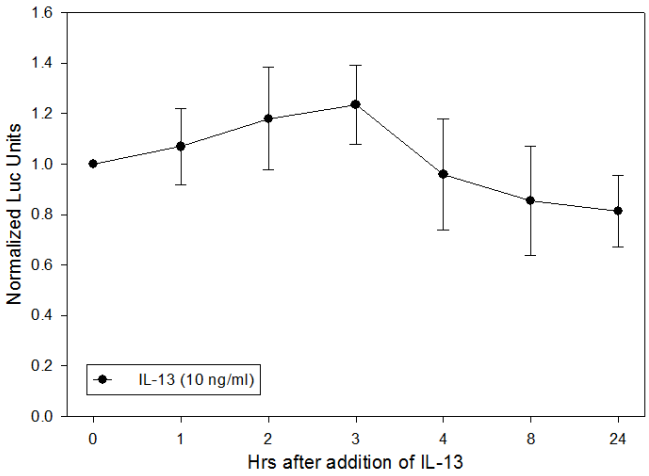

C.

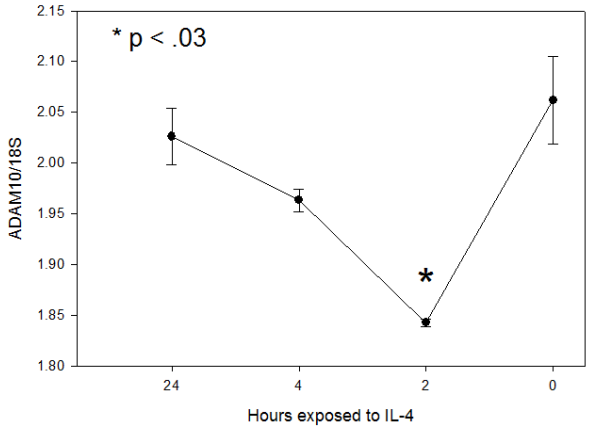

Figure 43: IL-21 increases promoter activity and mRNA expression. RPMI 8866 stably expressing the Luciferase gene under control of the ADAM10 promoter as explained in figure 41, were stimulated with (A) 25 ng/ml of IL-21 and compared to unstimulated cells. Shown is the average of two experiments. (B) Primary B cells were stimulated with 25 ng/ml of IL-21 alone or left unstimulated for 8 hours. mRNA was then isolated and ADAM10 levels were determined by qRT-PCR. Experiment was preformed once. Error bars represent standard deviation.

A.

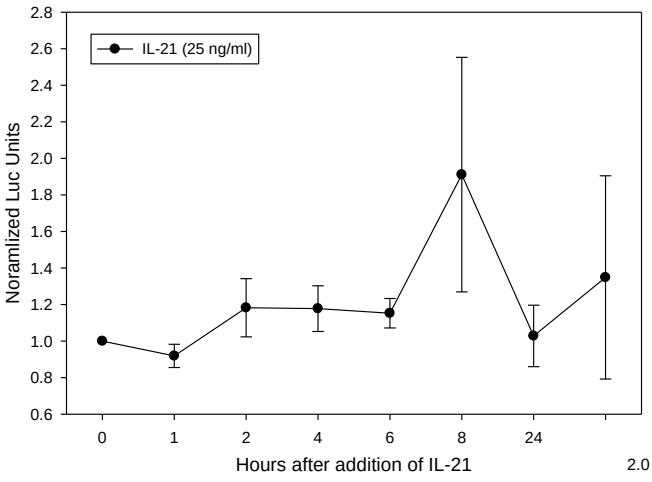

B.

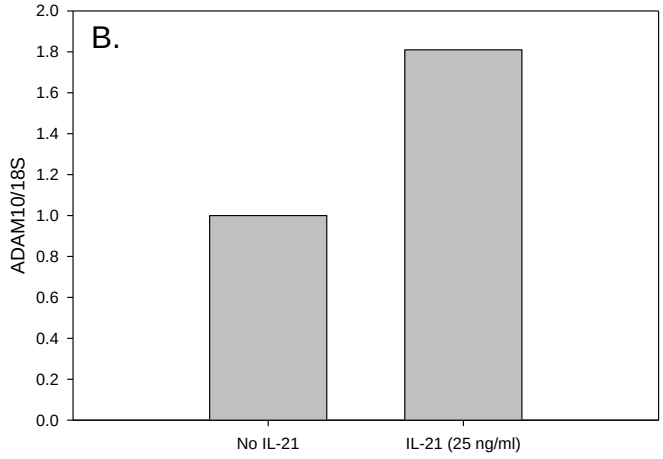

Figure 44: anti-CD40 also increases promoter activity, sCD23 and ADAM10 protein levels. RPMI 8866 stably expressing the luciferase gene under the ADAM10 promoter as explained in Figure 41 were stimulated (A) with anti-CD40 for 8 hours, and then compared to unstimulated control. To determine if this signaling was through the NFκB pathway in parallel experiments the Bay inhibitor was included at a concentration of 1 μM, n=1. (B) To determine if anti-CD40 also increased ADAM10 activity, RPMI 8866 at 50,000 cells/well were stimulated with anti-CD40 then 24 hours later the supernatants were collected and compared to unstimulated cells used as a control. (C) To determine if IL-21 and/or CD40 signaling were also having an effect on ADAM10 protein levels. RPMI 8866 cells were stimulated with anti-CD40 and IL-21 and then 24 hours later ADAM10 levels were determined by flow cytometry as explained in the material and methods. Error bars represent standard deviation.

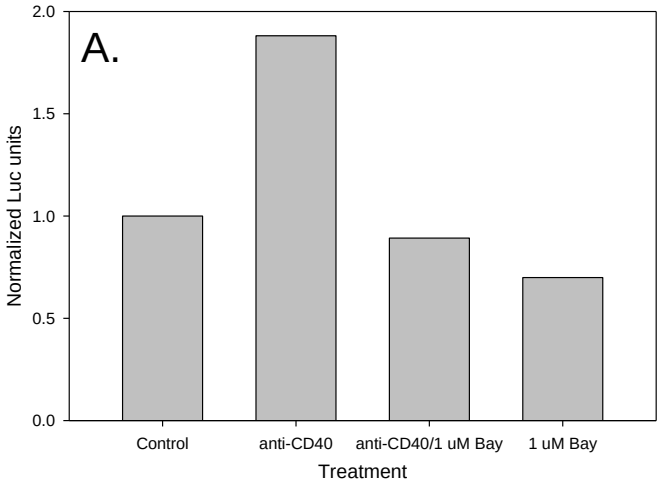

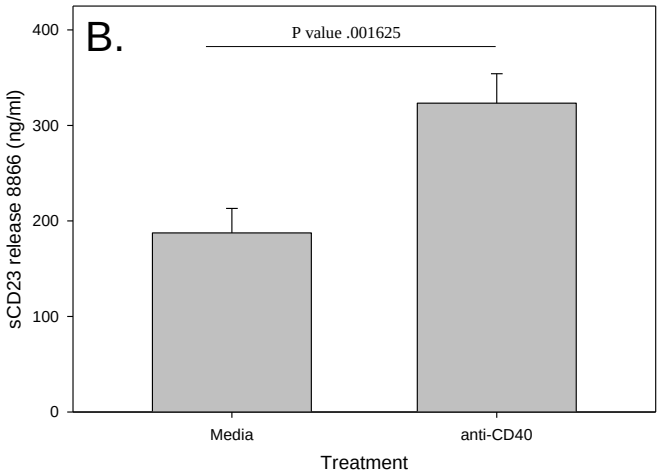

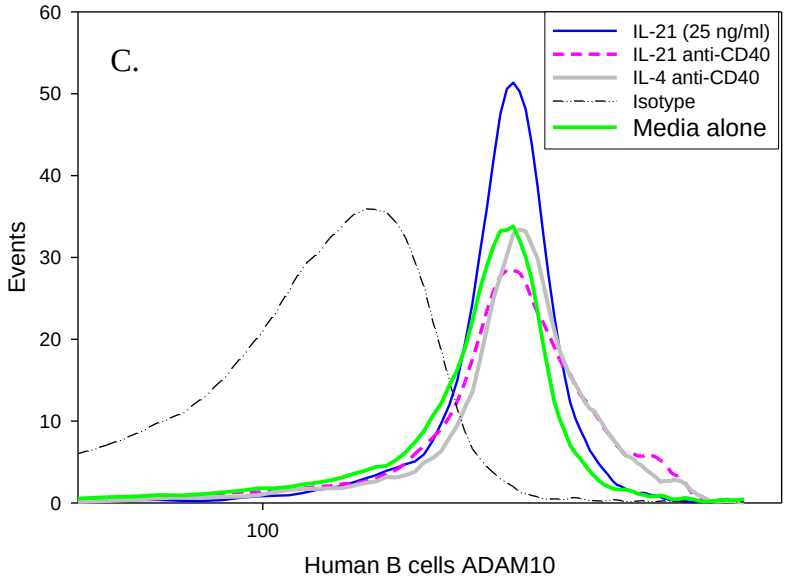

found that the human ADAM10 promoter contained several putative transcriptional factor binding sites, including GATA1, 2 and 3, Statx and NF-κ. Also in the studies by Prizen *et al.* (108) she had found that at least in HEK293 cells the region between 300 and 433 upstream of the transcriptional start site were most important for ADAM10 promoter activity. Thus we hypothesized that cytokines such as IL-4 which signaling causes the phosphorylation of Stat6 could possibly be regulating ADAM10 expression. The human ADAM10 vector, graciously provided by the Prinzen laboratory, was used to transfect RPMI 8866 cells to test our hypothesis that cytokines change ADAM10 promoter activity and ultimately expression. Transfected cells were then cultured with IL-4 (Figure 42a), IL-13 (Figure 42c), IL-21 (Figure 43) and anti-CD40 (Figure 44) to determine their respective effects on the ADAM10 promoter. As a control, cells were dually transfected with a vector expressing Renilla Luciferase to standardize our samples. Twenty-four hours after stimulation, promoter activity was determined and compared to unstimulated cells. These results (not shown) showed us initially that cytokines do have effects on ADAM10. However, transient transfection does not allow studying of the promoter beyond about 2 days. Additionally, with each transfection there is a difference in efficiency, thus making it hard to compare results. We therefore created a cell line stably expressing the luciferase gene under control of the ADAM10 promoter. These cells were then stimulated with the different cytokines stated above and compared to unstimulated cells. IL-4 was found to transiently decrease the promoter activity (Figure 42a), which also corresponded to a slight transient decrease in the mRNA levels (Figure 42b). Previously it was also found that IL-4 does not have an affect on protein levels of ADAM10 (48). Similar results were also found with IL-13 (Figure 42c). In contrast to

IL-4, IL-21 increased ADAM10 promoter activity as well as mRNA level (Figure 43a and b). Additionally we also found IL-21 increased the expression of ADAM10 (as seen by FACS (Figure 44c)). Anti-CD40 also increased ADAM10 promoter activity. This increase could be blocked by the addition of 1 μM of Bay inhibitor (11-7082, blocks IκB phosphorylation) (Figure 42a), thus showing that anti-CD40 was increasing ADAM10 promoter activity through NFκB signaling. Anti-CD40 also increased the levels of ADAM10 mRNA (Figure 44b) and protein expression (as seen by FACS (Figure 44c)). A caveat to these studies is that unstimulated RPMI 8866 have high levels of ADAM10, thus making it difficult to determine if the addition of cytokines was causing significant difference. Overall this data shows that some cytokines and membrane bound proteins can increase ADAM10 expression.

B. Effects of ADAM10 inhibitors on immunoglobulin production.

We found that inhibition of ADAM10 decreased IgE in the BALF compared to DMSO treated mice (Figure 21e) as well as the signs of experimental asthma (Figure 21). Additionally, we also found that cytokines affect the expression ADAM10. We thus sought to determine if blocking ADAM10 with an inhibitor would decrease the IgE production of primary tonsillar B cells cultured in activating condition. First to determine the correct concentration of inhibitor to use in these studies, we tested sCD23 release using increased doses of inhibitor. B cells were incubated for 5 days plus or minus three different inhibitors, the Glaxo ADAM10 inhibitor, the Incyte ADAM10 inhibitor or the Incyte ADAM17 inhibitor (included as a negative control) (Figure 45a). We found the Incyte ADAM10 inhibitor had an IC50 in the range of 5 μM, this concentration is very selective for ADAM10 (91). For the Glaxo ADAM10 inhibitor the IC50 was about 1.25

Figure 45: Dose response of ADAM10 inhibitors. (A) Primary B cells plated at 50,000 cells/well stimulated with 10 ng/ml of IL-4, 200 ng/ml of IL-21 and 1 µg/ml of anti-CD40 were cultured with different doses of either the Incyte or Glaxo ADAM10 inhibitors or the Incyte ADAM17 inhibitor (as ADAM17 is known not to be involved in CD23 cleavage, this inhibitor was used as a negative control) in order to determine the correct dose of inhibitor to inhibit sCD23 release. Supernatant was isolated after 5 days of culture and sCD23 levels were tested by ELISA and compared to control untreated cells. (B) Similar experiment as in A except cells were plated at 12,500 cells/well and isolated at day 14 and tested for immunoglobulin production by ELISA. Error bars represent standard deviation.

A.

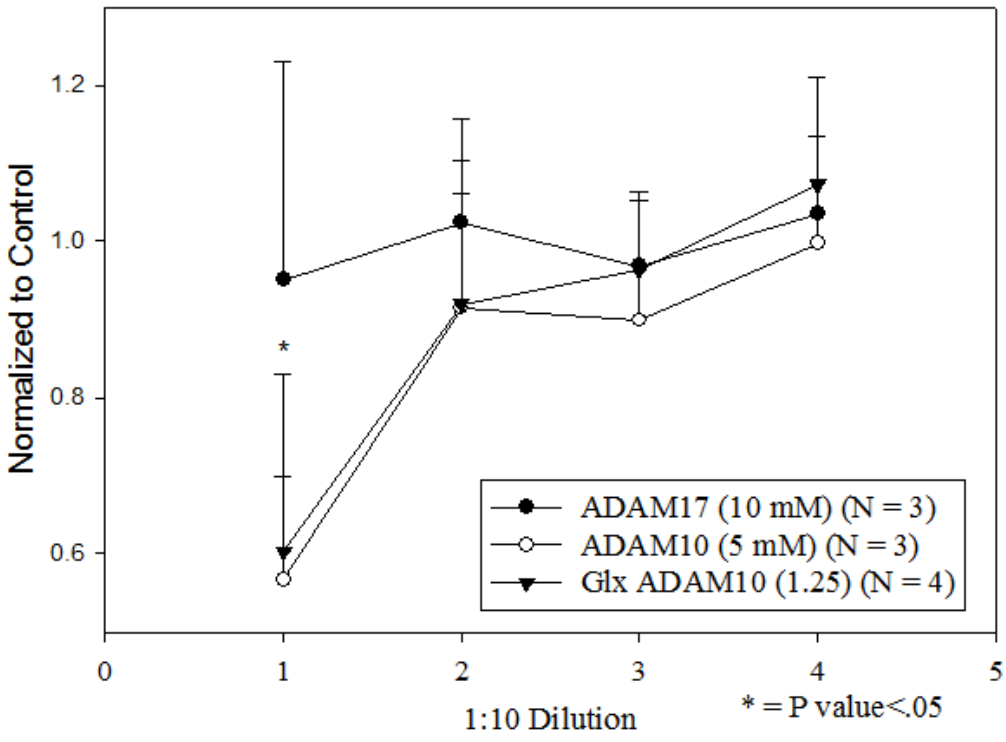

B.

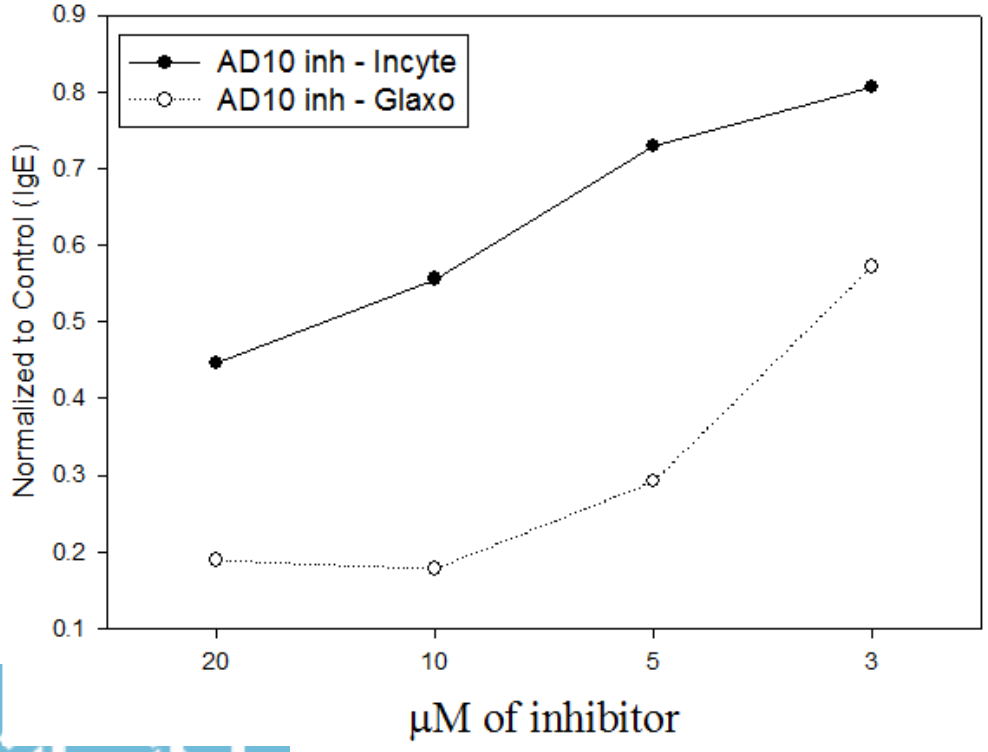

Figure 46: ADAM10 inhibitors decrease sCD23 and IgE but not proliferation. (A) Primary B cells plated at 12, 500 cells/well were stimulated as explained in Figure 45b +/- the Incyte ADAM10 inhibitor (INC008765) (10 µM). Production of immunoglobulin and sCD23 as measured by ELISA were normalized to the cells treated with equal amounts of DMSO and then averaged. Proliferation was determined by H^3-thymadine incorporation as explained in the Material and methods and was again normalized to cells treated with DMSO. (B) (ADAM10 is referred to as AD10 in this panel) Similarly to A except this time peripheral blood mononuclear cells (PBMC) isolated from whole blood as explained in the material and methods were plated at 300,000 cells/well and again stimulated with IL-4, IL-21 and anti-CD40 were used. Levels of IgE production were then measured on Day 14 and compared to DMSO treated cells. Shown is the average of three experiments. (C) To determine if inhibition of ADAM10 was affecting cell division, primary tonsilor B cells were stained with CFSE prior to being plated at 12,500 cells/well and stimulated with IL-4, IL-21 and anti-CD40. On day 5 cells were isolated and the number of cell division was then determined by flow cytometry as explained in the material and methods. Error bars represent standard deviation. * = P value < .05, ** = P value < .01.

A.

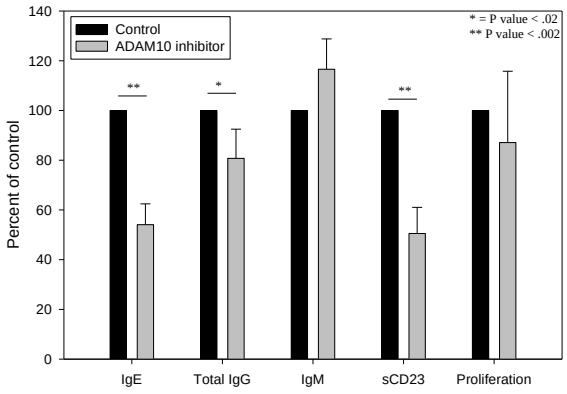

B.

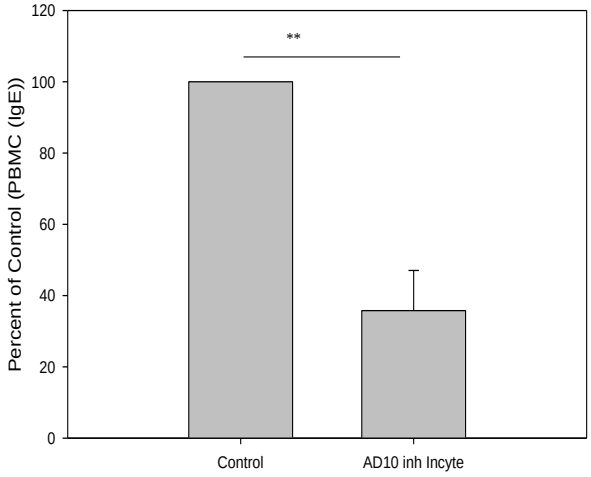

C.

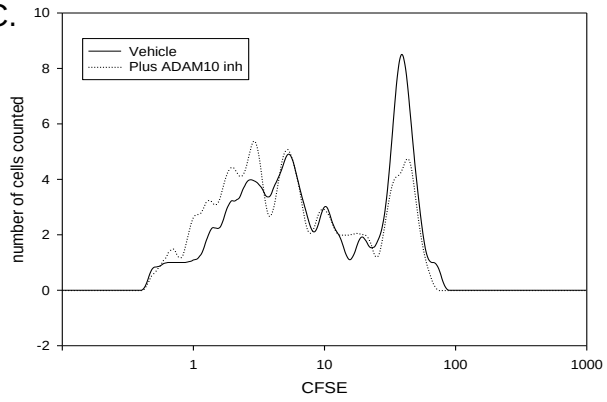

Figure 47: The number of IgE secreting cells is unaffected by the addition of ADAM10 inhibitors. (A) Primary tonsilor B cells were plated and stimulated as described in figure 45b and immunoglobulin levels were determined by ELISA. (B) Using cells isolated from the same tonsil as in A in a parallel experiment, cells were plated in triplicate at three different concentration as indicated in the figure and stimulated. Then on day 8 of the culture the cells were isolated and washed and restimulated with IL-4, IL-21 and anti-CD40. They were then replated on MultiScreen Filter plates pre-coated with mouse anti-human IgE (4.15) (5 µg/ml) and grown for 20 hours. Plates were then developed as explained the material and methods and spots (which indicates the number of IgE producing cells) were counted. (C) Same as B except with B cells were isolated from a second tonsil. Error bars represent standard deviation.

A.

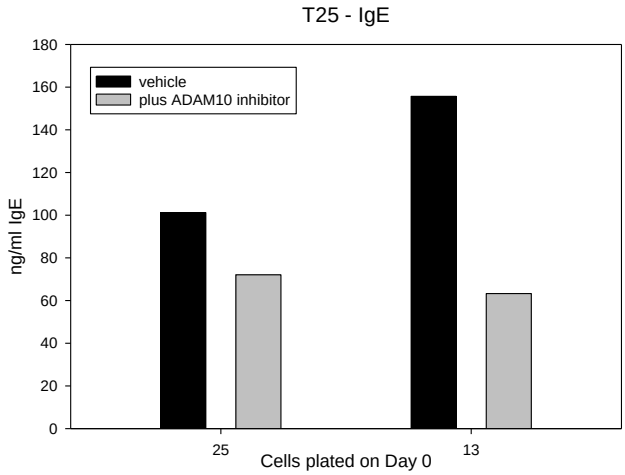

B.

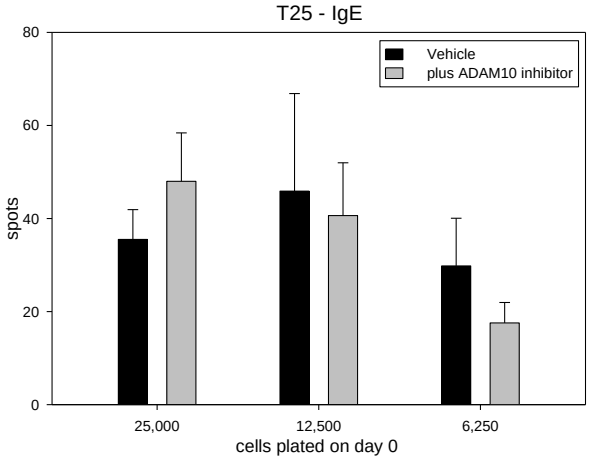

C.

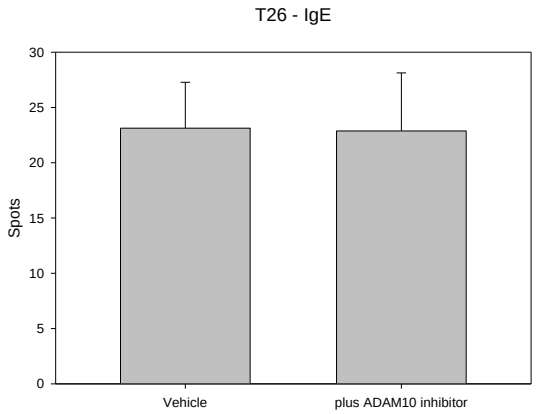

Figure 48: sCD23 does not rescue the ADAM10 inhibitor effect on IgE synthesis. B cells were stimulated +/- the ADAM10 inhibitor as explained in figure 45b. To determine if the decrease in immunoglobulin production was because of decreased sCD23, 2 µg/ml (approximately the decrease in sCD23 seen in cultures with the inhibitor compared to the vehicle control as determined by ELISA) of sCD23 (isolated from RPMI 8866) was added to the cultures treated with the ADAM10 inhibitor. Then on day 14 (A) IgG or (B) IgE levels were determined by ELISA. (C) To determine when ADAM10 was important in the production of IgE, the inhibitor was added on days 0, 5, and 8 of the culture and IgE levels were determined by ELISA on day 14. Shown are results from one experiment.

A.

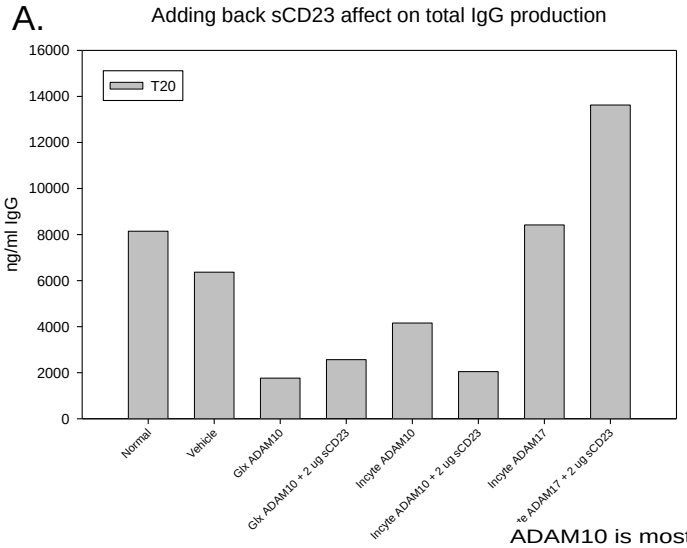

B.

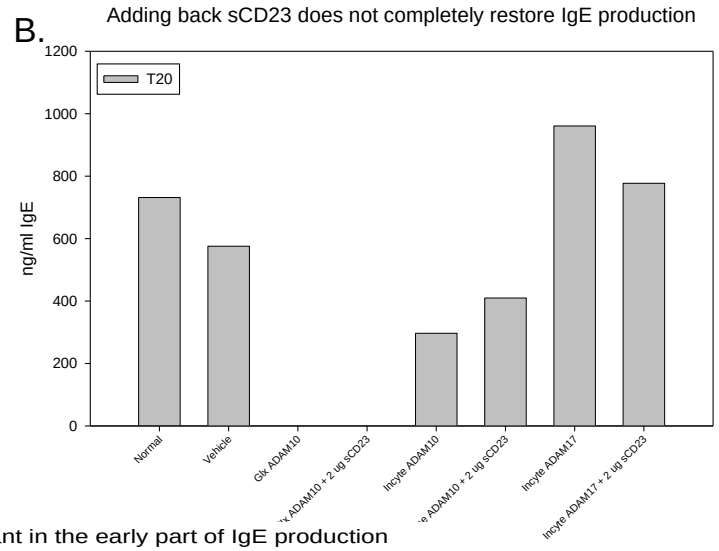

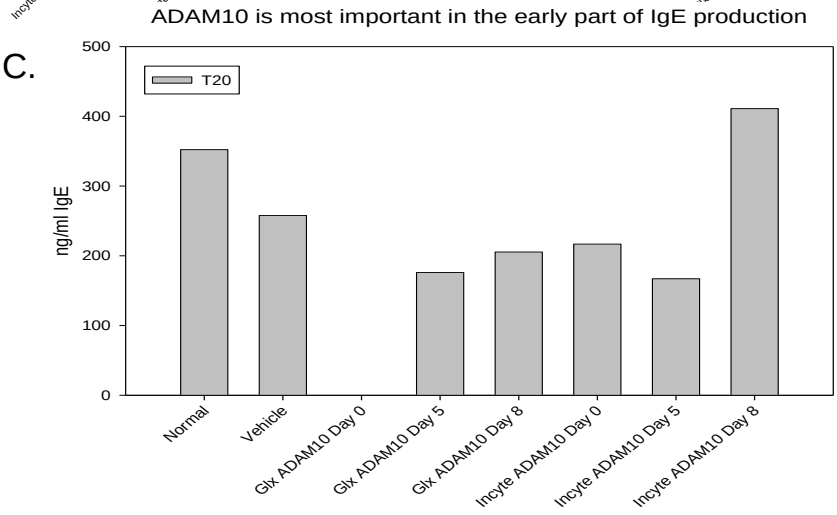

μM, however concentration above 2 μM are considered to not be selective for ADAM10 (125). When these same cultures were extended to 14 days and immunoglobulin levels were measured (Figure 45b), we found that blocking ADAM10's ability to cleave decreases the production of IgE. However, although the Glaxo inhibitor is was more effective at inhibiting IgE, it required levels that were not selective for ADAM10. Thus, most of the further studies were only done with the Incyte ADAM10 inhibitor. Figure 46a shows a combination of multiple experiments with the Incyte ADAM10 inhibitor (10 μM) and shows that inhibiting ADAM10 decreases IgE synthesis on average by about 50%. The same decrease is also seen when purified PBMC plated at 300,000 cells/well were used (Figure 46b).

It has previously been shown in both the mouse and human system that to class switch to IgE B cells must go through multiple rounds of cell divisions (15;126). Thus it is possible that inhibiting ADAM10 is decreasing cell division. To test this hypothesis tonsillar B cells +/- the Incyte ADAM10 inhibitor were cultured for 4 days. They were then pulsed as explained in the material and methods with H^3-thymidine. 24 hours later the cells were harvested and incorporation was measured. As shown in Figure 46a, the inclusion of the ADAM10 inhibitor as measured by H^3-thymidine had no effect on proliferation, while with CFSE (Figure 46c) there is a slight increase in cell division. Thus ADAM10 inhibition having little effect on the proliferation of B cells.

Another possibility is that ADAM10 inhibition is affecting B cell class switching. This possibility would seem to make sense as inhibiting ADAM10 also slightly decreases IgG production (Figure 46a). To test this, the amount of B cell producing IgE +/- the ADAM10 inhibitor was determined by elispot as explained in the Materials and Methods.

As is shown in Figure 47, opposite to what we expected, inhibiting ADAM10 had no effect on the amount of cells that produced IgE. These results thus show that ADAM10 has no effect on class switching, but that inhibiting ADAM10 decreases the production of IgE on a per cell basis.

Previously McCloskey *et al.* showed that if sCD23 is added to tonsillar B cells it can either increase IgE production or decrease based on oligomerization state of CD23 (127) . If it is a monomer it decreases IgE. If it is an oligomer it increases. They proposed that the ability of oligomers to increase IgE was due to trimeric CD23 ability to cross-link CD21 and mIgE on B cell. With the addition of the ADAM10 inhibitor we would be blocking sCD23 release, and possibly this sCD23 is needed to increase the production of IgE. To test this, we isolated sCD23 from RPMI 8866 cells and then determined its concentration by ELISA. It was then added to ADAM10 inhibited B cell cultures at a concentration of 2 µg/ml, which is the concentration we determined would be in cultures without the inhibitor. The sCD23 isolated from RPMI 8866 would be a mixture of monomers and oligomers, however as we showed in Figure 34a it is predominately composed of oligomers and would be expected to stimulate IgE production. However, we found that the addition of sCD23 could not reverse the effects of ADAM10 inhibition (Figure 48a, b). As the sCD23 we added back was a mixture of both monomeric and trimeric (see Fig 32a) the lack of reverse could be because it contains monomeric sCD23, which cannot crosslink CD21 and mIgE. But as this is the type of sCD23 mixture that the B cells cultures themselves would contain we can conclude that the reason that ADAM10 activity is important in IgE production is not because it increases the levels of sCD23.

Finally, Mayer *et al.* also showed previously with a broad spectrum inhibitor of metalloproteases, that metalloproteases activity is only needed early in the cultures. If the inhibitors were added at later time points in the cultures, the inhibition of IgE was not as pronounced (128). When we performed a similar experiment with the ADAM10 inhibitors we found the same thing (Figure 48c). ADAM10 was most important early in the cultures however later it was not as important. Mayer *et al.* also found that the inhibition pattern exactly paralleled that of anti-lectin antibodies. This suggests that membrane bound CD23 early in the cultures is important for controlling the switching of cells to high IgE producers but not in class switching (128). Overall, this data shows that ADAM10 is important in the early stages of *in vitro* B cells cultures, and increases IgE synthesis on a per cell bases. This increase however is not because it increases the levels of sCD23, but because it decreases the levels of membrane bound CD23. These results further shows that it is membrane bound CD23 that is involved in the regulation of IgE synthesis.

C. Knocking down ADAM10 does change proliferation

When we used the inhibitors above we found that blocking ADAM10 activity did not have an effect on proliferation in primary B cells. However in work done by Jamie Sturgill previously in the laboratory with a broad spectrum inhibitor of metalloproteases, marimastat, she had found that marimastat was added to RPMI 8866 there was a decrease in proliferation compared to untreated cells (data not shown). RPMI 8866 are a non-EBV infected human lymphoblastoid B cell line and thus ADAM10 in these cells could have been hijacked and be involved in the continual growth of these and other malignant B cells, while it is not in primary B cells. To test this hypothesis, RPMI 8866 were

Figure 49: Knocking down ADAM10 with siRNA decreases the proliferation of RPMI 8866. ADAM10 mRNA levels were knocked down in RPMI 8866 by the transfection with the plasmid shown in figure 12 as explained in the material and methods. Cells were also co-transfected with a GFP expressing plasmid. GFP^+ cells were then sorted. (A) mRNA from these cells were then isolated and ADAM10 mRNA levels were compared to cells only transfected with the GFP plasmid by RT-PCR. (B) Shown is the average of at least three experiments. (C) In parallel experiments sorted cells were plated at 50,000 cells/well and proliferation was determined by H^3 incorporation as explained in the material methods. Shown is the average of three experiments.

A.

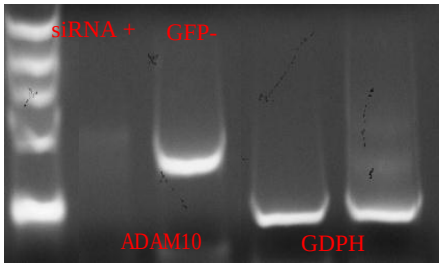

B.

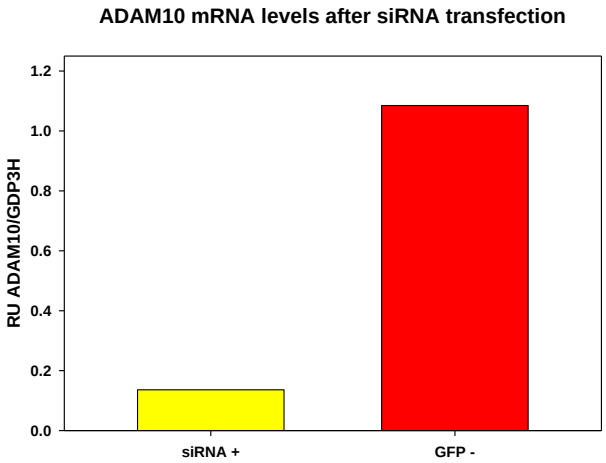

C.

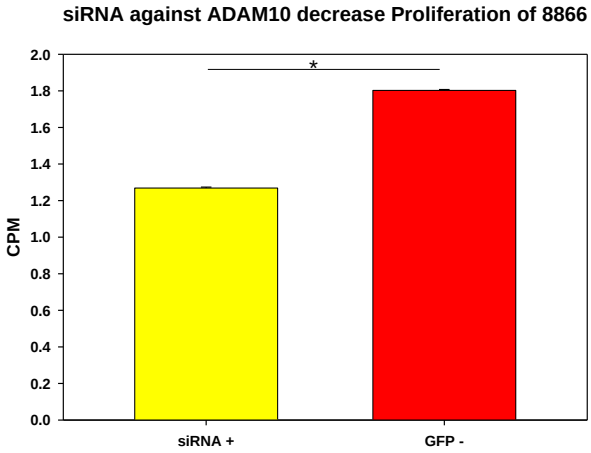

* = P value < .0001

Figure 50: Doxycycline decreases ADAM10 expression and kills RPMI 8866. (A) RPMI 8866 cells were transfected with two plasmids shown in Figure 13 and selected for with Blasticidin and G418 to create a inducible stably expressing siRNA cell line. The siRNA is induced by the addition of doxycycline. To ensure that doxycycline it self was not affecting RPMI 8866, ADAM10 levels were determined by qRT-PCR after the addition of increased amounts of doxycycline and compared to untreated cells. (B) Proliferation as determined by H^3- thymidine incorporation was determined following the addition of increasing amounts of doxycycline to both the inducible cell line plus untransfected RPMI 8866. These results are from one experiment.

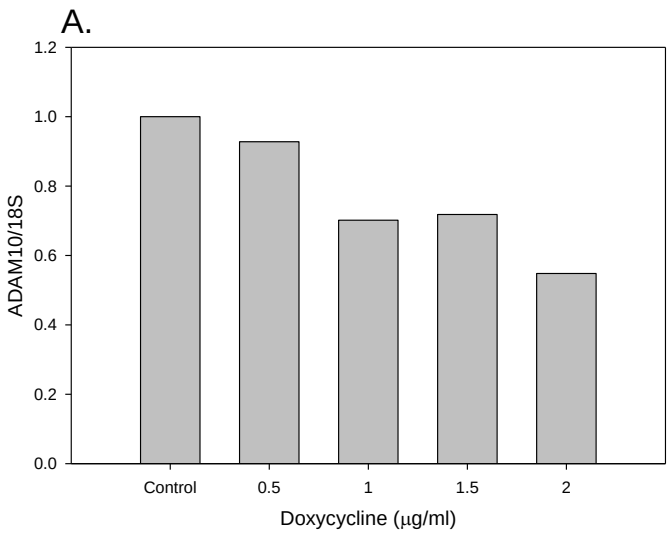

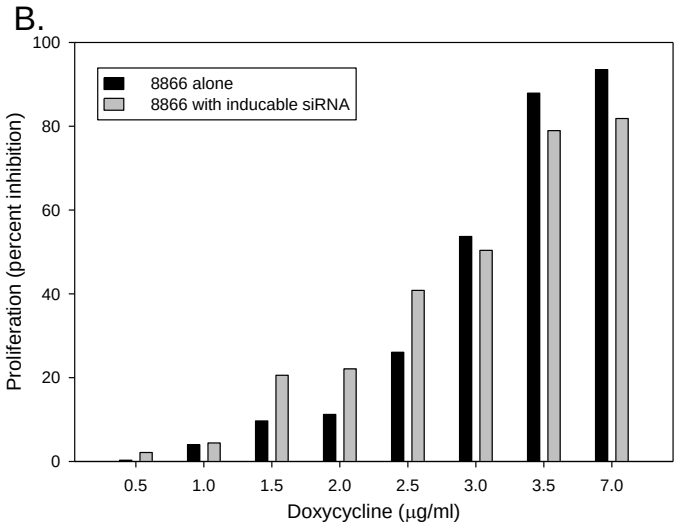

transfected with a siRNA plasmid (Figure 11) and then tested for the amount of proliferation compared to cells transfected with a plasmid containing a scrambled siRNA. As B cells have very low transfection efficiency, RPMI 8866 were co-transfected with a GFP constitutively expressing plasmid along with the siRNA plasmid (Figure 11). Twenty-four hours later GFP positive cells were sorted. The cells were then collected and mRNA was isolated. As is shown in (Figure 49a and b) siRNA caused an 80% knock down of ADAM10 mRNA. In parallel experiments after sorting, the cells were plated and proliferation was measured by H^3-thymidine incorporation (Figure 49c). We found that knocking down ADAM10 decreased proliferation by about one-third and thus confirmed our hypothesis that in a least in this malignant B cell line ADAM10 has been hijacked and is involved in increasing the cells proliferation.

As all these studies were done using transiently expressed siRNA, we did not have much control over the levels of siRNA expression. In addition, as the B cells had to be transfected each time there was some cell death associated with the transfection. We tried to control for this by always comparing our results to sorted cells transfected with just GFP or a scrambled siRNA/GFP. However, a better way is to create a stable tet-on siRNA cell line using the vectors shown in Figure 12. Unfortunately, we quickly learned that this would not work, as the inducer of the siRNA, doxycycline, decreased ADAM10 levels as well as the proliferation of the cells by itself (Figure 50a and b). Overall, the results in Figure 49 in combination with the inhibitors studies show that ADAM10 is involved in proliferation of at least one malignant B cell line and IgE production from PBMC or B cells.

Discussion

I. ADAM10 activity increases asthma induction in IgE dependent, but not IgE independent models of experimental asthma. It has previously been shown that if the cleavage of CD23 is blocked with a stabilizing antibody or if CD23 is overexpressed that the signs of lung inflammation were decreased (53). However, it was not known what role ADAM10 played in this or how CD23 was able to control lung inflammation. Herein we show that overexpression of CD23 or blocking ADAM10 decreases the Th2 response as well as the other signs of lung inflammation, including eosinophilia, AHR and IgE production.

Based on the findings reported we propose three possibilities of how ADAM10 is involved in the enhancement of asthma associated signs. As we found that administration of the inhibitor blocked IgE production (Figure 21e), this decrease in IgE would be reflected in decreased mediators released from mast cells after antigen challenge. This decrease in mediator release would result in decreased signs of experimental asthma, including AHR. One of the reasons for decreased IgE production is reduced cleavage of CD23, as we have previously shown that inhibitors of ADAM10 (109) and loss of ADAM10 (50) reduce CD23 cleavage both *in vitro* and *in vivo* respectively. Additionally, using a hu-PBL model in SCID mice, the inhibition of CD23 cleavage was previously shown to correlate with decreased IgE synthesis (128). However, as discussed earlier in mice where the B cells are deficient in ADAM10 were subjected to a model that is dependent on IgE but not on mast cells (Model B) there still was a reduction in asthma signs compared to WT. This thus shows that IgE must also work through other mechanisms. This could possibly be binding of FcεR1 on basophils as they are also

known to be increased in areas of allergic inflammation (129). Another possibility is that the binding of IgE complexes to CD23 causes enhance antigen presentation and immune responses. This has been well documented by the Heyman laboratory (reviewed in (60)). As we showed in Figure 31 and 34 and will be discussed later, ADAM10 is not only the sheddase of CD23, but also sorts CD23 into exosomes. Once released from the cell, the CD23 containing exosomes could bind IgE complexes and cause increased antigen presentation and T cell responses. The ADAM10 B cell conditional knockouts do not have these CD23 containing exosomes (Figure 34a), and the lack of these CD23 containing exosomes could possibly explain part of the inhibition of the Th1, as well as the Th2,cytokine responses. Such exosomes, containing bound IgE complexes, would be anticipated to enhance dendritic cell activation of T cells.

Lastly as discussed above, when the ADAM10 inhibitor was administered there was a decrease in the Th2 response. We found that this decrease could possibly be explained by decreased IL-33 production. The transcription factor Foxa2 has recently been shown to be one of the major regulatory proteins of lung inflammation. Mice that lack Foxa2 have spontaneous pulmonary eosinophilic inflammation as well as mucous production (130). Chen *et al.* also showed that this was because Foxa2, which is expressed in the epithelial cells of the lung, controls the production of eotaxin and IL-33, and thus, the Th2 response. Foxa2 has also been shown to be down-regulated by the ADAM10 substrate EGF signaling through its receptor (131). Additionally, in asthma patients there is an upregulation of EGFR (132) and inhibiting EGFR signaling in an experimental mouse model shows similar results to those we found with the ADAM10 inhibitor (133). Finally, as shown in Figure 21h and 23d blocking ADAM10 did not

cause a decrease in IL-13. We speculated above that ADAM10 cleavage of some protein must be required for IL-13 upregulation of AHR. In the human system, Zhen *et al.* (131) showed that EGFR signaling was required for both the IL-13 upregulation of mucous production by human epithelial cells as well as constitutive mucous production. Thus inhibition of ADAM10 could potentially be suppressing signaling through the EGF receptor.

II. ADAM10 is also required for CD23 sorting into B cell derived exosomes. CD23 ability to be cleaved has often been termed its stability; when destabilized its cleavage is increased while stabilizing does the converse. These results reported here help to clarify the mechanism of this observation. Basically with the addition of IgE (stabilizing) or 19G5 (destabilizing) to $CD23^+$ cells there is a change in internalization of CD23 (see Figure 27c), this change is then reflective in the amount of CD23 associated with exosomes (Figure 33b) and in soluble cleaved products. When CD23 is destabilized there is an increased amount of CD23 associated with exosomes. Conversely when CD23 is stabilized with monomeric IgE, CD23 associated with exosomes is decreased (Figure 33c). These results also might help explain previous findings (40) that although destabilization was believed to cause CD23 to unravel at the cell surface, when destabilizing antibodies were added there was no change in fluorescence resonance energy transfer between different sections of the trimer. Thus, the data in this study suggest that anti-stalk reagents increase internalization into endosomes. At endosomal pH levels, the ADAM10 cleavage site is evidently much more exposed as evidenced by the rapid cleavage when exosomal bound CD23 is resuspended at pH 5.8 (Figure 31). When the pH is closer to neutrality (pH 7.4) cleavage is much slower. We note also that

IgE partially inhibits ADAM10 and CD23 interaction (Figure 36c), which suggests that if CD23 is internalized while being complexed to IgE, there would be decreased binding of ADAM10 and thus be less efficiently incorporated into exosomes. Finally, CD23 inclusion in exosomes could also be blocked by growing $CD23^{+}$-CHO cells in the presence of NH_4Cl (Figure 33d) helping to explain our results shown in Figure 28a, where reduced cleavage is seen in the presence of this reagent. The SPR results were also quite informative. While the steady state affinity was not significantly different at pH 5.8 vs. 7.4, the Rmax increased about an order of magnitude (Figure 38a). This indicates that the accessibility of the ADAM10 binding site of CD23 was greatly increased by the lower pH, perhaps due to unraveling of the trimer at the lower pH. Most anti-lectin mAbs result in CD23 stabilization, analogous to IgE, and decrease internalization compared to untreated cells, and thereby also inhibit CD23 cleavage. The mechanism responsible for internalization changes is unknown, but changing of the conformation of the cytoplasmic domain is an intriguing possibility, as this domain was recently shown to control internalization (118). Internalized CD23 is internalized into clathrin coated pits and the endosomal pathway (see (36;118) and Table 2). Here ADAM10 has a higher ability to bind CD23 as is evidence by the increase Rmax (see Figure 37b and 38). These findings also beg the question if other ADAM10 substrates, (e.g. notch, EGF and LAG-3) might also bind ADAM10 with a higher Rmax at a lower pH. Once ADAM10 and CD23 interact sorting into exosomes occurs and the exosome is either secreted with intact CD23, or the CD23 is rapidly cleaved. In addition, with the use of an ADAM10 specific inhibitor, we showed that the first cleavages of CD23 was

ADAM10 dependent (see Figure 31c), while subsequent cleavage were by other proteases, which agrees with earlier published findings (48).

B cell derived exosomes are not simply a budding of the MVB or simply fragments of the plasma membrane as their protein constituency is different than the plasma membrane. For example, classical Fc receptors and transferrin receptors are not found in exosomes (120). Thus, for proteins to be secreted in exosomes they require a sort signal. Little is known about the signals required for sorting into exosomes. What is known is that the constitutive photomorphogenesis (COP9) signalosome (CSN) associated protein CSN5 regulates the quantity of some of the proteins in exosomes including ubiquitinated heat shock protein 70 (134). Ubiquitination, however, is not required for MHC II sorting into exosomes (135). For EGF receptor a one amino acid was shown to be important for its inclusion in exosomes (120), but little else is understood. We show that a protease, ADAM10, was essential for CD23 to be included in exosomes (Figure 33a). Of note, although we only saw an 80% drop in sCD23 when cells were cultured in media containing NH_4Cl, this is the same percentage drop seen in $ADAM10^{-/-}$ compared to WT after injection of 19G5 (50), and primary mouse B cells cultured in the presence of inhibitors of ADAM10 (49), showing that ADAM10s predominant role in the removal of CD23 was to sort it into exosomes. Even with the blocking of ADAM10 there still was shedding, which shows that although in both the human and mouse system ADAM10 cleavage in the endosomal pathway is the dominant way of removal of CD23 from the cell there are other proteases that have this role. These could include MMP9 (136) and ADAM8 (137) as both have been shown to be able to cleave CD23. Finally, when calcium is influxed into the cell it causes the MVB to fuse

with the plasma membrane and the exosomes to be released (73). Previously it was shown that the calcium ionophore, ionomycin, increases the levels of CD23 fragments in cell supernatant (49). Our findings may explain these findings, as ionomycin would increase the fusing of MVB and thus the release of CD23 containing exosomes.

Once sorted into exosomes CD23 was either rapidly cleaved by ADAM10 or secreted from the cell where cleavage by ADAM10 still occurred, albeit more slowly. Although the exact role of CD23 in exosomes is not known: the exosomal bound intact CD23 would retain its high affinity/avidity for IgE and thus, be able to bind both free IgE and IgE immune complexes. Thus this pathway could represent more than just a pathway to remove CD23 from the cell, as CD23 bound with IgE complexes represent a good target for dendritic cells and could help explain the increased antigen presentation capacity seen with IgE-antigen complexes (reviewed in (60)). In the case of parasite infection or the initiation of an immune response, an increase in Ag presentation would be advantageous, especially as exosome secretion increases with B cells activation (76). However, in the context of Type I allergic disease, delivery of antigens to APC by exosomal CD23 would be expected to cause increased reactions to allergens. Thus, blocking CD23 inclusion in exosomes or release as a soluble product, analogous to IgE (Figure 27c, 28b) is a possible allergy therapeutic strategy. As we showed in Figure 27c, a possible way to do this is with an anti-lectin mAb or potentially blocking ADAM10 activity with an inhibitor.

As part of this study we also explored alternative ways of inhibiting CD23 inclusion in exosomes. One alternative is to keep CD23 on the surface (IgE or anti-lectin binding), thus, preventing it from coming in contact with ADAM10. High CD23 cell

Figure 51: Model for CD23 entering the endosomal pathway and in contact with ADAM10. The amount of CD23 internalized is determined by its stability, with IgE/anti-lectin mAbs increasing internalization and anti-stalk mAbs increasing internalization. With the decrease in pH found in the endosomal pathway ADAM10 has increased accessibility to bind CD23 resulting in cleavage and/or sorting into exosomes. Exosome and endosomal contents are then released from the cell; this process is enhanced by cell activation and calcium influx.

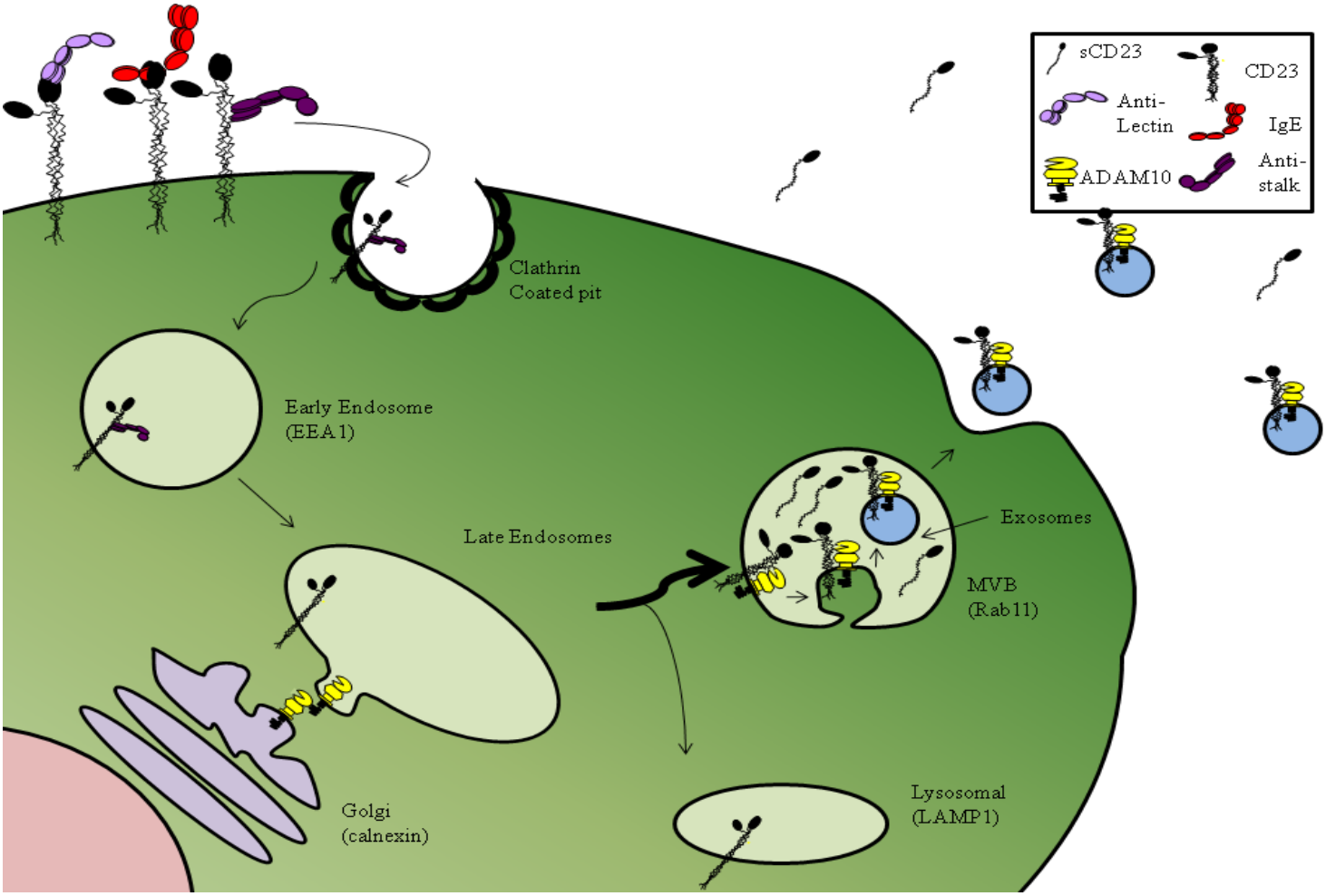

surface expression correlates with lower IgE synthesis. An additional alternative would be to block ADAM10 binding. This approach would be anticipated to increase cell surface CD23 levels; indeed B cells that lack ADAM10 were shown to have quite high cell surface CD23 (50). These studies indicate a mechanism for this cell surface increase, namely, ADAM10$^{-/-}$ B cells do not incorporate or secrete CD23 in exosomes and thus, blocking ADAM10 binding or cleavage is a second possible therapeutic target to regulate IgE synthesis. Although we only investigated the requirement of ADAM10 for CD23 inclusion in exosomes, we would hypothesize that ADAM10 would also be required for the other ADAM10 substrates known to be included in exosomes, L1 and CD44 (79). In addition, as exosomes have been shown to contained enzymatically active ADAM17 (79) it is possible that one role of the ADAMs family members is to sort proteins into exosomes. To block ADAM10 binding it has previously been found that an acidic pocket of the cysteine-rich region was important for binding to Eph, with three residues being specifically important (Glu573, Glu578, and Glu579) (25). As we found that ADAM10 bound CD23 in a protease independent manner, it is thus possible that this same region is also important for binding CD23 (see Figure 36a and b) this region could be thus be specifically targeted, with a small peptide or some other form of inhibitor. However, as the Glu could potentially be protonated at the lower pH found in the endosomal pathway this region might not be important in binding CD23 after it has been internalized. In addition, N-glycosylation of amino acid 280 of ADAM10 has been shown to be essential for ADAM10 shedding and sorting into exosomes. The mutation of this amino acid caused ADAM10 to be retained in the Golgi (138), offering another target region in blocking ADAM10's ability to cleave CD23.

In summary (Figure 51), we show that CD23 internalization is affected by its stability. Once internalized CD23 was trafficked to the MVB where ADAM10, because of the change in pH, has increased access to bind and sort CD23 into exosomes; CD23 was then either rapidly cleaved or secreted as intact CD23 bound to exosomes. Calcium influx enhances this exosome secretion, helping to explain the increase in sCD23 production post cell activation. Once secreted, cleavage is more gradual and the subsequent cleavages are ADAM independent. Blocking this cleavage represents a novel way of increasing surface CD23 and decreasing IgE synthesis.

III. Cytokine increase of ADAM10 could potentially be affecting IgE production

Hasbold *et al.* (126) were the first to show that class switching and synthesis of IgE requires multiple rounds of cell division. Two recent papers from of our laboratory have shown that signaling through cytokines or glutamate receptors can affect the amount of B cell proliferation and IgE production. The first paper by Caven *et al.* (15) showed that the addition of IL-21 both increased proliferation and IgE. In our studies we have also shown that IL-21 (Figure 43) increases ADAM10 mRNA expression. Sturgill *et al.* (109) also showed that with the addition of glutamate to B cell cultures there is a large increase in proliferation and IgE production. She also showed that there was an increase in ADAM10 mRNA expression and activity (sCD23 production). In our studies with the ADAM10 inhibitor (Figure 46a and b) all the cultures were grown in the presence of both IL-21 and glutamate and we did not see a change in proliferation. This thus shows that the change in proliferation caused by IL-21 and glutamate are most likely ADAM10 independent. On the other hand, blocking ADAM10 activity decreased IgE production

Figure 52: New proposal of the mechanism of how CD23 regulates IgE production. CD23 has been proposed to regulate IgE, through its binding of CD21 as shown in Figure 2. In our work, we found that CD23 possibly works through an additional mechanism. We found that CD23 is secreted from B cells in the context of exosomes. In the initial response as these exosomes contain full length CD23 they can bind IgE/antigen complexes and increasing the uptake of antigen and antigen presentation by dendritic cells, which will lead to increased immune reactions, including possible IgE production. However, as the levels of IgE increase, as shown in Figure 35, less CD23 will be incorporated into exosomes. Thus once IgE reaches a certain threshold CD23 will be blocked from entering exosomes. Upon a secondary antigen challenge, this IgE bound CD23 will bind its antigen and CD23 will once again be internalized and released from the cell in the context of exosomes.

Proposed Model

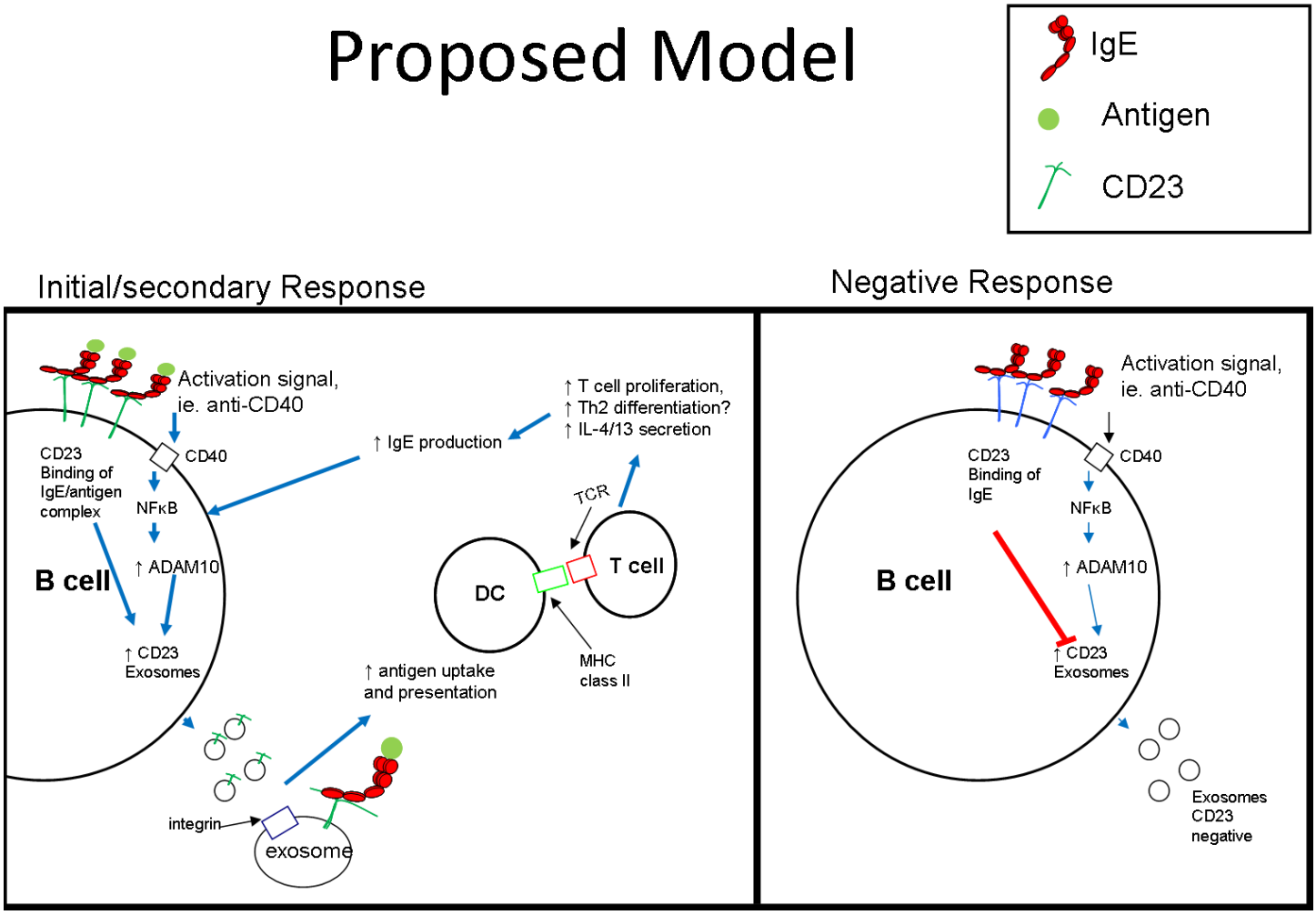

showing that the induction of in IgE synthesis by IL-21 and glutamate are possibly because they increase ADAM10 levels, thus decreasing the levels of membrane bound CD23. Additionally, it is known that activation of B cells through CD40 signaling causes increased secretion of exosomes (76). We additionally show that when B cells are activated by CD40 signaling they also have increased expression of ADAM10 (Figure 44), which is required for CD23 sorting into exosomes (Figure 33a). Thus it is easy to speculate that activation of B cells leads to increased levels of CD23+-exosome secretion and shows once again that exosomal CD23 could be involved in enhancing the initial immune response.

IV. Conclusion and significance

Previously it had been clearly shown that CD23 is involved in allergies (53). This was done through the use of overexpressing mice and stabilizing antibodies. Additionally, in work done by *Ford et al.* (87) it was shown that destabilization CD23 leads to increased IgE production. As shown in figure 2 this ability of CD23 to control IgE synthesis was believed to be because of changes in sCD23 binding to CD21. However, in the context of the mouse system, this theory never completely made sense as mouse sCD23 lacks the ability to bind CD21. Furthermore, as discussed in the introduction, binding by CD23 of injected IgE/antigen complexes increases the production of antigen specific IgG by 1000 fold. With the discovery of CD23 being in exosomes, we here propose an additional model (Figure 52) of how CD23 can have a dual role in both increasing inflammation as well as down regulating IgE synthesis. We see this model as an enhancement of the already proposed model. We propose that after an initial antigen challenge, the antigen will be taken up by dendritic cells and processed. Dendritic cells will then initiate T cell

activation. This initial activation will cause some IL-4 production. These T cells can then activate B cells and in the presence of the low level of IL-4 there will be minimal class switching to IgE. Activation of B cells will also cause increased expression of ADAM10 (see Figure 44), and increase the CD23+-exosome release. Additionally as we showed in Figure 27c and 33b, when ligands interact with the stalk region of CD23, the internalization and incorporation into exosomes of CD23 is increased. These exosomes can then bind IgE/antigen complexes and increase the uptake of antigen by dendritic cells, ultimately increasing the immune reaction against the antigen. This model could explain the data of Ford *et al.* (87), because the injection of 19G5 would increase the amount of CD23+-exosomes. The model also gives an explanation to how IgE can increase inflammation in a mast cell independent matter, as we found in our asthma studies, although IgE could also possible be binding basophils and have being affect. Later in the immune reaction, when IgE has reached a certain threshold, most membrane bound CD23 would be occupied by IgE/antigen complexes and internalization and exosome incorporation of CD23 would be blocked and provides a negative feedback for the immune response and IgE production. Overall our data provides a new explanation to the known enhancement of immunoglobulin and T cell responses by IgE-antigen complexes. It was known that these responses were dependent on CD23, but not how. Our work provides a potential explanation. In connection with this, in initial studies with B cells isolated from allergic patients, we have found that the ADAM10 levels are increased during allergy season when compared to the levels in non-allergic patients or to allergy patients out of allergy season (data not shown). The higher ADAM10 would result in enhanced CD23/exosome secretion and enhance specific IgE production.

Additionally, in our experiments with the ADAM10 inhibitor we found that ADAM10 was also important on non-B cells, and we proposed that these cells could possibly be epithelial cells. Without the cleavage of EFGR ligands, experimental asthma signs are not exacerbated, as EFGR signaling is required for the down regulation of Foxa2. In conclusion, these findings show that ADAM10 on both B and non-B cells is potentially a new target for asthma therapy.

Reference List

1. Eder W, Ege MJ, von ME. The asthma epidemic. N Engl J Med 2006 Nov 23;355(21):2226-2235.

2. Braman SS. The global burden of asthma. Chest 2006 Jul;130(1 Suppl):4S-12S.

3. Diaz-Sanchez D, Tsien A, Fleming J, Saxon A. Combined diesel exhaust particulate and ragweed allergen challenge markedly enhances human in vivo nasal ragweed-specific IgE and skews cytokine production to a T helper cell 2-type pattern. J Immunol 1997 Mar 1;158(5):2406-2413.

4. Holgate ST, Polosa R. Treatment strategies for allergy and asthma. Nat Rev Immunol 2008 Mar;8(3):218-230.

5. Galli SJ, Tsai M, Piliponsky AM. The development of allergic inflammation. Nature 2008 Jul 24;454(7203):445-454.

6. Prausnitz D, Kustner H. Studien uber die Ueberempfindlichkeit. Zentrabl Bakteriol [A] 1921;86:160-175.

7. Hamilton RG. Science behind the discovery of IgE. J Allergy Clin Immunol 2005 Mar;115(3):648-652.

8. Ishizaka K, Ishizaka T. Identification of IgE-antibodies as a carrier of reaginic activity. J Immunol 1967;99:1187-1198.

9. Stanworth DR, Humphrey JH, Bennich H, Johansson SG. Specific inhibition of the Prausnitz-Kustner reaction by an atypical human myeloma protein. Lancet 1967 Aug 12;2(7511):330-332.

10. Bennich HH, Ishizaka K, Johansson SG, Rowe DS, Stanworth DR, Terry WD. Immunoglobulin E. A new class of human immunoglobulin. Immunochemistry 1968 Jul;5(4):327-328.

11. Stavnezer J, Guikema JE, Schrader CE. Mechanism and regulation of class switch recombination. Annu Rev Immunol 2008;26:261-292.

12. Coffman RL, Carty J. A T cell activity that enhances polyclonal IgE production and its inhibition by interferon-gamma. J Immunol 1986 Feb 1;136(3):949-954.

13. Coffman RL, Lebman DA, Shrader B. Transforming growth factor beta specifically enhances IgA production by lipopolysaccharide-stimulated murine B lymphocytes. J Exp Med 1989 Sep 1;170(3):1039-1044.

14. Kiniwa M, Gately M, Gubler U, Chizzonite R, Fargeas C, Delespesse G. Recombinant interleukin-12 suppresses the synthesis of immunoglobulin E by

interleukin-4 stimulated human lymphocytes. J Clin Invest 1992 Jul;90(1):262-266.

15. Caven TH, Shelburne A, Sato J, Chan-Li Y, Becker S, Conrad DH. IL-21 dependent IgE production in human and mouse in vitro culture systems is cell density and cell division dependent and is augmented by IL-10. Cell Immunol 2005 Dec;238(2):123-134.

16. Jeannin P, Lecoanet S, Delneste Y, Gauchat JF, Bonnefoy JY. IgE versus IgG4 production can be differentially regulated by IL-10. J Immunol 1998 Apr 1;160(7):3555-3561.

17. Pene J, Rousset F, Briere F, Chretien I, Wideman J, Bonnefoy JY, et al. Interleukin 5 enhances interleukin 4-induced IgE production by normal human B cells. The role of soluble CD23 antigen. Eur J Immunol 1988 Jun;18(6):929-935.

18. Joshi PC, Choi YS. Human interleukin 7 is a B cell growth factor for activated B cells. Eur J Immunol 1991 Mar;21(3):681-686.

19. Vercelli D, Jabara HH, Arai K, Yokota T, Geha RS. Endogenous interleukin 6 plays an obligatory role in interleukin 4-dependent human IgE synthesis. Eur J Immunol 1989 Aug;19(8):1419-1424.

20. Holgate S, Casale T, Wenzel S, Bousquet J, Deniz Y, Reisner C. The anti-inflammatory effects of omalizumab confirm the central role of IgE in allergic inflammation. J Allergy Clin Immunol 2005 Mar;115(3):459-465.

21. Avila PC. Does anti-IgE therapy help in asthma? Efficacy and controversies. Annu Rev Med 2007;58:185-203.

22. Macglashan D, Jr. IgE and Fc{epsilon}RI regulation. Ann N Y Acad Sci 2005 Jun;1050:73-88.

23. Lawrence DA, Weigle WO, Spiegelberg HL. Immunoglobulins cytophilic for human lymphocytes, monocytes, and neutrophils. J Clin Invest 1975 Feb;55(2):368-376.

24. Gould HJ, Sutton BJ. IgE in allergy and asthma today. Nat Rev Immunol 2008 Mar;8(3):205-217.

25. Janes PW, Saha N, Barton WA, Kolev MV, Wimmer-Kleikamp SH, Nievergall E, et al. Adam meets Eph: an ADAM substrate recognition module acts as a molecular switch for ephrin cleavage in trans. Cell 2005 Oct 21;123(2):291-304.

26. Conrad DH. FcεRII/CD23: The low affinity receptor for IgE. Ann Rev Immunol 1990;8:623-45.

27. Wang F, Gregory CD, Rowe M, Rickinson AB, Wang D, Birkenbach M, et al. Epstein-Barr virus nuclear antigen 2 specifically induces expression of the B-cell activation antigen CD23. Proc Natl Acad Sci U S A 1987 May;84(10):3452-3456.

28. Thorley-Lawson DA, Nadler LM, Bhan AK, Schooley RT. BLAST-2 [EBVCS], an early cell surface marker of human B cell activation, is superinduced by Epstein Barr virus. J Immunol 1985 May;134(5):3007-3012.

29. Yukawa K, Kikutani H, Owaki H, Yamasaki K, Yokota A, Nakamura H, et al. A B cell-specific differentiation antigen, CD23, is a receptor for IgE (Fc epsilon R) on lymphocytes. J Immunol 1987 Apr 15;138(8):2576-2580.

30. Ikuta K, Takami M, Kim CW, Honjo T, Miyoshi T, Tagaya Y, et al. Human lymphocyte Fc receptor for IgE: sequence homology of its cloned cDNA with animal lectins. Proc Natl Acad Sci U S A 1987 Feb;84(3):819-823.

31. Kikutani H, Inui S, Sato R, Barsumian EL, Owaki H, Yamasaki K, et al. Molecular structure of human lymphocyte receptor for immunoglobulin E. Cell 1986 Dec 5;47(5):657-665.

32. Ludin C, Hofstetter H, Sarfati M, Levy CA, Suter U, Alaimo D, et al. Cloning and expression of the cDNA coding for a human lymphocyte IgE receptor. EMBO J 1987 Jan;6(1):109-114.

33. Bettler B, Maier R, Ruegg D, Hofstetter H. Binding site for IgE of the human lymphocyte low-affinity Fc epsilon receptor (Fc epsilon RII/CD23) is confined to the domain homologous with animal lectins. Proc Natl Acad Sci U S A 1989 Sep;86(18):7118-7122.

34. Conrad DH, Ford JW, Sturgill JL, Gibb DR. CD23: an overlooked regulator of allergic disease. Curr Allergy Asthma Rep 2007 Sep;7(5):331-337.

35. Boltz-Nitulescu G, Wiltschke C, Langer K, Nemet H, Holzinger C, Gessl A, et al. Augmentation of IgE receptor expression and IgE receptor-mediated phagocytosis of rat bone marrow-derived macrophages by murine interferons. Immunology 1988 Mar;63(3):529-535.

36. Karagiannis SN, Warrack JK, Jennings KH, Murdock PR, Christie G, Moulder K, et al. Endocytosis and recycling of the complex between CD23 and HLA-DR in human B cells. Immunology 2001 Jul;103(3):319-331.

37. Beavil AJ, Edmeades RL, Gould HJ, Sutton BJ. α-Helical coiled-coil stalks in the low-affinity receptor for IgE (FcεRII/CD23) and related C-type lectins. Proc Natl Acad Sci USA 1992;89(2):753-757.

38. Richards ML, Katz DH. The binding of IgE to murine FcεRII is calcium-dependent but not inhibited by carbohydrate. J Immunol 1990;144:2638-2646.

39. Shi J, Ghirlando R, Beavil RL, Beavil AJ, Keown MB, Young RJ, et al. Interaction of the low-affinity receptor CD23/Fc epsilonRII lectin domain with the Fc epsilon3-4 fragment of human immunoglobulin E. Biochemistry 1997 Feb 25;36(8):2112-2122.

40. Kilmon MA, Shelburne AE, Chan-Li Y, Holmes KL, Conrad DH. CD23 trimers are preassociated on the cell surface even in the absence of its ligand, IgE. J Immunol 2004 Jan 15;172(2):1065-1073.

41. Chen BH, Ma C, Caven TH, Chan-Li Y, Beavil A, Beavil R, et al. Necessity of the stalk region for immunoglobulin E interaction with CD23. Immunology 2002 Nov;107(3):373-381.

42. Munoz O, Brignone C, Grenier-Brossette N, Bonnefoy JY, Cousin JL. Binding of anti-CD23 monoclonal antibody to the leucine zipper motif of FcepsilonRII/CD23 on B cell membrane promotes its proteolytic cleavage. Evidence for an effect on the oligomer/monomer equilibrium. J Biol Chem 1998 Nov 27;273(48):31795-31800.

43. Lee WT, Rao M, Conrad DH. The murine lymphocyte receptor for IgE. IV. The mechanism of ligand-specific receptor upregulation on B cells. J Immunol 1987 Aug 15;139(4):1191-1198.

44. Defrance T, Aubry JP, Rousset F, Vanbervliet B, Bonnefoy JY, Arai N, et al. Human recombinant interleukin 4 induces Fc epsilon receptors (CD23) on normal human B lymphocytes. J Exp Med 1987 Jun 1;165(6):1459-1467.

45. Conrad DH, Keegan AD, Kalli KR, Van DR, Rao M, Levine AD. Superinduction of low affinity IgE receptors on murine B lymphocytes by lipopolysaccharide and IL-4. J Immunol 1988 Aug 15;141(4):1091-1097.

46. Sukumar S, Conrad DH, Szakal AK, Tew JG. Differential T cell-mediated regulation of CD23 (Fc epsilonRII) in B cells and follicular dendritic cells. J Immunol 2006 Apr 15;176(8):4811-4817.

47. Marolewski AE, Buckle DR, Christie G, Earnshaw DL, Flamberg PL, Marshall LA, et al. CD23 (FcepsilonRII) release from cell membranes is mediated by a membrane-bound metalloprotease. Biochem J 1998 Aug 1;333 (Pt 3):573-579.

48. Lemieux GA, Blumenkron F, Yeung N, Zhou P, Williams J, Grammer AC, et al. The low affinity IgE receptor (CD23) is cleaved by the metalloproteinase ADAM10. J Biol Chem 2007 May 18;282(20):14836-14844.

49. Weskamp G, Ford JW, Sturgill J, Martin S, Docherty AJ, Swendeman S, et al. ADAM10 is a principal 'sheddase' of the low-affinity immunoglobulin E receptor CD23. Nat Immunol 2006 Dec;7(12):1293-1298.

50. Gibb DR, El SM, Kang DJ, Rowe WJ, El SR, Cichy J, et al. ADAM10 is essential for Notch2-dependent marginal zone B cell development and CD23 cleavage in vivo. J Exp Med 2010 Mar 15;207(3):623-635.

51. Fujiwara H, Kikutani H, Suematsu S, Naka T, Yoshida K, Yoshida K, et al. The absence of IgE antibody-mediated augmentation of immune responses in CD23-deficient mice. Proc Natl Acad Sci U S A 1994 Jul 19;91(15):6835-6839.

52. Yu P, Kosco-Vilbois M, Richards M, Kohler G, Lamers MC. Negative feedback regulation of IgE synthesis by murine CD23. Nature 1994 Jun 30;369(6483):753-756.

53. Haczku A, Takeda K, Hamelmann E, Loader J, Joetham A, Redai I, et al. CD23 exhibits negative regulatory effects on allergic sensitization and airway hyperresponsiveness. Am J Respir Crit Care Med 2000 Mar;161(3 Pt 1):952-960.

54. Ford JW, Sturgill JL, Conrad DH. 129/SvJ mice have mutated CD23 and hyper IgE. Cell Immunol 2009;254(2):124-134.

55. Texido G, Eibel H, Le Gros G, Van der Putten H. Transgene CD23 expression on lymphoid cells modulates IgE and IgG1 responses. J Immunol 1994;153:3028-3042.

56. Payet ME, Woodward EC, Conrad DH. Humoral response suppression observed with CD23 transgenics. J Immunol 1999 Jul 1;163(1):217-223.

57. Rosenwasser LJ, Meng J. Anti-CD23. Clin Rev Allergy Immunol 2005 Aug;29(1):61-72.

58. Byrd JC, Kipps TJ, Flinn IW, Castro J, Lin TS, Wierda W, et al. Phase 1/2 study of lumiliximab combined with fludarabine, cyclophosphamide, and rituximab in patients with relapsed or refractory chronic lymphocytic leukemia. Blood 2010 Jan 21;115(3):489-495.

59. Behring, Wernicke. Ueber Immunisirung und Heilung von Versuchsthieren bei der Diphtherie. Medical Microbiology and Immunology 1892 Dec 27;12(1):10-44.

60. Hjelm F, Carlsson F, Getahun A, Heyman B. Antibody-mediated regulation of the immune response. Scand J Immunol 2006 Sep;64(3):177-184.

61. Gustavsson S, Hjulstrom S, Liu T, Heyman B. CD23/IgE-mediated regulation of the specific antibody response in vivo. J Immunol 1994 May 15;152(10):4793-4800.

62. Gustavsson S, Wernersson S, Heyman B. Restoration of the antibody response to IgE/antigen complexes in CD23-deficient mice by CD23+ spleen or bone marrow cells. J Immunol 2000 Apr 15;164(8):3990-3995.

63. Getahun A, Hjelm F, Heyman B. IgE enhances antibody and T cell responses in vivo via CD23+ B cells. J Immunol 2005 Aug 1;175(3):1473-1482.

64. Rooke J, Pan D, Xu T, Rubin GM. KUZ, a conserved metalloprotease-disintegrin protein with two roles in Drosophila neurogenesis. Science 1996 Aug 30;273(5279):1227-1231.

65. Hartmann D, De SB, Serneels L, Craessaerts K, Herreman A, Annaert W, et al. The disintegrin/metalloprotease ADAM 10 is essential for Notch signalling but not for alpha-secretase activity in fibroblasts. Hum Mol Genet 2002 Oct 1;11(21):2615-2624.

66. Tanigaki K, Honjo T. Regulation of lymphocyte development by Notch signaling. Nat Immunol 2007 May;8(5):451-456.

67. Blobel CP. ADAMs: key components in EGFR signalling and development. Nat Rev Mol Cell Biol 2005 Jan;6(1):32-43.

68. Reiss K, Saftig P. The "a disintegrin and metalloprotease" (ADAM) family of sheddases: physiological and cellular functions. Semin Cell Dev Biol 2009 Apr;20(2):126-137.

69. Nagano O, Murakami D, Hartmann D, De SB, Saftig P, Iwatsubo T, et al. Cell-matrix interaction via CD44 is independently regulated by different metalloproteinases activated in response to extracellular Ca(2+) influx and PKC activation. J Cell Biol 2004 Jun 21;165(6):893-902.

70. Gutwein P, Mechtersheimer S, Riedle S, Stoeck A, Gast D, Joumaa S, et al. ADAM10-mediated cleavage of L1 adhesion molecule at the cell surface and in released membrane vesicles. FASEB J 2003 Feb;17(2):292-294.

71. Sahin U, Weskamp G, Kelly K, Zhou HM, Higashiyama S, Peschon J, et al. Distinct roles for ADAM10 and ADAM17 in ectodomain shedding of six EGFR ligands. J Cell Biol 2004 Mar 1;164(5):769-779.

72. Radtke F, Fasnacht N, MacDonald HR. Notch signaling in the immune system. Immunity 2010 Jan 29;32(1):14-27.

73. Thery C, Zitvogel L, Amigorena S. Exosomes: composition, biogenesis and function. Nat Rev Immunol 2002 Aug;2(8):569-579.

74. Viaud S, Thery C, Ploix S, Tursz T, Lapierre V, Lantz O, et al. Dendritic cell-derived exosomes for cancer immunotherapy: what's next? Cancer Res 2010 Feb 15;70(4):1281-1285.

75. Clayton A, Turkes A, Dewitt S, Steadman R, Mason MD, Hallett MB. Adhesion and signaling by B cell-derived exosomes: the role of integrins. FASEB J 2004 Jun;18(9):977-979.

76. McLellan AD. Exosome release by primary B cells. Crit Rev Immunol 2009;29(3):203-217.

77. Saunderson SC, Schuberth PC, Dunn AC, Miller L, Hock BD, MacKay PA, et al. Induction of exosome release in primary B cells stimulated via CD40 and the IL-4 receptor. J Immunol 2008 Jun 15;180(12):8146-8152.

78. Muntasell A, Berger AC, Roche PA. T cell-induced secretion of MHC class II-peptide complexes on B cell exosomes. EMBO J 2007 Oct 3;26(19):4263-4272.

79. Stoeck A, Keller S, Riedle S, Sanderson MP, Runz S, Le NF, et al. A role for exosomes in the constitutive and stimulus-induced ectodomain cleavage of L1 and CD44. Biochem J 2006 Feb 1;393(Pt 3):609-618.

80. Bruce C, Thomas PS. The effect of marimastat, a metalloprotease inhibitor, on allergen-induced asthmatic hyper-reactivity. Toxicol Appl Pharmacol 2005 Jun 1;205(2):126-132.

81. Paulissen G, Rocks N, Gueders MM, Crahay C, Quesada-Calvo F, Bekaert S, et al. Role of ADAM and ADAMTS metalloproteinases in airway diseases. Respir Res 2009;10:127.

82. Dijkstra A, Postma DS, Noordhoek JA, Lodewijk ME, Kauffman HF, ten Hacken NH, et al. Expression of ADAMs ("a disintegrin and metalloprotease") in the human lung. Virchows Arch 2009 Apr;454(4):441-449.

83. Di VE, Crahay C, Garbacki N, Hennuy B, Gueders M, Noel A, et al. New asthma biomarkers: lessons from murine models of acute and chronic asthma. Am J Physiol Lung Cell Mol Physiol 2009 Feb;296(2):L185-L197.

84. Lopez-Perez E, Zhang Y, Frank SJ, Creemers J, Seidah N, Checler F. Constitutive alpha-secretase cleavage of the beta-amyloid precursor protein in the furin-deficient LoVo cell line: involvement of the pro-hormone convertase 7 and the disintegrin metalloprotease ADAM10. J Neurochem 2001 Mar;76(5):1532-1539.

85. Amour A, Knight CG, Webster A, Slocombe PM, Stephens PE, Knauper V, et al. The in vitro activity of ADAM-10 is inhibited by TIMP-1 and TIMP-3. FEBS Lett 2000 May 19;473(3):275-279.

86. Horiuchi K, Le GS, Schulte M, Yamaguchi T, Reiss K, Murphy G, et al. Substrate selectivity of epidermal growth factor-receptor ligand sheddases and their regulation by phorbol esters and calcium influx. Mol Biol Cell 2007 Jan;18(1):176-188.

87. Ford JW, Kilmon MA, Haas KM, Shelburne AE, Chan-Li Y, Conrad DH. In vivo murine CD23 destabilization enhances CD23 shedding and IgE synthesis. Cell Immunol 2006 Oct;243(2):107-117.

88. Schwartz W, J.Jiao, J.Ford, D.Conrad, J.F.Hamel, P.Santabien, et al. Application of chemically-stable immunoglobulin-selective sorbents: capture and purification of antibodies with resolution of aggregate. BioProcessing Journal 2004;3:53-62.

89. Bohn A, Konig W. Generation of monoclonal murine anti-DNP-IgE, IgM and IgG1 antibodies: biochemical and biological characterization. Immunology 1982 Oct;47(2):297-311.

90. Kelly AE, Chen B-H, Woodward EC, Conrad DH. Production of a chimeric form of CD23 that is oligomeric and blocks IgE binding to the Fc epsilonRI. J Immunol 1998;161(12):6696-704.

91. Zhou BB, Peyton M, He B, Liu C, Girard L, Caudler E, et al. Targeting ADAM-mediated ligand cleavage to inhibit HER3 and EGFR pathways in non-small cell lung cancer. Cancer Cell 2006 Jul;10(1):39-50.

92. Galichet A, Weibel M, Heizmann CW. Calcium-regulated intramembrane proteolysis of the RAGE receptor. Biochem Biophys Res Commun 2008 May 23;370(1):1-5.

93. Pan D, Rubin GM. Kuzbanian controls proteolytic processing of Notch and mediates lateral inhibition during Drosophila and vertebrate neurogenesis. Cell 1997 Jul 25;90(2):271-280.

94. Poole JA, Meng J, Reff M, Spellman MC, Rosenwasser LJ. Anti-CD23 monoclonal antibody, lumiliximab, inhibited allergen-induced responses in antigen-presenting cells and T cells from atopic subjects. J Allergy Clin Immunol 2005 Oct;116(4):780-788.

95. Squire CM, Studer EJ, Lees A, Finkelman FD, Conrad DH. Antigen presentation is enhanced by targeting antigen to the Fc epsilon RII by antigen-anti-Fc epsilon RII conjugates. J Immunol 1994 May 1;152(9):4388-4396.

96. Williams CM, Galli SJ. Mast cells can amplify airway reactivity and features of chronic inflammation in an asthma model in mice. J Exp Med 2000 Aug 7;192(3):455-462.

97. Williams CM, Galli SJ. The diverse potential effector and immunoregulatory roles of mast cells in allergic disease. J Allergy Clin Immunol 2000 May;105(5):847-859.

98. Kelly-Welch AE, Melo ME, Smith E, Ford AQ, Haudenschild C, Noben-Trauth N, et al. Complex role of the IL-4 receptor alpha in a murine model of airway inflammation: expression of the IL-4 receptor alpha on nonlymphoid cells of bone marrow origin contributes to severity of inflammation. J Immunol 2004 Apr 1;172(7):4545-4555.

99. Kelly-Welch AE, Melo ME, Smith E, Ford AQ, Haudenschild C, Noben-Trauth N, et al. Complex role of the IL-4 receptor alpha in a murine model of airway inflammation: expression of the IL-4 receptor alpha on nonlymphoid cells of bone marrow origin contributes to severity of inflammation. J Immunol 2004 Apr 1;172(7):4545-4555.

100. REITMAN S, FRANKEL S. A colorimetric method for the determination of serum glutamic oxalacetic and glutamic pyruvic transaminases. Am J Clin Pathol 1957 Jul;28(1):56-63.

101. Wang SY, Yang M, Xu XP, Qiu GF, Ma J, Wang SJ, et al. Intranasal delivery of T-bet modulates the profile of helper T cell immune responses in experimental asthma. J Investig Allergol Clin Immunol 2008;18(5):357-365.

102. Ishii A, Oboki K, Nambu A, Morita H, Ohno T, Kajiwara N, et al. Development of IL-17-mediated delayed-type hypersensitivity is not affected by down-regulation of IL-25 expression. Allergol Int 2010 Dec;59(4):399-408.

103. Patki V, Virbasius J, Lane WS, Toh BH, Shpetner HS, Corvera S. Identification of an early endosomal protein regulated by phosphatidylinositol 3-kinase. Proc Natl Acad Sci U S A 1997 Jul 8;94(14):7326-7330.

104. Kannan K, Stewart RM, Bounds W, Carlsson SR, Fukuda M, Betzing KW, et al. Lysosome-associated membrane proteins h-LAMP1 (CD107a) and h-LAMP2 (CD107b) are activation-dependent cell surface glycoproteins in human peripheral blood mononuclear cells which mediate cell adhesion to vascular endothelium. Cell Immunol 1996 Jul 10;171(1):10-19.

105. Savina A, Vidal M, Colombo MI. The exosome pathway in K562 cells is regulated by Rab11. J Cell Sci 2002 Jun 15;115(Pt 12):2505-2515.

106. Krijnse-Locker J, Parton RG, Fuller SD, Griffiths G, Dotti CG. The organization of the endoplasmic reticulum and the intermediate compartment in cultured rat hippocampal neurons. Mol Biol Cell 1995 Oct;6(10):1315-1332.

107. Lipschultz CA, Li Y, Smith-Gill S. Experimental design for analysis of complex kinetics using surface plasmon resonance. Methods 2000 Mar;20(3):310-318.

108. Prinzen C, Muller U, Endres K, Fahrenholz F, Postina R. Genomic structure and functional characterization of the human ADAM10 promoter. FASEB J 2005 Sep;19(11):1522-1524.

109. Sturgill JL, Mathews J, Scherle P, Conrad DH. Glutamate signaling through the kainate receptor enhances human immunoglobulin production. J Neuroimmunol 2011 Jan 5.

110. Hirschowitz EA. Autologous dendritic cell vaccines for non-small-cell lung cancer. 2004 Jul 15.

111. Lambrecht BN, Hammad H. The role of dendritic and epithelial cells as master regulators of allergic airway inflammation. Lancet 2010 Sep 4;376(9743):835-843.

112. Fridman JS, Caulder E, Hansbury M, Liu X, Yang G, Wang Q, et al. Selective inhibition of ADAM metalloproteases as a novel approach for modulating ErbB pathways in cancer. Clin Cancer Res 2007 Mar 15;13(6):1892-1902.

113. Chvatchko Y, Kosco-Vilbois MH, Herren S, Lefort J, Bonnefoy JY. Germinal center formation and local immunoglobulin E (IgE) production in the lung after an airway antigenic challenge. J Exp Med 1996 Dec 1;184(6):2353-2360.

114. Barrett NA, Austen KF. Innate cells and T helper 2 cell immunity in airway inflammation. Immunity 2009 Sep 18;31(3):425-437.

115. Walter DM, McIntire JJ, Berry G, McKenzie AN, Donaldson DD, DeKruyff RH, et al. Critical role for IL-13 in the development of allergen-induced airway hyperreactivity. J Immunol 2001 Oct 15;167(8):4668-4675.

116. Akbari O, Stock P, Meyer E, Kronenberg M, Sidobre S, Nakayama T, et al. Essential role of NKT cells producing IL-4 and IL-13 in the development of allergen-induced airway hyperreactivity. Nat Med 2003 May;9(5):582-588.

117. Soroosh P, Doherty TA. Th9 and allergic disease. Immunology 2009 Aug;127(4):450-458.

118. Montagnac G, Molla-Herman A, Bouchet J, Yu LC, Conrad DH, Perdue MH, et al. Intracellular trafficking of CD23: differential regulation in humans and mice by both extracellular and intracellular exons. J Immunol 2005 May 1;174(9):5562-5572.

119. Ohkuma S, Poole B. Fluorescence probe measurement of the intralysosomal pH in living cells and the perturbation of pH by various agents. Proc Natl Acad Sci U S A 1978 Jul;75(7):3327-3331.

120. Keller S, Sanderson MP, Stoeck A, Altevogt P. Exosomes: from biogenesis and secretion to biological function. Immunol Lett 2006 Nov 15;107(2):102-108.

121. Keegan AD, Conrad DH. The murine lymphocyte receptor for IgE. V. Biosynthesis, transport, and maturation of the B cell Fc epsilon receptor. J Immunol 1987 Aug 15;139(4):1199-1205.

122. Letellier M, Sarfati M, Delespesse G. Mechanisms of formation of IgE-binding factors (soluble CD23)--I. Fc epsilon R II bearing B cells generate IgE-binding factors of different molecular weights. Mol Immunol 1989 Dec;26(12):1105-1112.

123. Le Gall SM, Bobe P, Reiss K, Horiuchi K, Niu XD, Lundell D, et al. ADAMs 10 and 17 represent differentially regulated components of a general shedding machinery for membrane proteins such as transforming growth factor alpha, L-selectin, and tumor necrosis factor alpha. Mol Biol Cell 2009 Mar;20(6):1785-1794.

124. Rabin E, Cong YZ, Wortis HH. Loss of CD23 is a consequence of B-cell activation. Implications for the analysis of B-cell lineages. Ann N Y Acad Sci 1992 May 4;651:130-142.

125. Hundhausen C, Misztela D, Berkhout TA, Broadway N, Saftig P, Reiss K, et al. The disintegrin-like metalloproteinase ADAM10 is involved in constitutive cleavage of CX3CL1 (fractalkine) and regulates CX3CL1-mediated cell-cell adhesion. Blood 2003 Aug 15;102(4):1186-1195.

126. Hasbold J, Lyons AB, Kehry MR, Hodgkin PD. Cell division number regulates IgG1 and IgE switching of B cells following stimulation by CD40 ligand and IL-4. Eur J Immunol 1998 Mar;28(3):1040-1051.

127. McCloskey N, Hunt J, Beavil RL, Jutton MR, Grundy GJ, Girardi E, et al. Soluble CD23 monomers inhibit and oligomers stimulate IGE synthesis in human B cells. J Biol Chem 2007 Aug 17;282(33):24083-24091.

128. Mayer RJ, Bolognese BJ, Al-Mahdi N, Cook RM, Flamberg PL, Hansbury MJ, et al. Inhibition of CD23 processing correlates with inhibition of IL-4-stimulated IgE production in human PBL and hu-PBL-reconstituted SCID mice. Clin Exp Allergy 2000 May;30(5):719-727.

129. Rorsman H. Basophil leucocytes in urticaria, asthma and atopic dermatitis. Acta Allergol 1958;12(2-3):205-216.

130. Chen G, Wan H, Luo F, Zhang L, Xu Y, Lewkowich I, et al. Foxa2 programs Th2 cell-mediated innate immunity in the developing lung. J Immunol 2010 Jun 1;184(11):6133-6141.

131. Zhen G, Park SW, Nguyenvu LT, Rodriguez MW, Barbeau R, Paquet AC, et al. IL-13 and epidermal growth factor receptor have critical but distinct roles in epithelial cell mucin production. Am J Respir Cell Mol Biol 2007 Feb;36(2):244-253.

132. Puddicombe SM, Polosa R, Richter A, Krishna MT, Howarth PH, Holgate ST, et al. Involvement of the epidermal growth factor receptor in epithelial repair in asthma. FASEB J 2000 Jul;14(10):1362-1374.

133. Vargaftig BB, Singer M. Leukotrienes mediate part of Ova-induced lung effects in mice via EGFR. Am J Physiol Lung Cell Mol Physiol 2003 Oct;285(4):L808-L818.

134. Liu Y, Shah SV, Xiang X, Wang J, Deng ZB, Liu C, et al. COP9-associated CSN5 regulates exosomal protein deubiquitination and sorting. Am J Pathol 2009 Apr;174(4):1415-1425.

135. Gauvreau ME, Cote MH, Bourgeois-Daigneault MC, Rivard LD, Xiu F, Brunet A, et al. Sorting of MHC class II molecules into exosomes through a ubiquitin-independent pathway. Traffic 2009 Oct;10(10):1518-1527.

136. Jackson L, Cady CT, Cambier JC. TLR4-mediated signaling induces MMP9-dependent cleavage of B cell surface CD23. J Immunol 2009 Aug 15;183(4):2585-2592.

137. Fourie AM, Coles F, Moreno V, Karlsson L. Catalytic activity of ADAM8, ADAM15, and MDC-L (ADAM28) on synthetic peptide substrates and in ectodomain cleavage of CD23. J Biol Chem 2003 Aug 15;278(33):30469-30477.

138. Escrevente C, Morais VA, Keller S, Soares CM, Altevogt P, Costa J. Functional role of N-glycosylation from ADAM10 in processing, localization and activity of the enzyme. Biochim Biophys Acta 2008 Jun;1780(6):905-913.

Vita

Joel Andrews Mathews was born February 19, 1981 at Good Samaritan Hospital in Corvallis, OR. He grew up in Toledo, OR and graduated as Valedictorian from Toledo High School Class of 1999. He earned a Bachelor of Science in Molecular Biology in April 2006 from Brigham Young University in Provo, Utah. He then enrolled in the Department of Microbiology and Immunology PhD program at Virginia Commonwealth University in August 2006.